

# Estimation of Reference Evapotranspiration Using Climatic Data

A THESIS SUBMITTED TO THE GRADUATE DIVISION OF THE  
UNIVERSITY OF HAWAII AT MĀNOA IN PARTIAL FULFILLMENT  
OF THE REQUIREMENTS FOR THE DEGREE OF  
MASTER OF SCIENCE  
IN  
CIVIL AND ENVIRONMENTAL ENGINEERING  
April 2017

By  
Margaret K. Lum

Thesis Committee:

Sayed Bateni, Chairperson  
Roger Babcock  
Oceana Francis

## **ACKNOWLEDGEMENTS**

I would like to thank Dr. Bateni, Dr. Babcock, and Dr. Francis for being on my thesis committee and for providing feedback. I would also like to thank Dr. Jalal Shiri and Emily Stack for their contributions.

## ABSTRACT

In this study, daily reference evapotranspiration ( $ET_0$ ) was estimated from climatic data using Multivariate Adaptive Regression Splines (MARS), M5 Model Tree (M5MT), and Gene Expression Programming (GEP). These approaches were trained with climatic data from eight weather stations in Iran for years 2000-2007. Thereafter, they were tested with data from the same eight weather stations in Iran for year 2008 and fourteen weather stations in California for year 2015. Four data combinations were evaluated: daily mean air temperature, daily mean wind speed, daily mean relative humidity, and solar radiation (configuration 1); daily mean air temperature and solar radiation (configuration 2); daily mean air temperature and daily mean relative humidity (configuration 3); daily maximum, minimum, and mean air temperature, and extraterrestrial radiation (configuration 4). In the first part of the study, MARS, M5MT, and GEP models were tested with data from the same Iran stations they were trained with. In the second part of the study, these approaches were tested with data from stations in California. The performance of MARS, M5MT, and GEP models were evaluated using mean absolute error ( $MAE$ ), root mean square error ( $RMSE$ ), and the coefficient of determination ( $R^2$ ). For all approaches, configuration 1 produced the most accurate results. Configuration 4 was found to be region dependent and is suggested when region specific data is limited (i.e., only temperature data is available). Results indicated MARS, M5MT and GEP could successfully predict  $ET_0$  from climatic data. Comparison of these approaches showed that GEP yielded the most accurate results. Also, it was found that MARS outperformed M5MT.

## TABLE OF CONTENTS

ACKNOWLEDGEMENTS .....	ii
ABSTRACT .....	iii
LIST OF FIGURES .....	v
LIST OF TABLES .....	vii
1. INTRODUCTION.....	1
2. METHODOLOGY.....	5
2.1 Multivariate Adaptive Regression Splines (MARS).....	5
2.2 M5 Model Tree (M5MT).....	7
2.3 Gene Expression Programming (GEP).....	10
2.4 Penman-Monteith (PM) Equation .....	13
3. DATA.....	14
3.1 Iran.....	14
3.2 California.....	15
3.3 Training and Testing Data .....	17
3.3.1 Data Combinations.....	18
3.4 Statistical Analysis .....	19
4. RESULTS .....	20
4.1 MARS.....	20
4.2 M5MT.....	40
4.3 GEP.....	80
4.4 Comparing Performance of MARS, M5MT, and GEP .....	99
5. CONCLUSION.....	102
APPENDIX: M5MT Output Reference Guide.....	104
REFERENCES.....	105

## LIST OF FIGURES

Figure 1a. M5MT separates training data set into regions. ....	8
Figure 1b. Dividing process of M5MT.....	8
Figure 1c. M5MT pruned nodes are replaced with linear models.....	9
Figure 1d. Example of final M5MT and corresponding input space. ....	9
Figure 2a. Example of GEP chromosome mutation.....	12
Figure 2b. Example of GEP chromosome IS transposition.....	12
Figure 2c. Example of GEP chromosome RIS transposition. ....	12
Figure 2d. Example of GEP chromosome gene transposition.....	12
Figure 2e. Example of GEP one-point recombination with two chromosomes. ....	12
Figure 2f. Example of GEP two-point recombination with two chromosomes. ....	12
Figure 2g. Example of GEP gene recombination with two chromosomes.....	13
Figure 3. Location of weather stations in Iran.....	15
Figure 4. Location of CIMIS weather stations. ....	16
Figure 5. Variation in RMSE and $R^2$ of $ET_0$ estimates from MARS1–MARS4 versus number of basis functions. ....	21
Figure 6. Estimated $ET_0$ values from MARS1 versus observations.....	25
Figure 7. Estimated $ET_0$ values from MARS2 versus observations.....	26
Figure 8. Estimated $ET_0$ values from MARS3 versus observations.....	27
Figure 9. Estimated $ET_0$ values from MARS4 versus observations.....	28
Figure 10. Time series of observed and estimated $ET_0$ values from MARS1.....	30
Figure 11. Time series of observed and estimated $ET_0$ values from MARS2.....	32
Figure 12. Time series of observed and estimated $ET_0$ values from MARS3.....	34
Figure 13. Time series of observed and estimated $ET_0$ values from MARS4.....	36
Figure 14. Comparing performance of MARS models in different stations. ....	37
Figure 15. Estimated $ET_0$ values from M5MT1 versus observations. ....	65
Figure 16. Estimated $ET_0$ values from M5MT2 versus observations. ....	66
Figure 17. Estimated $ET_0$ values from M5MT3 versus observations. ....	67
Figure 18. Estimated $ET_0$ values from M5MT4 versus observations. ....	68
Figure 19. Time series of observed and estimated $ET_0$ values from M5MT1. ....	70
Figure 20. Time series of observed and estimated $ET_0$ values from M5MT2. ....	72

Figure 21. Time series of observed and estimated $ET_0$ values from M5MT3. ....	74
Figure 22. Time series of observed and estimated $ET_0$ values from M5MT4. ....	76
Figure 23. Comparing performance of M5MT models in different stations. ....	77
Figure 24. Estimated $ET_0$ values from GEP1 versus observations. ....	84
Figure 25. Estimated $ET_0$ values from GEP2 versus observations. ....	85
Figure 26. Estimated $ET_0$ values from GEP3 versus observations. ....	86
Figure 27. Estimated $ET_0$ values from GEP4 versus observations. ....	87
Figure 28. Time series of observed and estimated $ET_0$ values from GEP1. ....	89
Figure 29. Time series of observed and estimated $ET_0$ values from GEP2. ....	91
Figure 30. Time series of observed and estimated $ET_0$ values from GEP3. ....	93
Figure 31. Time series of observed and estimated $ET_0$ values from GEP4. ....	95
Figure 32. Comparing performance of GEP models in different stations. ....	96
Figure 33. Performance of MARS, M5MT, and GEP models tested with Iran and California stations. ....	101

## LIST OF TABLES

Table 1. Locations, altitudes, latitudes, and longitudes of weather stations in Iran. ....	14
Table 2. Locations, altitudes, latitudes, and longitudes of weather stations in California. ....	16
Table 3. Training and testing data. ....	17
Table 4. Parameter values for each MARS model. ....	21
Table 5. Basis functions and corresponding coefficients in MARS1-MARS4. ....	24
Table 6. Statistical metrics of $ET_0$ estimates from MARS1 and MARS2. ....	38
Table 7. Statistical metrics of $ET_0$ estimates from MARS3 and MARS4. ....	39
Table 8. Performance of M5MT for different testing options. ....	40
Table 9. M5MT1 model tree and corresponding linear models. ....	43
Table 10. M5MT2 model tree and corresponding linear models. ....	56
Table 11. M5MT3 model tree and corresponding linear models. ....	58
Table 12. M5MT4 model tree and corresponding linear models. ....	60
Table 13. Statistical metrics of $ET_0$ estimates from M5MT1 and M5MT2. ....	78
Table 14. Statistical metrics of $ET_0$ estimates from M5MT3 and M5MT4. ....	79
Table 15. Summary of GEP model parameters. ....	80
Table 16. GEP equations corresponding to each model. ....	83
Table 17. Statistical metrics of $ET_0$ estimates from GEP1 and GEP2. ....	97
Table 18. Statistical metrics of $ET_0$ estimates from GEP3 and GEP4. ....	98
Table 19. Mean $R^2$ , MAE, and RMSE of $ET_0$ estimates from MARS, M5MT and GEP models (tested with Iran and California stations). ....	100

## 1. INTRODUCTION

Evapotranspiration (ET) is an important component of the hydrologic cycle and water resource management. ET involves the loss of water into the atmosphere through evaporation from the soil surface, and transpiration from the stomata of leaves. This process is dependent upon numerous climatologic variables and is responsible for the water stored in the atmosphere (Traore et al., 2010). About 90% of water in the atmosphere is due to evaporation from the land surface (i.e., water bodies and soil), while transpiration of plants is responsible for the remaining 10% (USGS, 2016). On a global scale, roughly 80% of water allotted for crop production and irrigation, is lost through ET (Xu et al., 2016; Lui et al. 2009).

The demand for water has intensified due to global climate change and the significant increase of Earth's population. In the last century, the United Nations reported water use was two times greater than the world's population growth. At this rate, 1.8 billion people will be residing in areas with insufficient water by the year 2025 (National Geographic Society, 2016). In response to droughts and the exhaustion of surface water availability, roughly 10% of the world's food is grown by over pumping groundwater sources. In addition, many water intensive crops are cultivated in arid conditions further exhausting water resources (Postel, 2015). Due to the aforementioned reasons, improving water use efficiency is imperative. An accurate estimation of ET enables proper computation of water budgeting, water planning and water allocation.



Several *in situ* methods have been used to measure ET. Although these methods can provide an accurate estimate of ET over homogeneous areas, limitations and inadequacies exist. For instance, the lysimeter technique utilizes water mass balance to estimate ET. Intricate planning and groundwork are required to obtain field measurements. These measurements only pertain to a small field area and may differ from surrounding areas due to the land surface heterogeneity (Verstraeten et al., 2008). Aside from the arduous installation and maintenance, it is also unsuitable to utilize the lysimeter technique in large areas with mixed vegetation because of the inability to obtain a representative sample (Garcia-Navarro et al., 2004).

Due to the high cost of *in situ* methods and the challenges of determining the relationship between multiple factors affecting evaporative demand and ET, other approaches were developed. The Penman-Monteith (PM) equation is an accepted mathematical expression to estimate reference ET ( $ET_0$ ) (described in Section 2.4). However, this method requires a large amount of climatic data.

To further improve  $ET_0$  estimation, artificial intelligence (AI) systems were used to estimate  $ET_0$ . A number of studies showed that AI approaches (e.g., Gene Expression Programming (GEP), Multivariate Adaptive Regression Splines (MARS), and M5 Model Tree (M5MT)) could estimate  $ET_0$  accurately (Pour Ali Baba et al., 2013; Rahimikhoob, 2008; Shiri and Kisi, 2011; Shiri et al., 2014).

Güven et al. (2008) used GEP to model  $ET_0$  with the following hydrologic inputs: humidity, solar energy, wind speed, and average air temperature. Results indicated the GEP model could perform better than the PM equation. Building upon this study, Shiri et al. (2011) evaluated the feasibility of GEP to estimate  $ET_0$ , in which GEP estimates were compared to those obtained from the Adaptive Neuro-Fuzzy Inference System (ANFIS), Hargreaves-Samani,

Priestley-Taylor and the PM equation. Both studies found that GEP provided the most accurate estimate of  $ET_0$ .

Multivariate Adaptive Regression Splines (MARS) exhibit comparable advantages to GEP. Adamowski et al. (2012) used MARS, Artificial Neural Networks (ANN), and Wavelet Artificial Neural Network (WANN) to estimate mountainous watershed runoff and compared the performance of the models. Results showed MARS and WANN performed similarly in estimating runoff, and both produced better results than ANN. Additionally, Yang et al. (2004) found MARS estimated soil temperature at varying depths more accurately than ANN.

Kisi and Parmar (2016) modeled river water pollution utilizing MARS, M5MT, and Least Square Support Vector Machine (LSSVM). Results indicated MARS and LSSVM obtained similar results and both outperformed M5MT. Using inputs of solar radiation, relative humidity, air temperature and wind speed, Kisi (2015) estimated pan evaporation via MARS, LSSVM, and M5MT. It was concluded MARS performed better than LSSVM and M5MT.

Pal and Deswal (2009) found  $ET_0$  estimates from M5MT to be comparable to those from the PM and Hargreaves-Samani equations. Although ANN surpassed M5MT in Sattari et al. (2013), M5MT delivered simple linear relationship between the inputs and output. In predicting wave height, the M5MT proved to be advantageous over ANN because it generates slightly better estimates and provides rules that can be easily understood by the user (Etemad-Shahidi and Mahjoobi, 2009).

The first objective of this study is to estimate  $ET_0$  from climatic data using MARS, M5MT, and GEP approaches. The second goal is to compare the performance of models created from these three approaches using four different data combinations. The third purpose is to

assess which combination has the most significant contribution towards the estimation of  $ET_0$ .

Lastly, we will investigate whether these models can be applied to another region.

## 2. METHODOLOGY

### 2.1 Multivariate Adaptive Regression Splines (MARS)

MARS performs linear regression in steps, and has the ability to model non-linearities (Friedman, 1991; Bansal and Salling, 2013). MARS is efficient in producing models dealing with high dimensional input data sets as well as establishing the connection between dependent and independent variables. The models created are adaptive and are modified through multiple iterations to form a polynomial expression.

The process of constructing the MARS model involves splitting the data into multiple sections. For each section, containing  $p$  input variables  $X_j$  ( $j = 1, \dots, p$ ), linear regression functions (i.e., basis functions) are generated describing the data (Sharda et al., 2006). The basis functions consist of the following reflected pair functions:

$$(X_j - t)_+ = \max(0, X_j - t) = \begin{cases} X_j - t, & X_j > t \\ 0, & X_j \leq t \end{cases} \quad (1a)$$

$$(t - X_j)_+ = \max(0, t - X_j) = \begin{cases} t - X_j, & X_j < t \\ 0, & X_j \geq t \end{cases} \quad (1b)$$

where  $t$  is the junction formed between two basis functions (i.e., the knot) at an observed value. MARS then takes the reflected pairs (Equations (1a) and (1b)) and creates a collection of basis functions,  $C$ :

$$C = \left\{ (X_j - t)_+, (t - X_j)_+ \right\}; t \in \{x_{1j}, x_{2j}, x_{3j}, \dots, x_{kj}\}; k = 1, 2, \dots, n; j = 1, 2, \dots, p \quad (2)$$

where  $x_{kj}$  is the  $n^{\text{th}}$  observed value of input variable  $X_j$ . The user then specifies the constraints, which involve the number of variables inputted into the model, the maximum number of basis functions, and the maximum permissible degree of interaction (described Section 4.1). Once specified, MARS implements two stepwise evaluations (Kisi, 2015). The first process (i.e., forward step) involves a robust model containing a large amount of knots where the MARS

algorithm is trialing functions in  $C$  to determine which basis functions reduce inaccuracy. Immediately following is the backward step, in which the unnecessary surplus of basis functions is eliminated to correct the over-fitted model. Through this piecewise method, the function created by MARS ( $f$ ) is generally in the form of:

$$f(x) = \beta_0 + \sum_{i=1}^A \beta_i h_i(x) \quad (3)$$

where  $h_i(x)$  is the function created from the selected basis functions in  $C$ ,  $\beta_0$  is the bias,  $\beta_i$  is the coefficient estimated from the least square method, and  $A$  is the number of terms in the final model after implementation of forward and backward steps (Adamowski et al., 2012; Kisi, 2015).

## 2.2 M5 Model Tree (M5MT)

M5MT is an extension of a regression tree and provides the user with multiple linear functions (Witten and Frank, 2005; Pal and Deswal, 2009). Its main objective is to generate a model that is capable of determining the relationship between the independent variables and target values (i.e., dependent variables) (Bhattacharya and Solomatine, 2005). The performance of the final model is examined by comparing its estimates with the target values.

The input data is subjected to two different stages to generate a final model. In the first stage, the input space is divided into a number of regions (Figure 1a), which corresponds to the nodes in a tree-like structure. The amount of error for each of these nodes corresponds to the standard deviation of each region. For each value that propagates to a specific node, the expected error reduction is calculated, which is referred to as the standard deviation reduction (SDR) (Pal and Deswal, 2009). The formula utilized to calculate the SDR is as follows:

$$SDR = sd(T) - \sum_{i=1}^A \frac{|T_i|}{|T|} sd(T_i) \quad (4)$$

where  $T$  is the set of instances that reach a node,  $T_i$  is the subset of instances exhibiting the  $i^{th}$  outcome of a potential set,  $A$  is the final amount of instances in set  $T$ , and  $sd$  is the standard deviation. After the SDRs are calculated, the model begins to execute computational iterations. This involves the dividing process (Figure 1b), which produces subsequent nodes with a reduced standard deviation from the previous nodes. This dividing process is continued where all possible splits are considered, and terminates when the maximum expected error reduction is achieved (Rahimikhoob et al., 2013). At the end of the first stage, the model tree exhibits a large structure with region-specific linear regression models (Bhattacharya and Solomatine, 2005). This stage is

prone to over-fitting (or poor generalization) and leads to the second stage of pruning the overgrown model tree.

Pruning will occur when the estimated error at a specific node is less than or equal to the error of the all nodes branched below (Atiaa and Ghalib, 2008; Pal and Deswal, 2009). The pruned nodes are then replaced with linear equations (i.e., linear models (LM)) (Figure 1c). This process simplifies and increases the overall accuracy of the model tree (Wang and Witten, 1997; Etemad-Shahidi and Mahjoobi, 2009). See Figure 1d for an example of a final version of a model tree with an input space divided into six regions corresponding to six linear models.

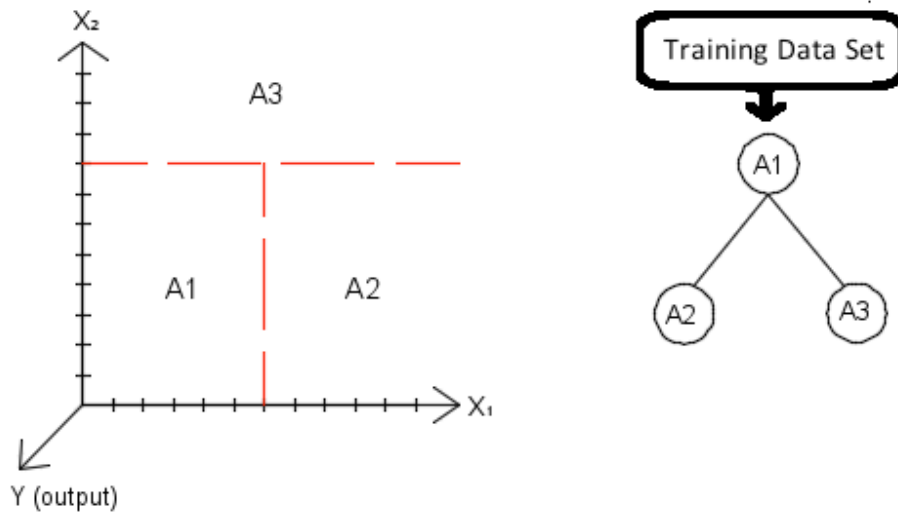


Figure 1a. M5MT separates training data set into regions.

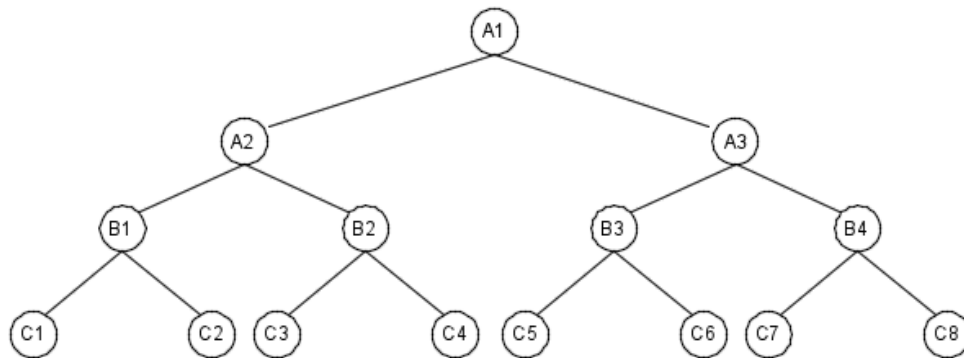


Figure 1b. Dividing process of M5MT.

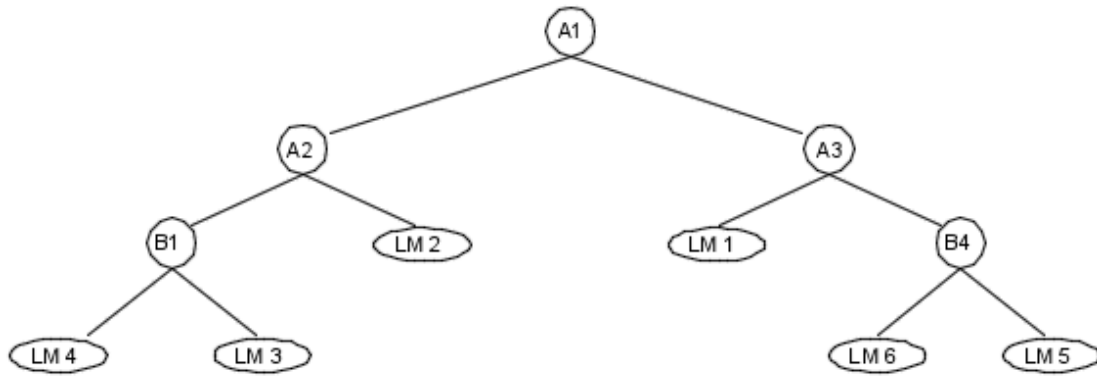


Figure 1c. M5MT pruned nodes are replaced with linear models.

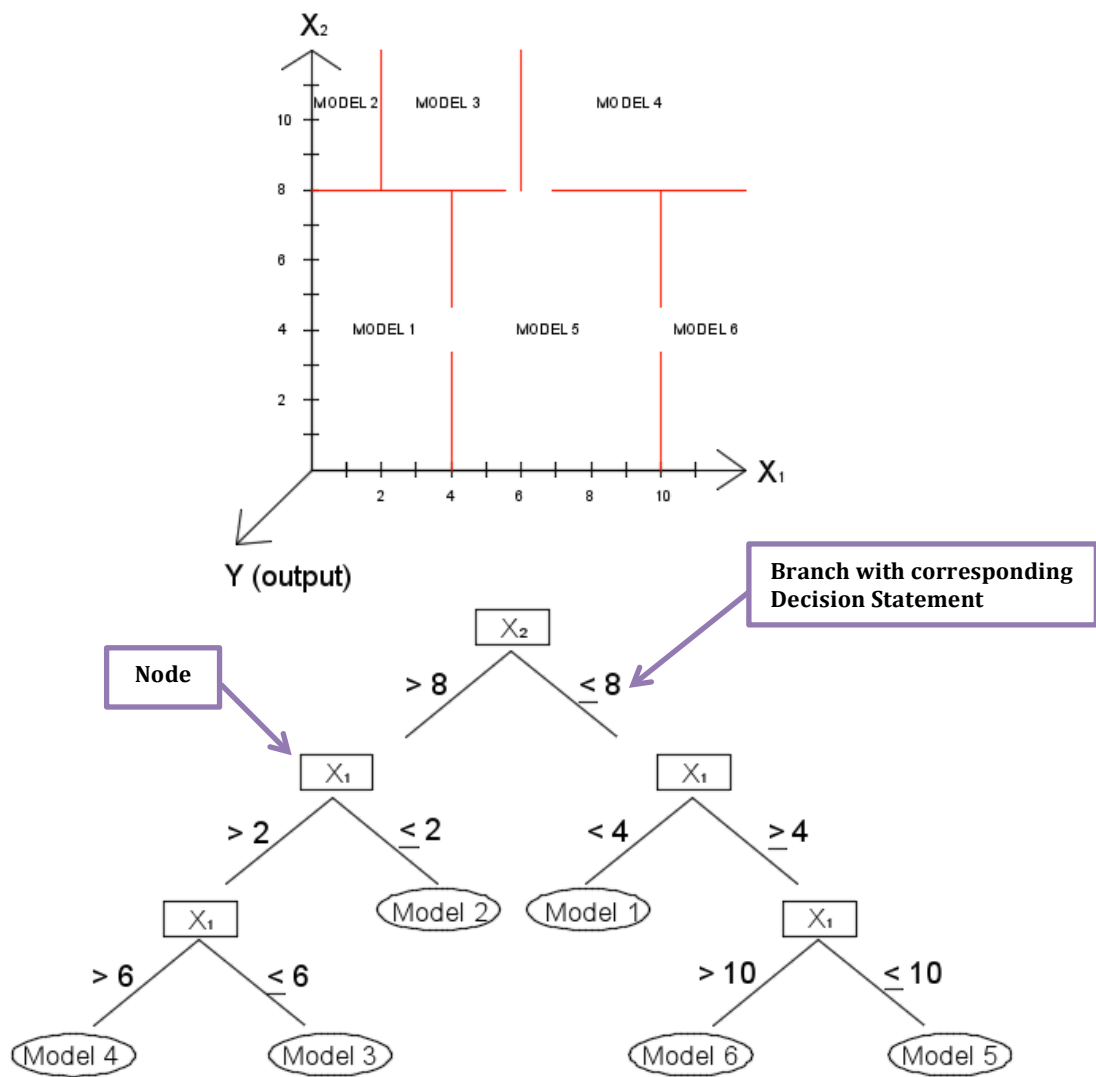


Figure 1d. Example of final M5MT and corresponding input space.



### 2.3 Gene Expression Programming (GEP)

GEP is a progressive algorithm that continuously adapts to determine the relationship between a given set of inputs and output(s) (Ferreira, 2001). GEP utilizes evolving computer programs (expression trees) of different sizes that are encoded with a finite linear string of input data (chromosomes). A final expression tree is produced consisting of mathematical expressions and polynomials (Güven and Günel, 2008).

GEP begins with a random generation of chromosomes for a specific program. These chromosomes are made up of genes (finite linear string containing input data) that are linked by arithmetic operators (e.g., +, -, ×, /) (Oltean and Grosan, 2003). GEP genes are made up of two parts: the head and the tail. The head consists of both terminal symbols (independent variables) and functional symbols (e.g., Arctan). The tail only consists of terminal symbols and is calculated as follows:

$$t = (n - 1)h + 1 \quad (5)$$

where  $t$  is the tail length,  $n$  is the amount of arguments in the functions, and  $h$  is the head length chosen by the user.

After the chromosomes are generated and used in the program, the accuracy of the program is evaluated using a fitness function (e.g., Root Mean Square Error (*RMSE*)) and fitness cases (i.e., the training data). The fitness function compares the dependent variable (e.g.,  $ET_0$ ) from the given training dataset to the values created by the program. The program will either be selected or rejected based upon its ability to simulate the dependent variable of the dataset. If the program is selected, then it is replicated and further improved through chromosome modifications.

The chromosomes are modified through replication, mutation, transposition, and crossover (i.e., recombination) (Ferreira, 2001). Replication copies an existing chromosome and uses it in the next generation. Mutation of a chromosome is when symbols in the head of a gene changes into other functional or terminal symbols, and symbols in the tail changes into other terminal symbols (Figure 2a).

Transposition is the random selection of segments within a chromosome and moves it to another position. Three types of transposition can occur: insertion sequence (IS), root insertion sequence (RIS), and gene transposition. In IS, random segments with functional or terminal symbols move and replace existing segments (Figure 2b). In RIS, random segments starting with a functional symbol move to the beginning of the gene. The whole head then shifts downstream (i.e., to the right), while losing the last symbols of the head (Figure 2c). Gene transposition moves a randomly selected gene to the beginning of the chromosome (Figure 2d).

Recombination affects two random chromosomes that exchange terminal and functional symbols at arbitrary points. There are three types of recombination: one-point recombination, two-point recombination, and gene recombination. One-point recombination splits the two chromosomes at the same arbitrary point and all symbols after that point will be exchanged between the chromosomes (Figure 2e). Two-point recombination separates the chromosomes at two points and the symbols between the points are exchanged (Figure 2f). Gene recombination involves the entire gene of a chromosome to be swapped with the other chromosome (Figure 2g).

After the aforementioned modifications, the newly improved chromosomes are used in the next iteration. This process is repeated for a programmed set of generations (iterations) or until a solution is reached.

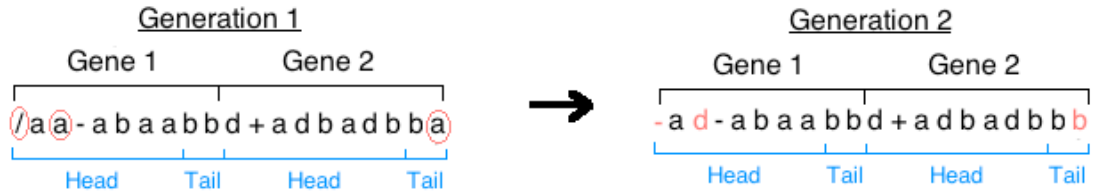


Figure 2a. Example of GEP chromosome mutation.

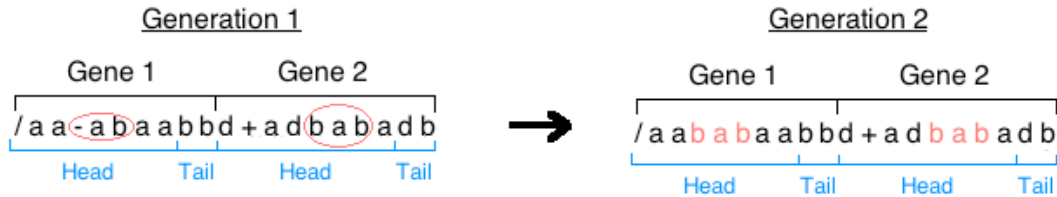


Figure 2b. Example of GEP chromosome IS transposition.

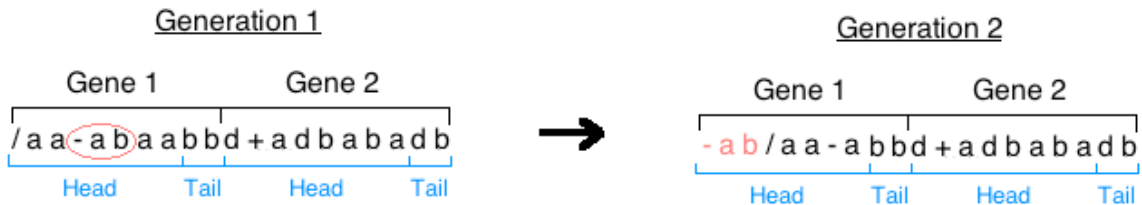


Figure 2c. Example of GEP chromosome RIS transposition.

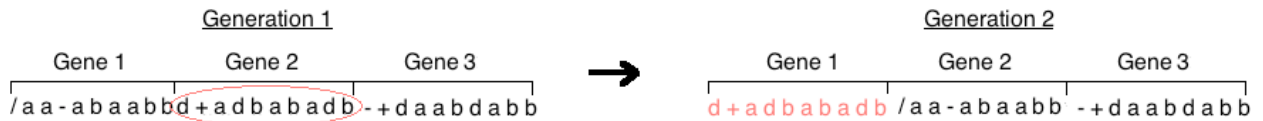


Figure 2d. Example of GEP chromosome gene transposition.

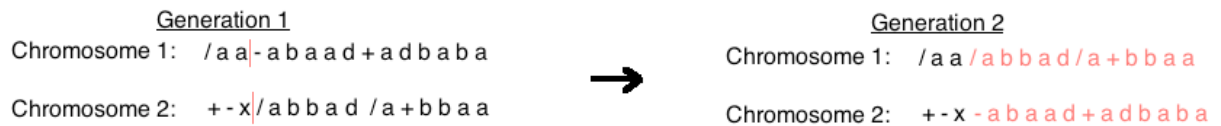


Figure 2e. Example of GEP one-point recombination with two chromosomes.



Figure 2f. Example of GEP two-point recombination with two chromosomes.

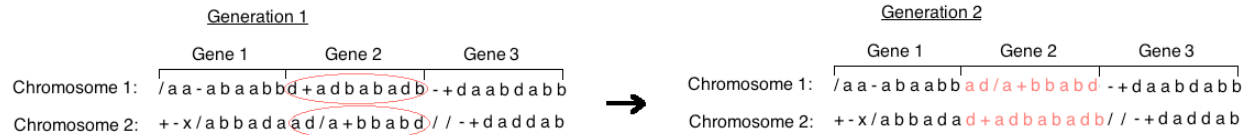


Figure 2g. Example of GEP gene recombination with two chromosomes.

## 2.4 Penman-Monteith (PM) Equation

The PM equation has been accepted as a reference equation for  $ET_0$  estimation (Shahidian et al., 2012).  $ET_0$  is defined as evapotranspiration that occurs when using a theoretical grass surface with an assumed height of 0.12 meter, a surface resistance (i.e., resistance of vapor leaving the surface) of 70 seconds per meter and a surface albedo (i.e., reflectivity of surface) of 0.23 (Allen et al, 1998). Other  $ET_0$  equations have been calibrated based upon the PM equation (Allen et al., 1998; Shiri et al., 2013). The PM equation is given by:

$$ET_0 = \frac{0.408\Delta(R_n - G) + \gamma \frac{900}{T_{mean} + 273} W_s (e_s - e_a)}{\Delta + \gamma(1 + 0.34W_s)} \quad (6)$$

where  $ET_0$  is the reference evapotranspiration (mm/d),  $\Delta$  is the slope of saturation vapor pressure function (kPa/°C),  $R_n$  is the net radiation (MJ/m<sup>2</sup>day),  $G$  is the soil heat flux density (MJ/m<sup>2</sup>day),  $\gamma$  is the psychrometric constant (kPa/°C),  $T_{mean}$  is the mean air temperature (°C),  $W_s$  is the daily mean wind speed at a height of 2 m (m/s),  $e_s$  is the saturation vapor pressure (kPa), and  $e_a$  is the actual vapor pressure (kPa).

### 3. DATA

#### 3.1 Iran

Daily climatic data from January 1, 2000 to December 31, 2008 was collected from 8 weather stations in the coastal regions of Iran. The recorded data were daily average relative humidity, daily mean wind speed at a reference height of 2 meters, daily maximum, minimum and mean air temperatures, and incoming solar radiation. The hydrological data and the corresponding calculated  $ET_0$  (from Equation (6)) were used to train and test the models (see Section 3.3). The locations, altitudes, longitudes and latitudes of the weather stations are shown in Table 1 and Figure 3.

Table 1. Locations, altitudes, latitudes, and longitudes of weather stations in Iran.

Station	Altitude, m	Latitude, °	Longitude, °
Abadan	6.6	30.2	48.2
Ahwaz	22.5	31.2	48.4
Bandar-e-Abbas	9.8	27.1	56.2
Bandar-e-Lenge	22.7	26.3	54.2
Bushehr	9	28.6	50.5
Gorgan	13.3	36.5	54.1
Rasht	-8.6	37.1	49.4
Sari	23	36.3	53.0



Figure 3. Location of weather stations in Iran.

### 3.2 California

Daily climatic data from January 1, 2015 to December 31, 2015 was collected from 14 California Irrigation Management Information System (CIMIS) weather stations. The collected data were daily average relative humidity, daily mean wind speed at a reference height of 2 meters, daily maximum, minimum and mean air temperature, and incoming solar radiation. The hydrological data and the corresponding calculated  $ET_0$  (from Equation (6)) were used to test the models (see Section 3.3). The locations, altitudes, longitudes, and latitudes of the CIMIS weather stations are shown in Table 2 and Figure 4.

Table 2. Locations, altitudes, latitudes, and longitudes of weather stations in California.

Station	Altitude, m	Latitude, °	Longitude, °
Bishop	1271	37.4	-118.4
King City Oasis Rd.	164.6	36.1	-121.1
Blythe NE	83.8	33.7	-114.6
Atascadero	269.8	35.5	-120.6
Delano	91.4	35.8	-119.3
Gilroy	56.4	37.0	-121.5
Arleta	298.7	34.3	-118.4
Gerber South	75	40.0	-122.2
Woodland	25	38.7	-121.8
Diamond Springs	624.8	38.6	-120.8
Lompoc	16.8	34.7	-120.5
Santa Maria II	65.5	34.9	-120.5
Macdoel II	1300	41.8	-122.0
Moreno Valley	488.9	33.9	-117.2

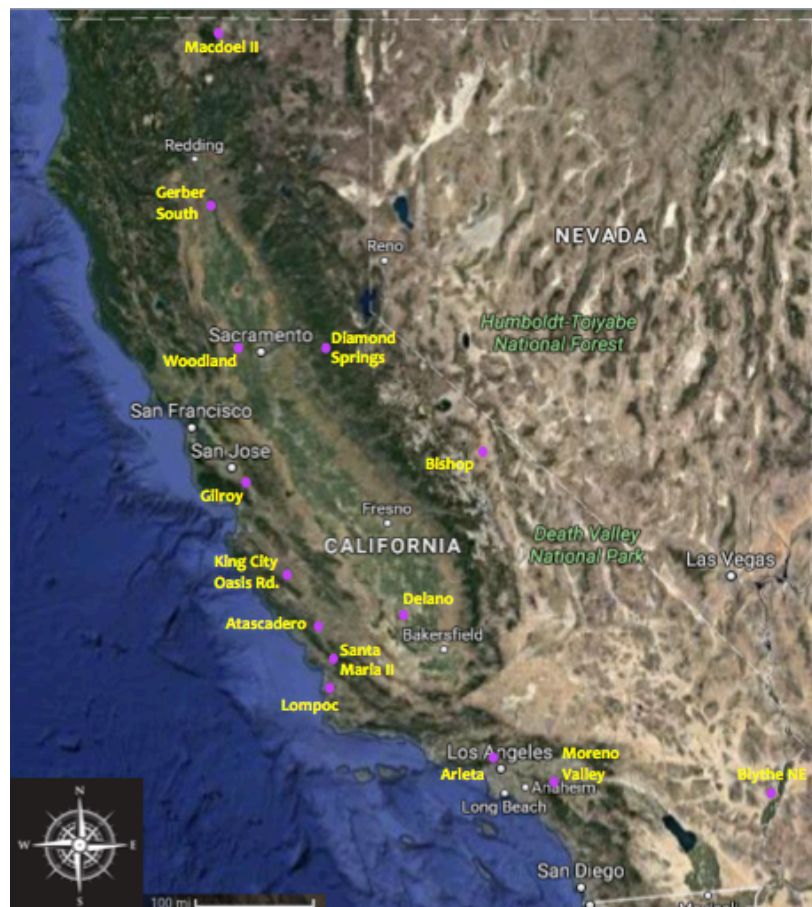


Figure 4. Location of CIMIS weather stations.

### 3.3 Training and Testing Data

The training dataset contained the climatic data from the 8 stations located in Iran (Table 1) and the corresponding  $ET_0$  estimates from the PM equation. The dataset was limited to the years 2000-2007, while the data from 2008 was reserved for testing. MARS, M5MT, and GEP used the training data to generate models (i.e., equations), which described the relationship between the input data (e.g., mean air temperature, solar radiation, etc.) from the 8 stations in Iran and the corresponding  $ET_0$  values.

The testing dataset contained the climatic data from the same 8 stations in Iran (year 2008 only) and 14 CIMIS stations in California (year 2015) (Section 3.2). The testing dataset was used to assess the capabilities of MARS, M5MT, and GEP models to predict  $ET_0$ . These predicted  $ET_0$  values were compared to  $ET_0$  estimates from the PM equation (6).

The MARS, M5MT and GEP training and testing data is outlined in Table 3. In the first part of this study, MARS, M5MT, and GEP models were tested with data from same Iran stations it was trained with. In the second part of this study, MARS, M5MT, and GEP models were tested with data from 14 CIMIS stations in California.

Table 3. Training and testing data.

	<b>Approach</b>	<b>Training Data</b>	<b>Testing Data</b>
<b>1<sup>st</sup> Part of Study</b>	MARS	Iran (2000-2007)	Iran (2008)
	M5MT		
	GEP		
<b>2<sup>nd</sup> Part of Study</b>	M5MT	Iran (2000-2007)	California (2015)
	MARS		
	GEP		



### 3.3.1 Data Combinations

The PM equation requires several hydrological variables (i.e., net radiation, soil heat flux, air temperature, relative humidity, and wind speed), which are typically unavailable. As a result, different combinations of hydrological data were investigated, which were based upon equations requiring fewer climatic data to estimate  $ET_0$  (e.g., Makkink, Romanenko, and Hargreaves-Samani).

The Makkink equation utilizes solar radiation (Makkink, 1957):

$$ET_0 = 0.61 \frac{\Delta R_s}{(\Delta + \gamma)\lambda} - 0.12 \quad (7)$$

where  $R_s$  is the incoming solar radiation (MJ/m<sup>2</sup>day) and  $\lambda$  is the latent heat of evaporation (MJ/kg).

The Romanenko equation uses the concept water mass transfer, and requires relative humidity and air temperature (Romanenko, 1961):

$$ET_0 = 0.0018(T_{mean} + 25)^2(100 - RH) \quad (8)$$

where  $RH$  is relative humidity (%).

The Hargreaves-Samani method uses air temperature and extraterrestrial radiation (Hargreaves and Samani, 1985):

$$ET_0 = 0.0023 \frac{R_a}{\lambda} (T_{mean} + 17.8) \sqrt{T_{max} - T_{min}} \quad (9)$$

where  $R_a$  is extraterrestrial radiation (mm/d),  $T_{max}$  is the daily maximum air temperature (°C) and  $T_{min}$  is the daily minimum air temperature (°C).

Based on the required inputs in equations (6) – (9) and the study conducted by Shiri et al. (2014), the data combinations used to train and test MARS, M5MT, and GEP are:

- i. Configuration 1:  $W_s, RH_{mean}, T_{mean}, R_s$  [MARS1, M5MT1, GEP1]
- ii. Configuration 2:  $T_{mean}, R_s$  [MARS2, M5MT2, GEP2]
- iii. Configuration 3:  $T_{mean}, RH_{mean}$  [MARS3, M5MT3, GEP3]
- iv. Configuration 4:  $T_{mean}, T_{max}, T_{min}, R_a$  [MARS4, M5MT4, GEP4]

### 3.4 Statistical Analysis

To evaluate the performance of MARS, M5MT, and GEP models, statistical metrics such as mean absolute error ( $MAE$ ), root mean square error ( $RMSE$ ), and the coefficient of determination ( $R^2$ ) were used and are defined as follows:

$$MAE = \frac{\sum_{i=1}^n |O_i - P_i|}{n} \quad (10)$$

$$RMSE = \sqrt{\frac{\sum_{i=1}^n (O_i - P_i)^2}{n}} \quad (11)$$

$$R^2 = \left[ \frac{\sum_{i=1}^n (O_i - \bar{O})(P_i - \bar{P})}{\sqrt{\sum_{i=1}^n (O_i - \bar{O})^2} \sqrt{\sum_{i=1}^n (P_i - \bar{P})^2}} \right]^2 \quad (12)$$

where  $n$  is the number of observations,  $O_i$  and  $P_i$  are the  $i^{th}$  observed and estimated  $ET_0$ , respectively, and  $\bar{O}$  and  $\bar{P}$  are the mean of observed and simulated  $ET_0$  values.

## 4. RESULTS

### 4.1 MARS

In this study, the MATLAB ARESLab toolbox was used. It consisted of multiple functions enabling the creation of piecewise linear and cubic regression MARS models. Parameters in ARESLab that were optimized based on trial and error were ‘*maxInteractions*’, ‘*c*’, and ‘*maxFuncs*’. The parameter ‘*maxInteractions*’ controlled the largest amount of interactions that can occur between the data variables, the ‘*c*’ parameter dictated smoothness of the model (the larger the value, the fewer the knots), and the ‘*maxFuncs*’ determined the highest number of basis functions to be included in the model during the forward phase (see Equations (1a) and (1b) in Section 2.1).

Figure 5 shows the variations in *RMSE* and  $R^2$  of  $ET_0$  estimates from MARS1–MARS4 versus the number of basis functions. As shown, MARS1 and MARS2 generated the lowest *RMSE* and the highest  $R^2$  with 15 basis functions. To obtain optimal values of  $R^2$  and *RMSE*, MARS3 and MARS4 utilized 6 and 3 basis functions, respectively. Due to the large amount of training data, Friedman (1991) recommended a ‘*c*’ value of 0, which will optimize knot production. Maximum interactivity (value of -1) between variables was allowed because it was shown to yield better results (Emamgolizadeh et al., 2015). The parameters used in each MARS model are presented in Table 4.

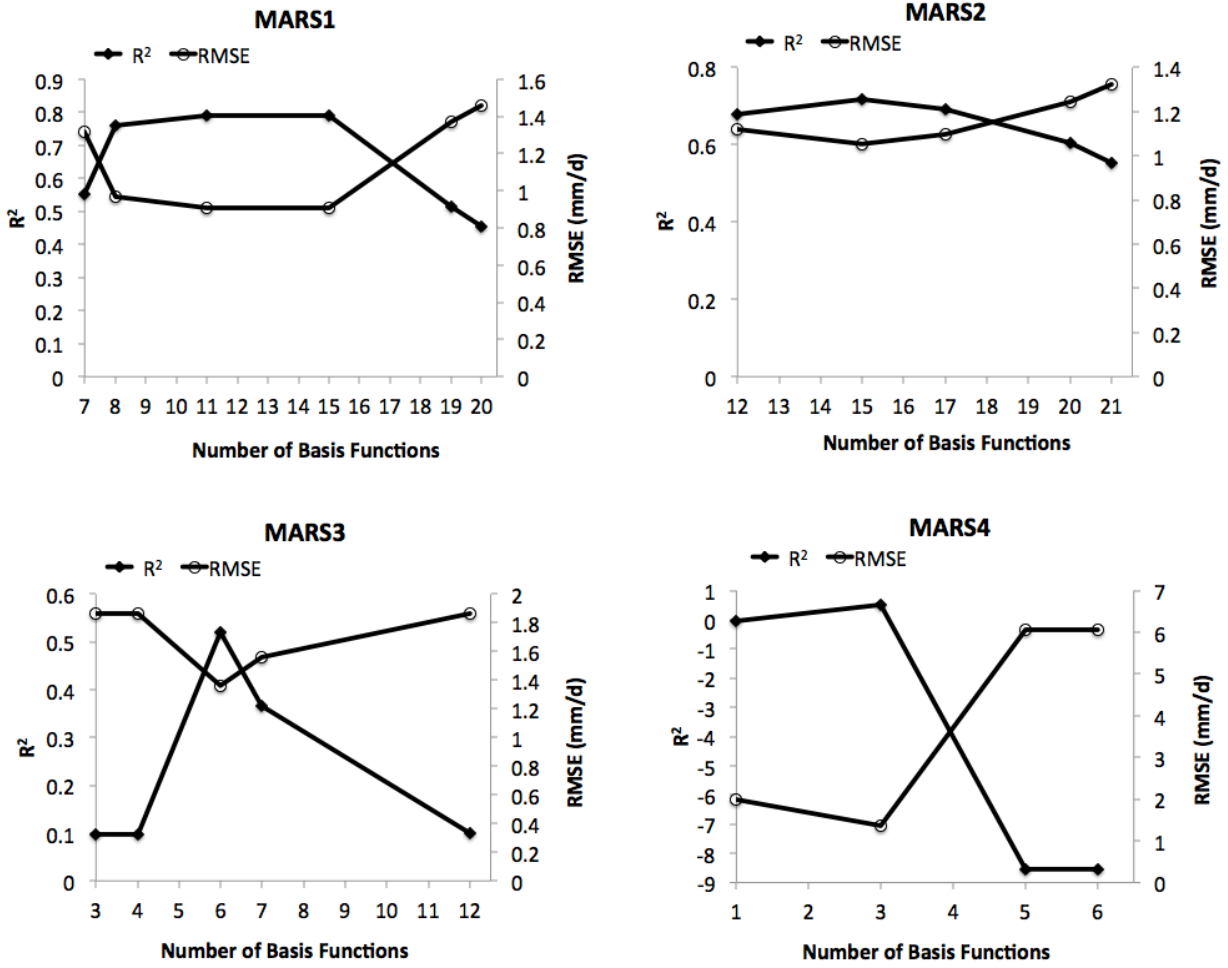


Figure 5. Variation in  $RMSE$  and  $R^2$  of  $ET_0$  estimates from MARS1–MARS4 versus number of basis functions.

Table 4. Parameter values for each MARS model.

Model	Parameters	Value
MARS1	<i>maxInteractions</i>	-1
	<i>c</i>	0
	<i>maxFuncs</i>	15
MARS2	<i>maxInteractions</i>	-1
	<i>c</i>	0
	<i>maxFuncs</i>	15
MARS3	<i>maxInteractions</i>	-1
	<i>c</i>	0
	<i>maxFuncs</i>	6
MARS4	<i>maxInteractions</i>	-1
	<i>c</i>	0
	<i>maxFuncs</i>	3

Summarized in Table 5 are the coefficients and basis functions generated by the four MARS models. The coefficients ( $\beta_i$ ) represent the weight (i.e., importance) of the variable in terms of contributing towards the estimation of  $ET_0$  (see Equation (3)). It is noteworthy that MARS1-MARS3 models effectively established a relationship between all input variables and  $ET_0$ . In contrast, three (i.e.,  $T_{mean}$ ,  $T_{min}$ , and  $R_a$ ) of the four inputs in the MARS4 model were eliminated.

Figures 6-9 compare  $ET_0$  estimates from the four MARS models with those from the PM equation for the different stations located in California and Iran. MARS1 and MARS2 yielded  $ET_0$  values more concentrated within the vicinity of the “best fit” line compared to MARS3 and MARS4. Figures 10-13 show the time series of predicted  $ET_0$  values from the four MARS models. Calculated  $ET_0$  values from the PM equation were also plotted on the same figures for comparison. The general trend in Figures 10-13 suggests an underestimation of  $ET_0$  in California. This is due to measurement errors and also the fact that none of the stations in California were used for training the MARS models. Nevertheless, the  $ET_0$  estimates from the MARS models were able to capture the daily oscillations of the observed  $ET_0$  values.

The performance of the MARS models was compared in Figure 14 using  $MAE$ ,  $RMSE$  and  $R^2$ . In all stations, MARS1 provided the best results, and MARS2 provided better estimates than MARS3 and MARS4. For California stations, average  $MAE$  of  $ET_0$  estimates from MARS2, MARS3, and MARS4 were 18%, 50%, and 52% greater than those of MARS1, respectively. Also, their average  $RMSE$  values were respectively 19%, 58%, and 57% greater than those of MARS1. When applied to the Iran stations, MARS1 resulted in the lowest  $MAE$  and  $RMSE$  values (0.44 mm/d and 0.603 mm/d, respectively) and the highest  $R^2$  value (0.94). MARS2 tested

with Iran stations resulted in better  $ET_0$  estimates compared to MARS3 and MARS4, with lower  $MAE$  (0.66 mm/d) and  $RMSE$  (0.93 mm/d) and higher  $R^2$  (0.84).

The statistical metrics of  $ET_0$  estimates from MARS1-MARS4 are given in Tables 6 and 7. High variability in  $MAE$ ,  $RMSE$ , and  $R^2$  can be observed for all California and Iran stations. Compared to MARS3 and MARS4, MARS1 and MARS2 models were able to more robustly learn the relationship between the input data and  $ET_0$  (see Tables 6 and 7). For all stations, the average  $MAE$  of MARS1 was 20%, 53%, and 56% less than those of MARS2, MARS3, and MARS4, respectively. Similarly, the average  $RMSE$  of all stations tested with MARS1 was reduced by 20%, 59%, and 61% when compared with those of MARS2, MARS3, and MARS4, respectively.

On average, MARS1 and MARS2 achieved better results than MARS3 and MARS4. The outcomes from MARS1 and MARS2 tested with California stations provided validation that MARS is a feasible approach to estimate  $ET_0$ . Furthermore, statistics from MARS2 indicated the ability of MARS to generate an equation to estimate  $ET_0$  from limited climatic data, which can be useful for areas with limited resources.

Table 5. Basis functions and corresponding coefficients in MARS1-MARS4.

Model	Basis Functions, $h_i(x)$	Coefficients, $\beta_i$
MARS1	Intercept ( $\beta_0$ )	11.9
	$(R_s - 10.8)_+$	0.249
	$(10.8 - R_s)_+$	-7.63E-02
	$(6.3 - W_s)_+ \times (RH_{\text{mean}} - 31.9)_+$	1.62E-02
	$(6.3 - W_s)_+ \times (31.9 - RH_{\text{mean}})_+$	3.30E-02
	$(W_s - 6.3)_+$	0.109
	$(6.3 - W_s)_+$	-0.964
	$(RH_{\text{mean}} - 30.8)_+$	-0.126
	$(30.8 - RH_{\text{mean}})_+$	-0.242
	$(T_{\text{mean}} - 42.6)_+$	-4.19E-03
	$(42.6 - T_{\text{mean}})_+$	-0.185
	$(R_s - 10.8)_+ \times (T_{\text{mean}} - 42.6)_+$	-1.49E-05
	$(R_s - 10.8)_+ \times (42.6 - T_{\text{mean}})_+$	-5.28E-03
	$(RH_{\text{mean}} - 30.8)_+ \times (T_{\text{mean}} - 31)_+$	8.33E-04
$(RH_{\text{mean}} - 30.8)_+ \times (31 - T_{\text{mean}})_+$	2.48E-03	
MARS2	Intercept ( $\beta_0$ )	4.08
	$(10.8 - R_s)_+$	-5.07E-02
	$(R_s - 10.8)_+ \times (T_{\text{mean}} - 42.7)_+$	-2.46E-02
	$(R_s - 10.8)_+ \times (42.7 - T_{\text{mean}})_+$	1.11E-02
	$(42.7 - T_{\text{mean}})_+$	-0.321
	$(33.5 - T_{\text{mean}})_+$	0.233
	$(T_{\text{mean}} - 1006.2)_+$	-7.76E-02
	$(1006.2 - T_{\text{mean}})_+$	2.43E-03
	$(R_s - 10.8)_+ \times (T_{\text{mean}} - 27.2)_+$	2.45E-02
	$(R_s - 10.8)_+ \times (27.2 - T_{\text{mean}})_+$	-1.52E-02
$(T_{\text{mean}} - 42.7)_+ \times (17.1 - R_s)_+$	-1.37E-04	
MARS3	Intercept ( $\beta_0$ )	10.8
	$(T_{\text{mean}} - 42)_+$	-3.22E-03
	$(42 - T_{\text{mean}})_+$	-0.208
	$(RH_{\text{mean}} - 31.6)_+$	-6.67E-02
	$(31.6 - RH_{\text{mean}})_+$	-0.253
MARS4	Intercept ( $\beta_0$ )	0.449
	$(T_{\text{max}} - 12.2)_+$	0.221
	$(12.2 - T_{\text{max}})_+$	0.330

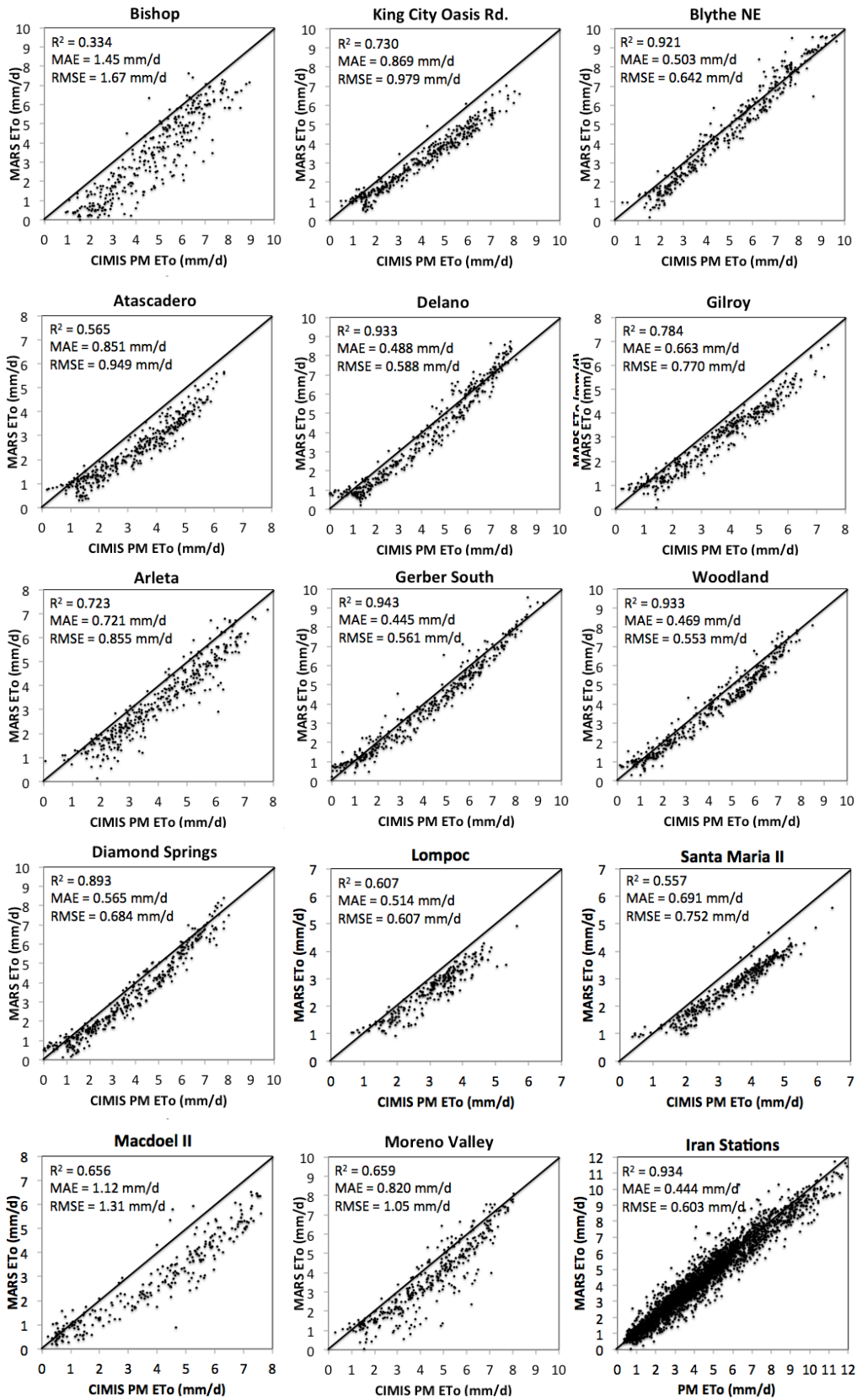


Figure 6. Estimated  $ET_0$  values from MARS1 versus observations.



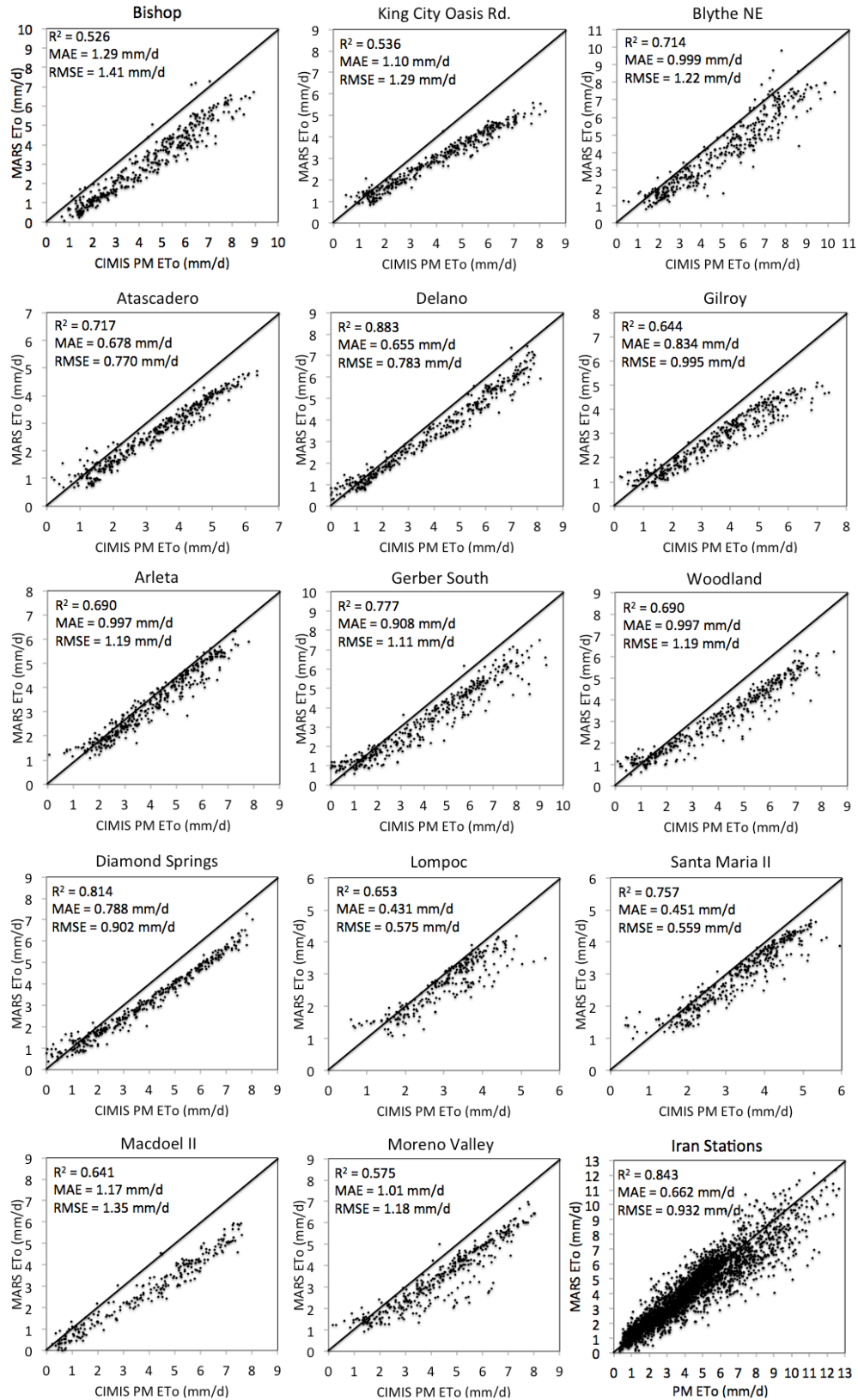


Figure 7. Estimated  $ET_0$  values from MARS2 versus observations.

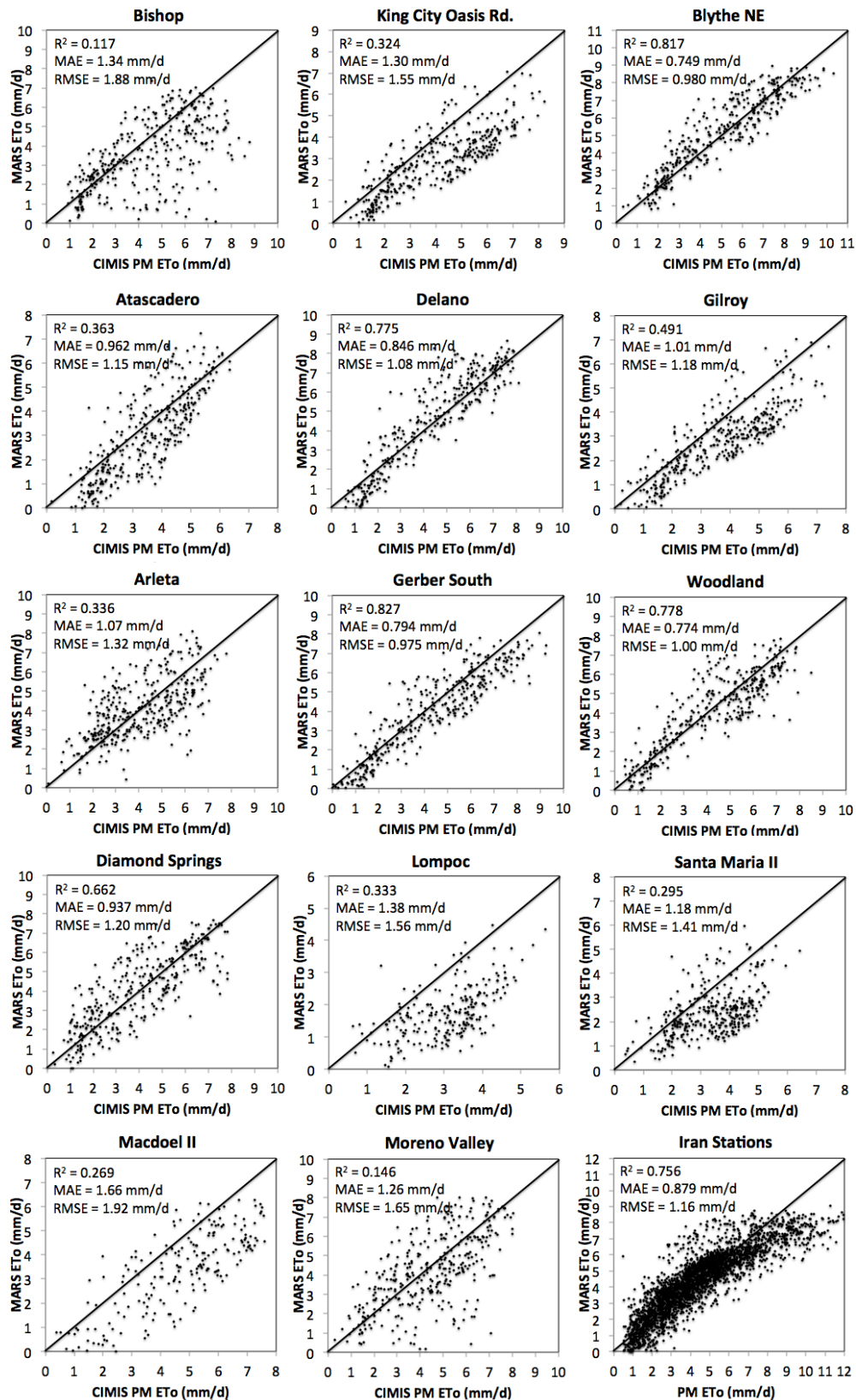


Figure 8. Estimated  $ET_0$  values from MARS3 versus observations.

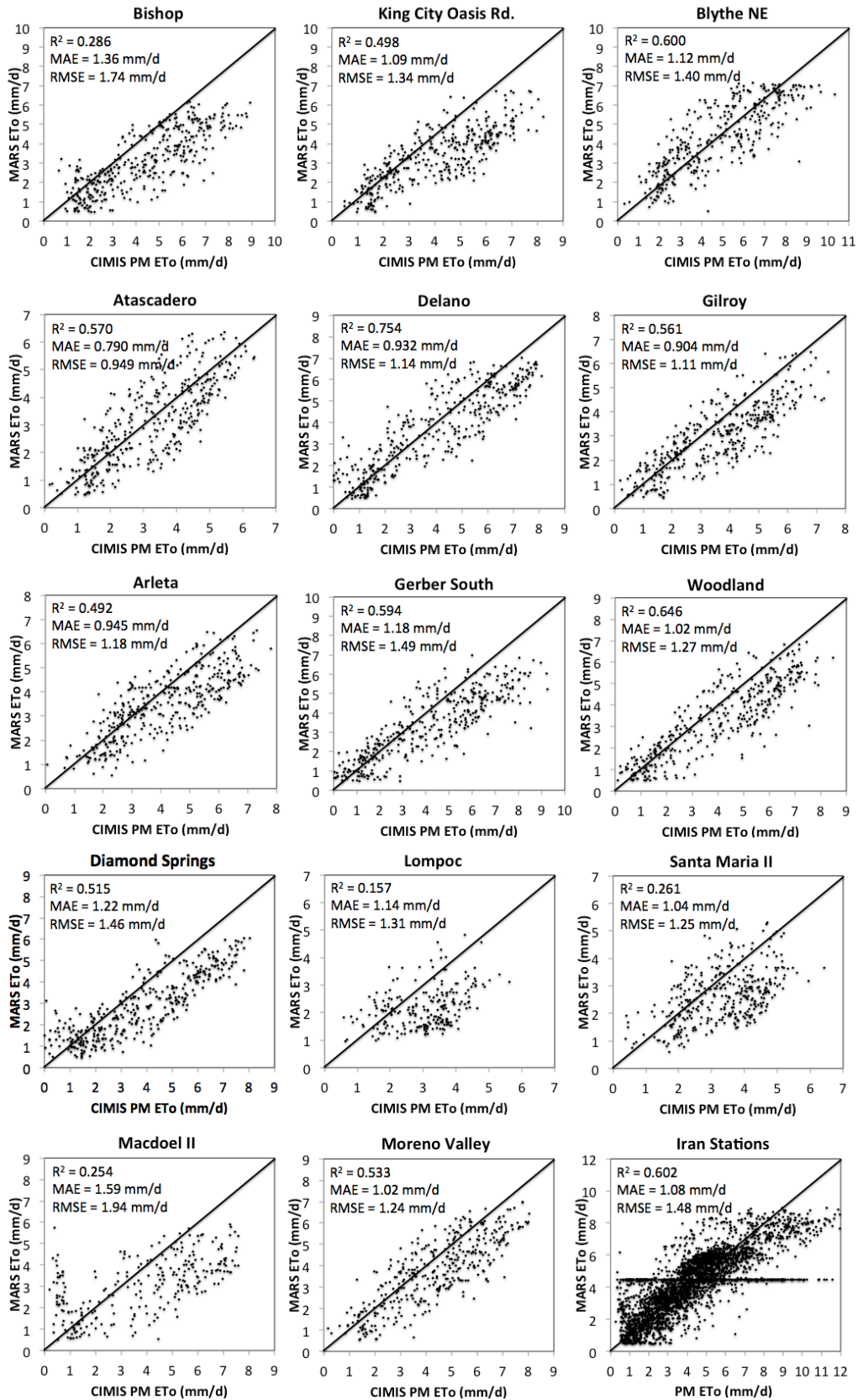
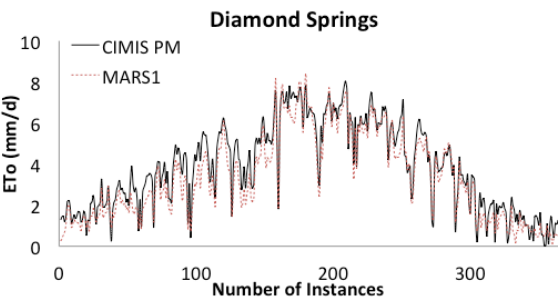
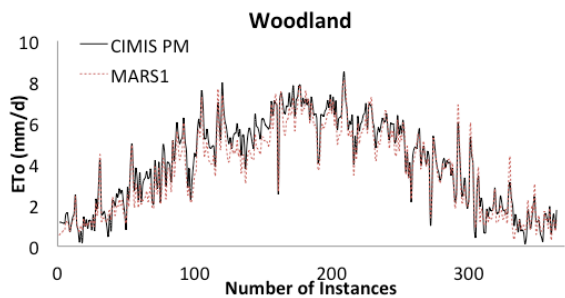
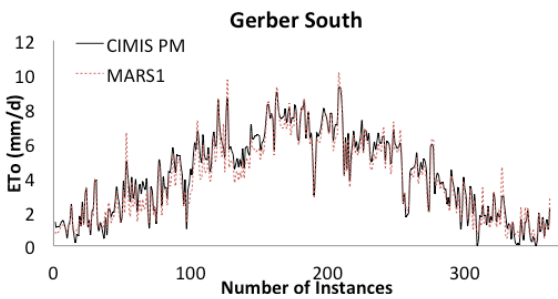
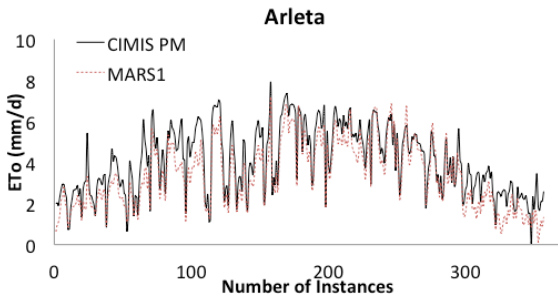
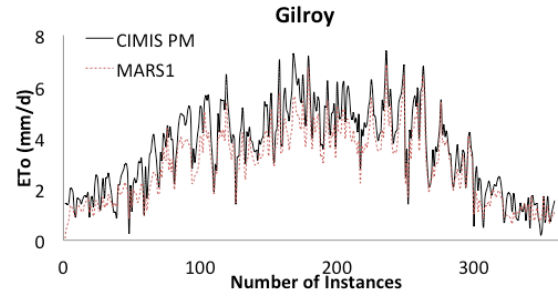
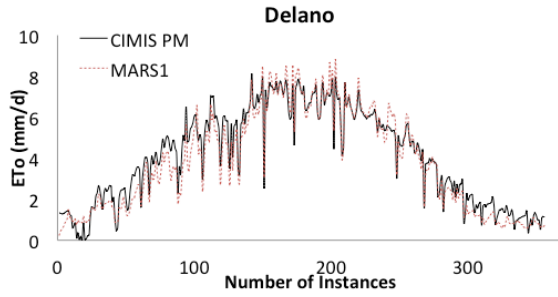
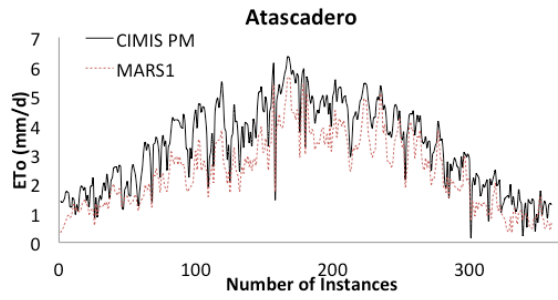
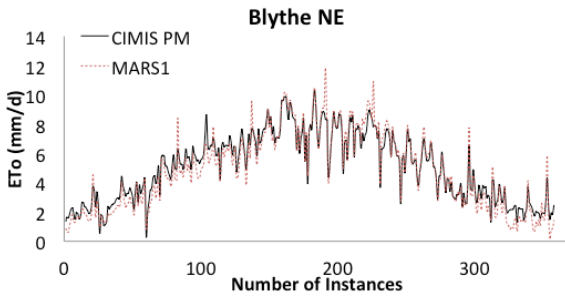
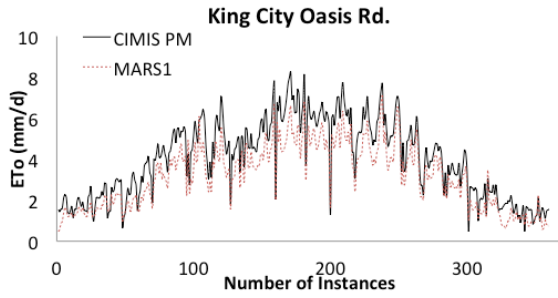
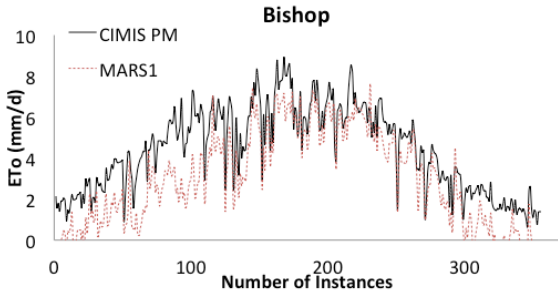


Figure 9. Estimated  $ET_0$  values from MARS4 versus observations.



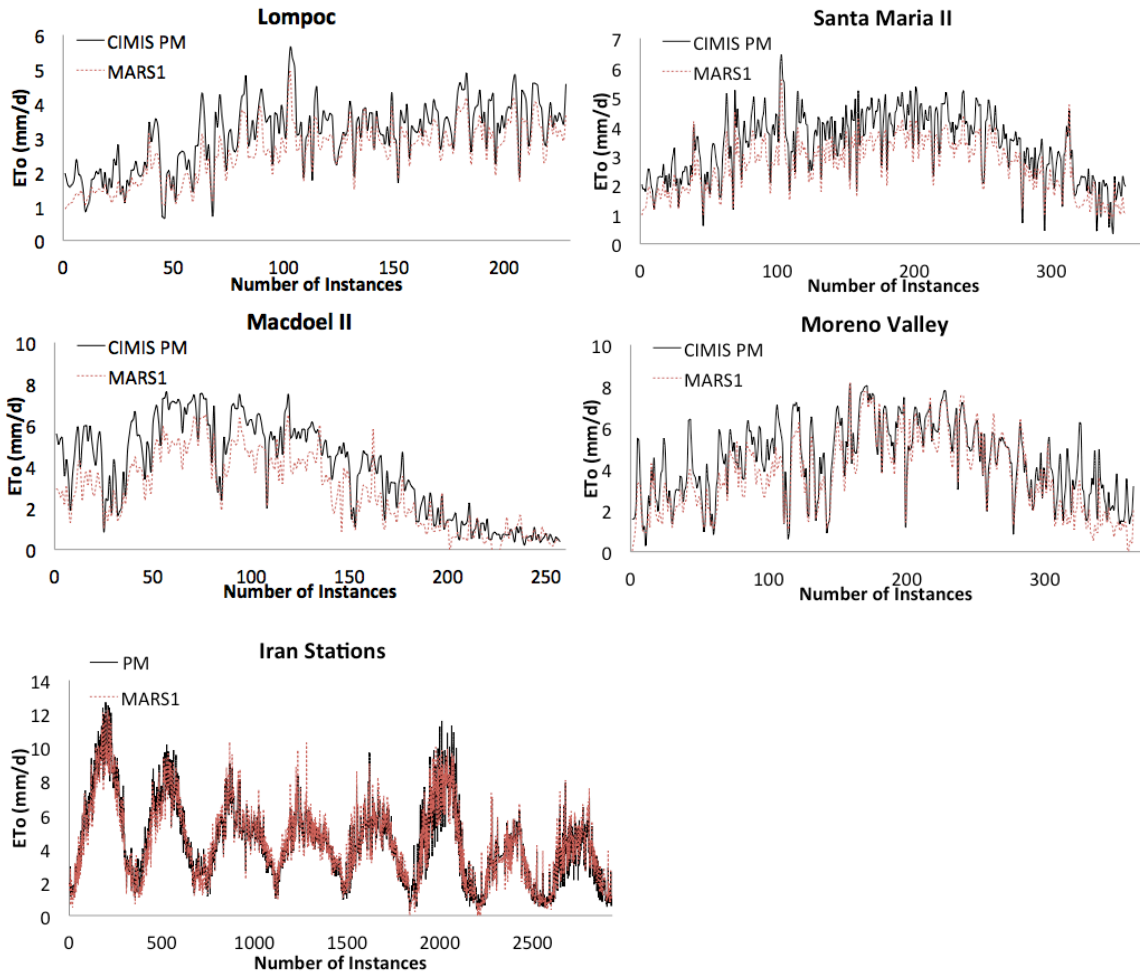
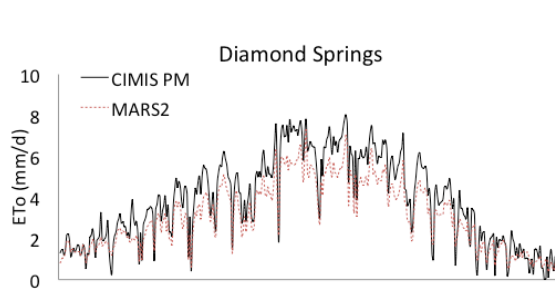
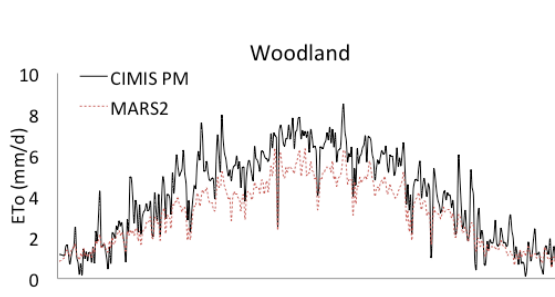
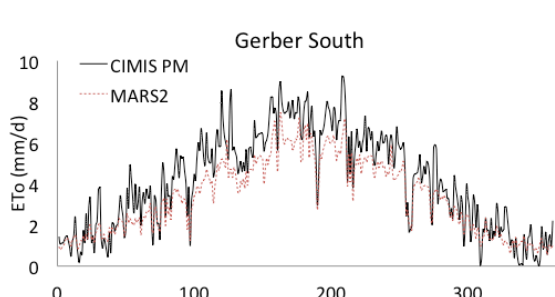
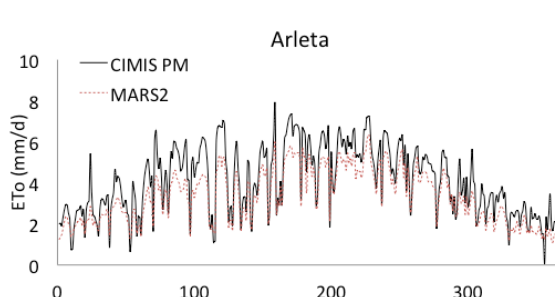
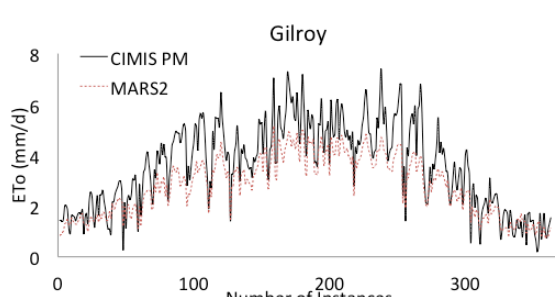
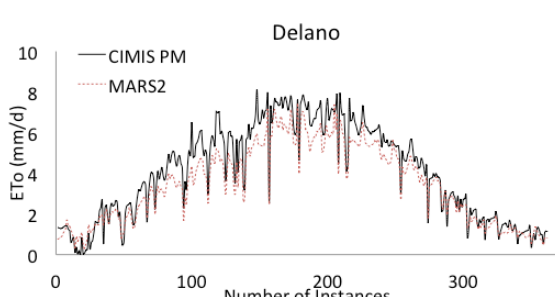
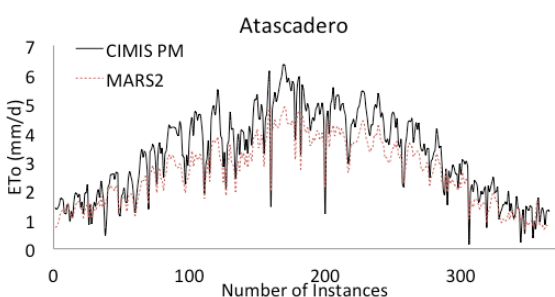
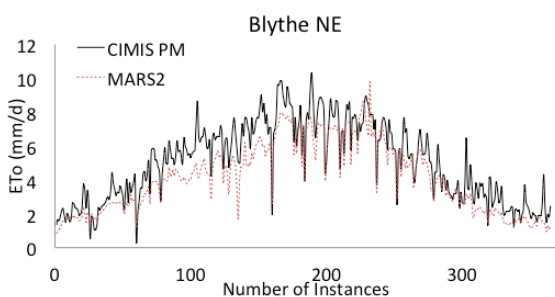
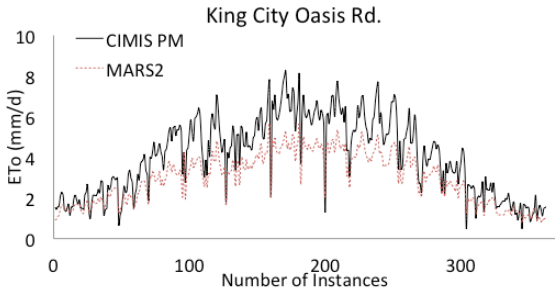
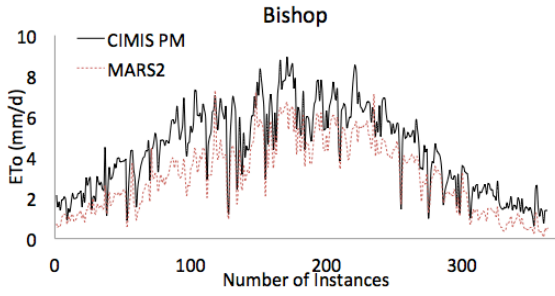


Figure 10. Time series of observed and estimated  $ET_0$  values from MARS1.



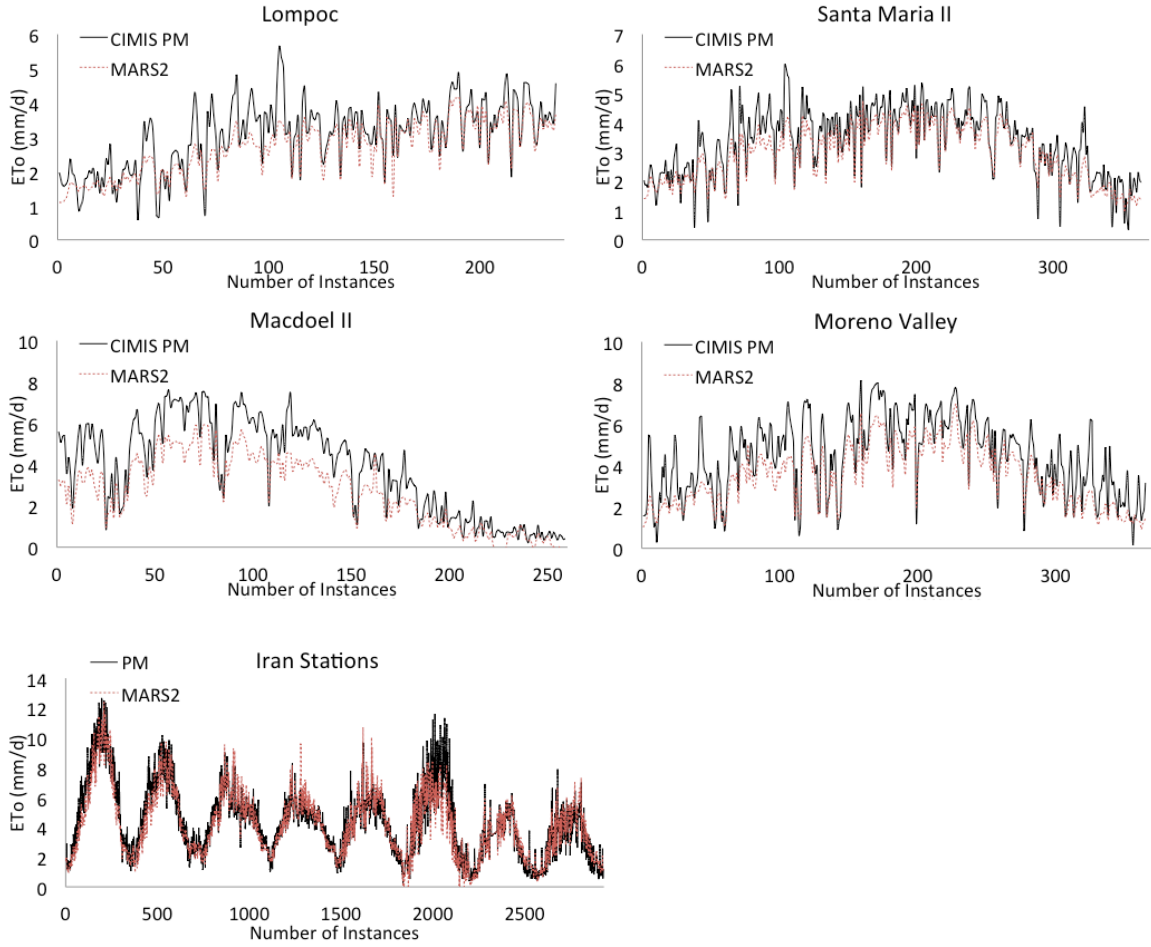
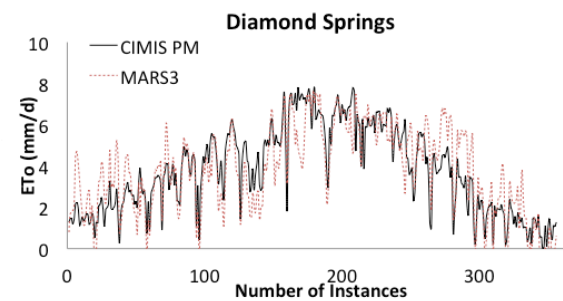
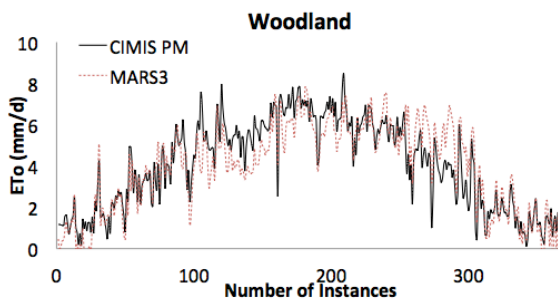
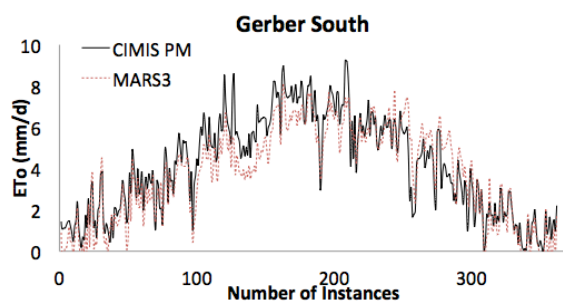
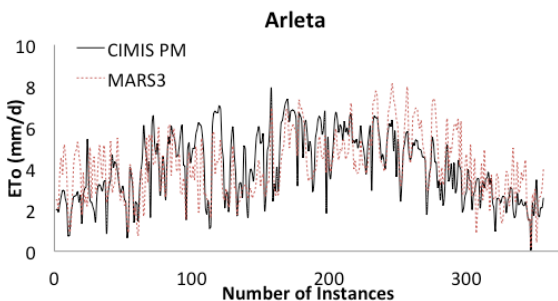
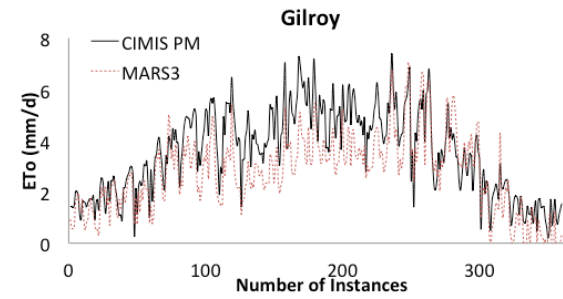
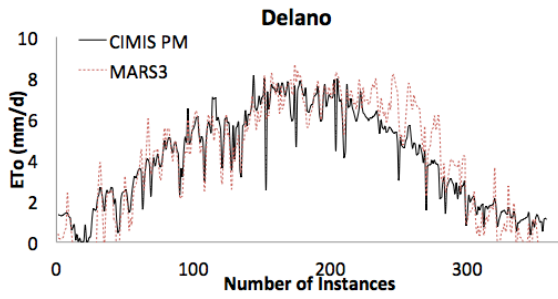
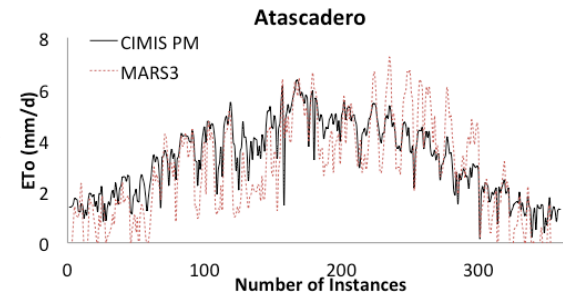
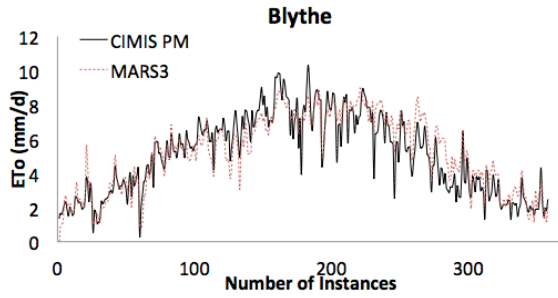
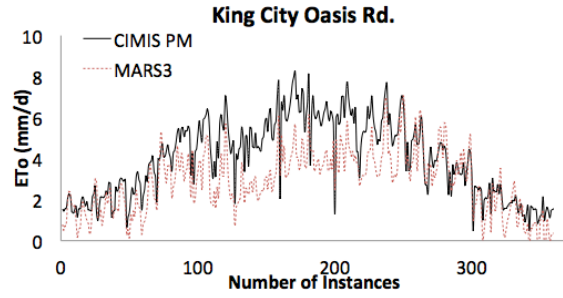
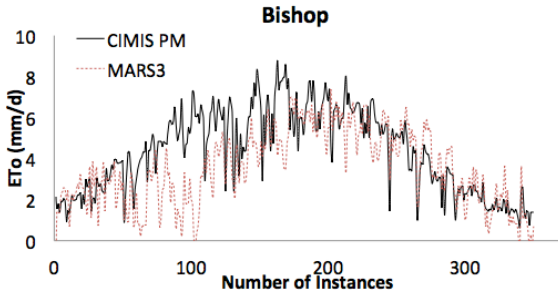


Figure 11. Time series of observed and estimated  $ET_0$  values from MARS2.





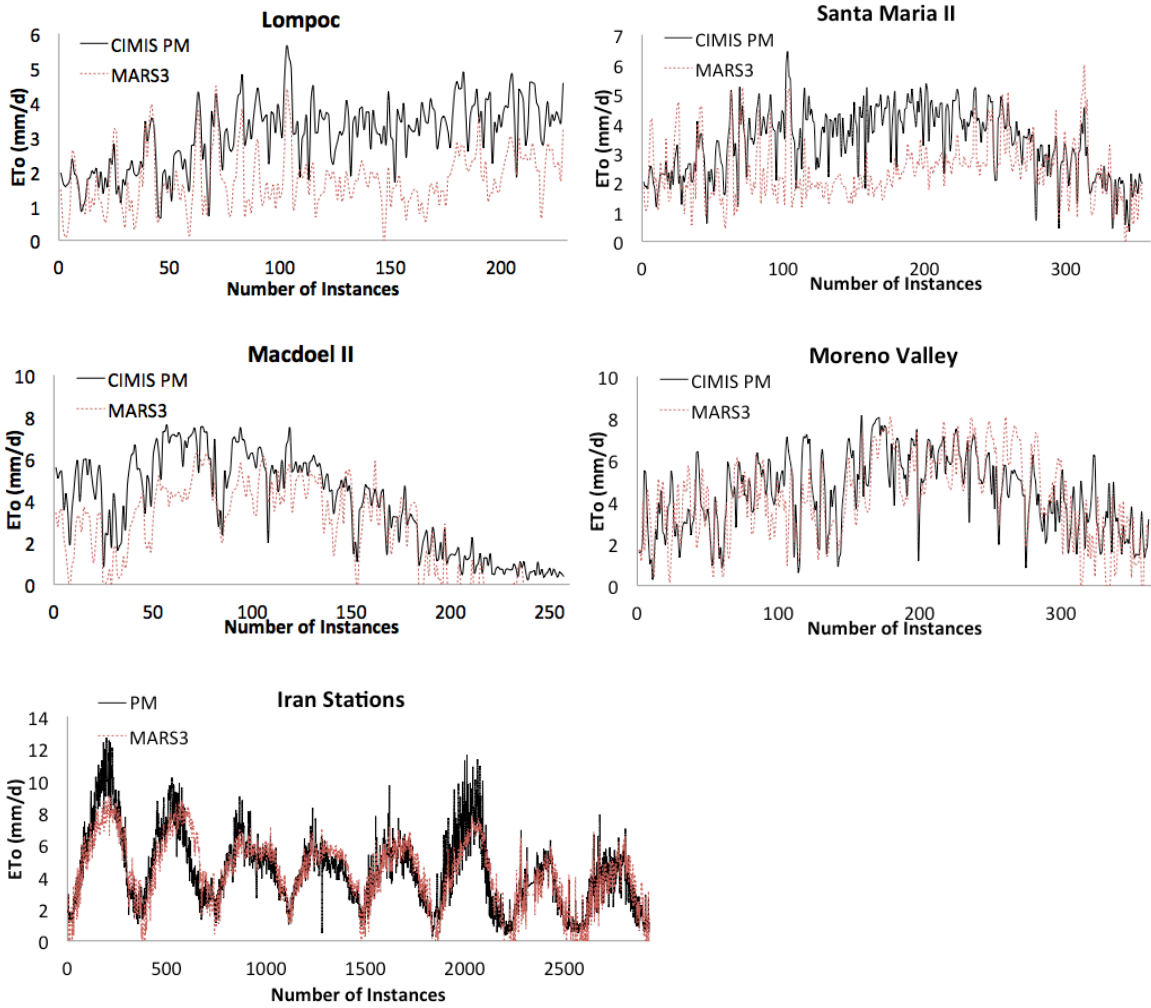
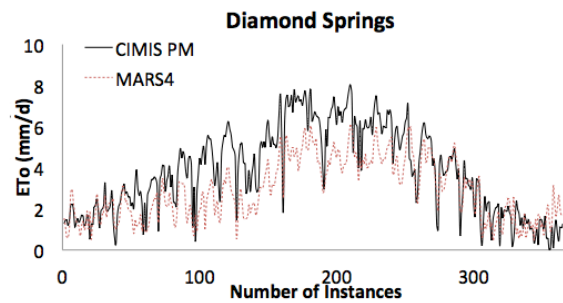
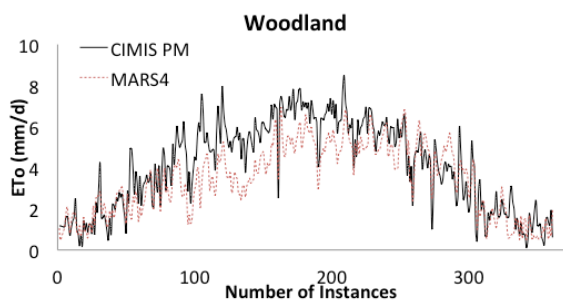
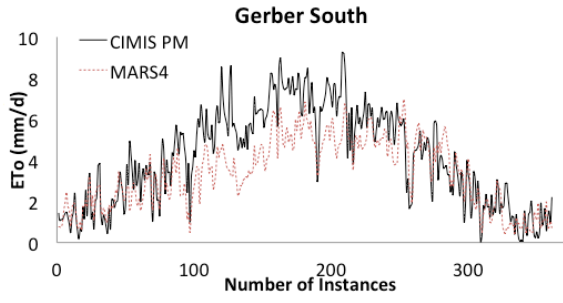
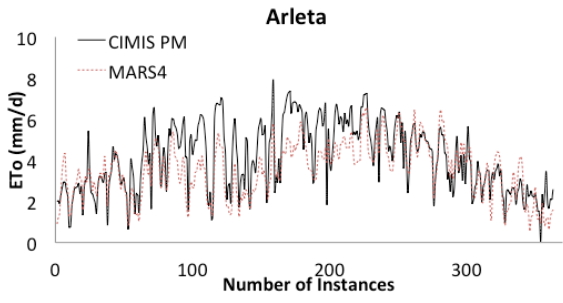
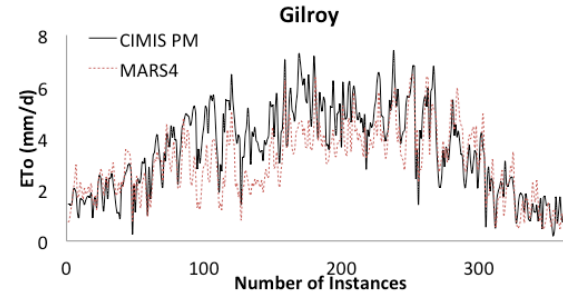
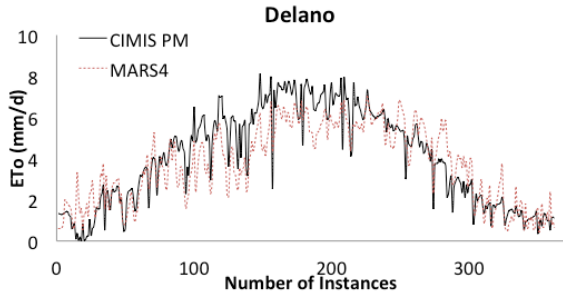
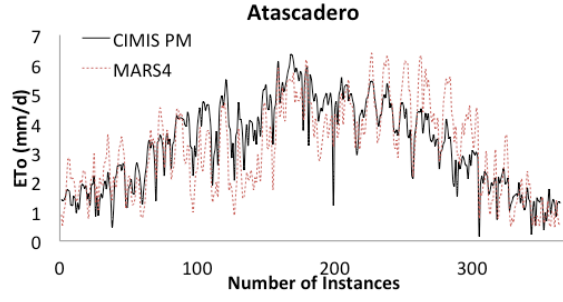
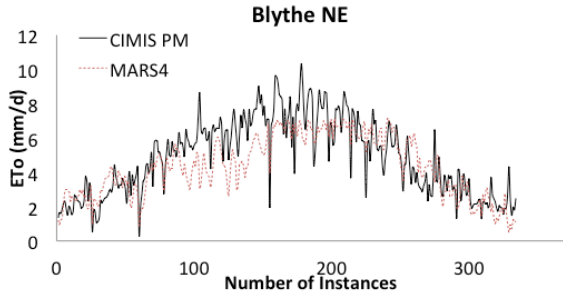
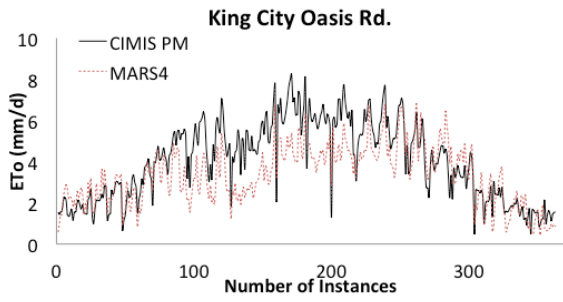
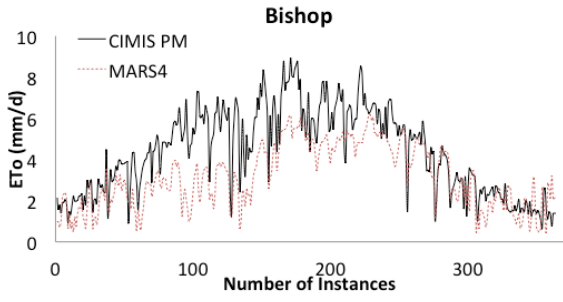


Figure 12. Time series of observed and estimated  $ET_0$  values from MARS3.



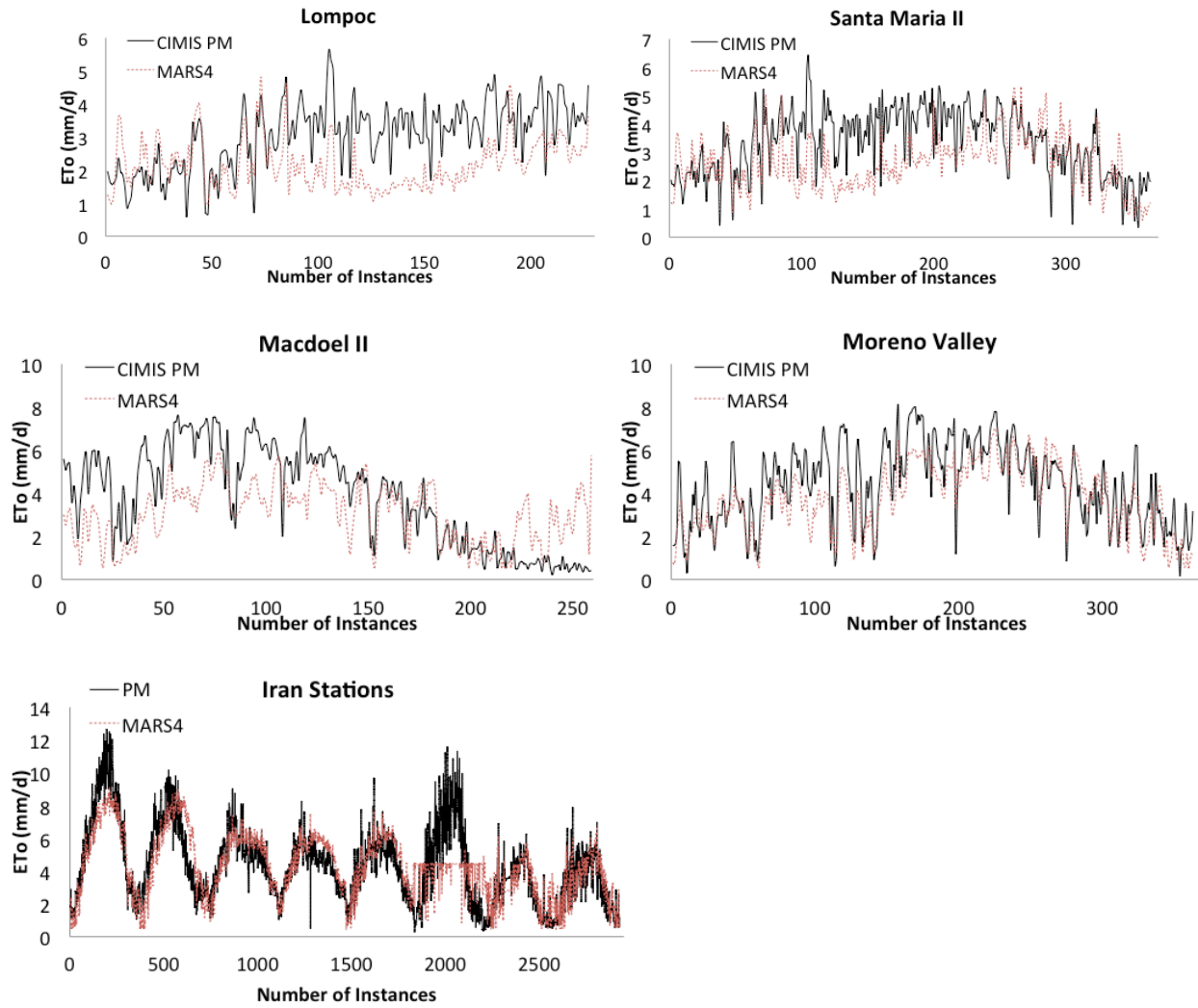


Figure 13. Time series of observed and estimated  $ET_0$  values from MARS4.

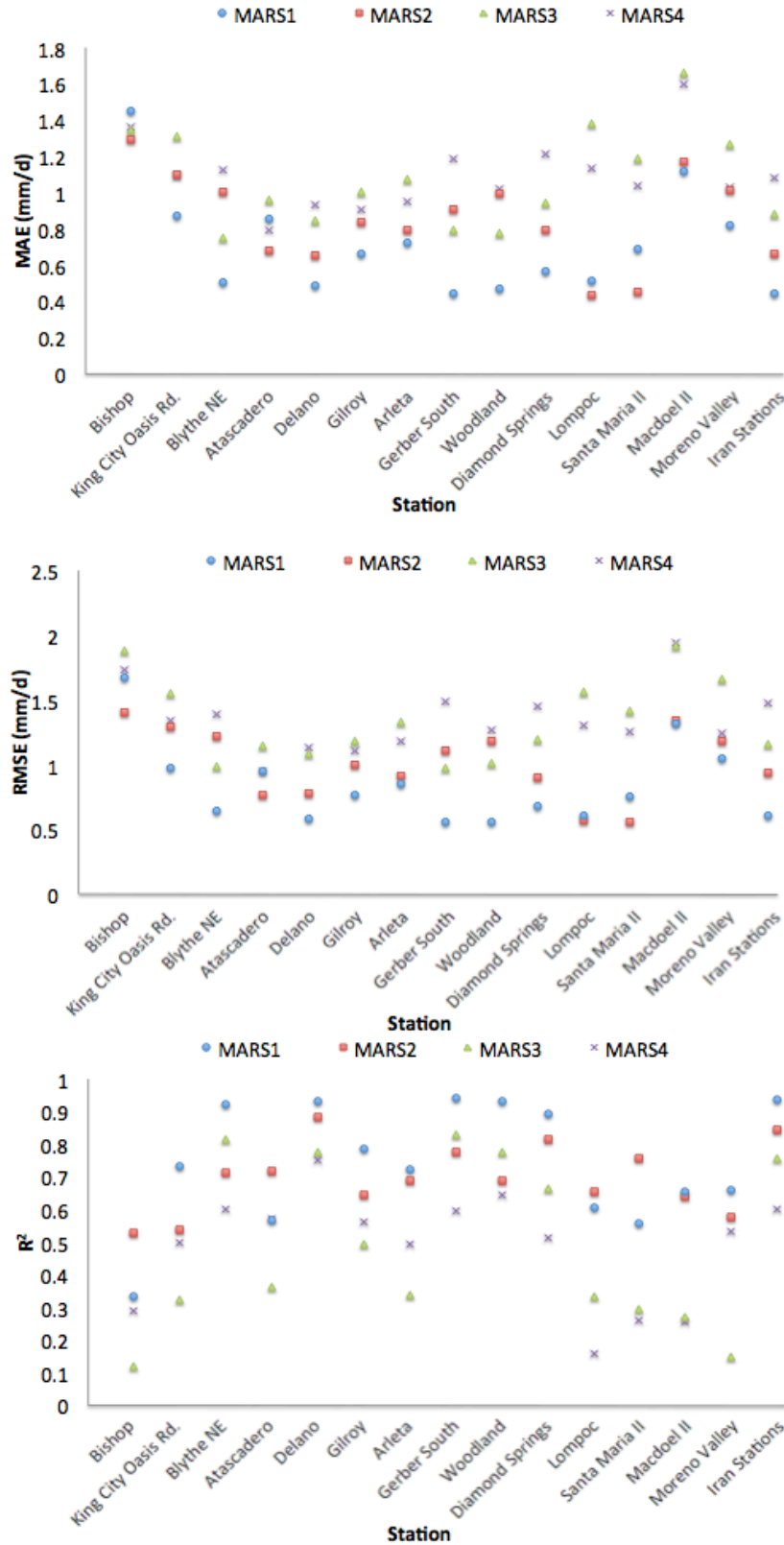


Figure 14. Comparing performance of MARS models in different stations.

Table 6. Statistical metrics of  $ET_0$  estimates from MARS1 and MARS2.

<b>Model</b>	<b>Station</b>	<b>MAE (mm/d)</b>	<b>RMSE (mm/d)</b>	<b>R<sup>2</sup></b>
MARS1	Bishop	1.45	1.67	0.33
	King City Oasis Rd.	0.87	0.98	0.73
	Blythe NE	0.50	0.64	0.92
	Atascadero	0.85	0.95	0.57
	Delano	0.49	0.59	0.93
	Gilroy	0.66	0.77	0.78
	Arleta	0.72	0.86	0.72
	Gerber South	0.44	0.56	0.94
	Woodland	0.47	0.55	0.93
	Diamond Springs	0.56	0.68	0.89
	Lompoc	0.51	0.61	0.61
	Santa Maria II	0.69	0.75	0.56
	Macdoel II	1.12	1.31	0.66
	Moreno Valley	0.82	1.05	0.66
All Iran Stations	0.44	0.60	0.93	
MARS2	Bishop	1.29	1.41	0.53
	King City Oasis Rd.	1.10	1.29	0.54
	Blythe NE	1.00	1.22	0.71
	Atascadero	0.68	0.77	0.72
	Delano	0.65	0.78	0.88
	Gilroy	0.83	0.99	0.64
	Arleta	0.79	0.92	0.69
	Gerber South	0.91	1.11	0.78
	Woodland	1.00	1.19	0.69
	Diamond Springs	0.79	0.90	0.81
	Lompoc	0.43	0.57	0.65
	Santa Maria II	0.45	0.56	0.76
	Macdoel II	1.17	1.35	0.64
	Moreno Valley	1.01	1.18	0.58
All Iran Stations	0.66	0.93	0.84	

Table 7. Statistical metrics of  $ET_0$  estimates from MARS3 and MARS4.

<b>Model</b>	<b>Station</b>	<b>MAE (mm/d)</b>	<b>RMSE (mm/d)</b>	<b>R<sup>2</sup></b>
MARS3	Bishop	1.34	1.88	0.12
	King City Oasis Rd.	1.30	1.55	0.32
	Blythe NE	0.75	0.98	0.82
	Atascadero	0.96	1.15	0.36
	Delano	0.85	1.08	0.78
	Gilroy	1.01	1.18	0.49
	Arleta	1.07	1.32	0.34
	Gerber South	0.79	0.97	0.83
	Woodland	0.77	1.00	0.78
	Diamond Springs	0.94	1.20	0.66
	Lompoc	1.38	1.56	0.33
	Santa Maria II	1.18	1.41	0.29
	Macdoel II	1.66	1.92	0.27
	Moreno Valley	1.26	1.65	0.15
All Iran Stations	0.88	1.16	0.76	
MARS4	Bishop	1.36	1.74	0.29
	King City Oasis Rd.	1.09	1.34	0.50
	Blythe NE	1.12	1.40	0.60
	Atascadero	0.79	0.95	0.57
	Delano	0.93	1.14	0.75
	Gilroy	0.90	1.11	0.56
	Arleta	0.95	1.18	0.49
	Gerber South	1.18	1.49	0.59
	Woodland	1.02	1.27	0.65
	Diamond Springs	1.22	1.46	0.51
	Lompoc	1.14	1.31	0.16
	Santa Maria II	1.04	1.25	0.26
	Macdoel II	1.59	1.94	0.25
	Moreno Valley	1.02	1.24	0.53
All Iran Stations	1.08	1.48	0.60	

## 4.2 M5MT

To create a model tree, a data mining software known as WEKA (Waikato Environment for Knowledge Analysis) was used (Frank et al., 2016). This software contained a variety of machine learning algorithms, including M5MT. To assist with the modeling process, WEKA provided percentage split, train-test, and cross validation testing options.

The percentage split option partitioned input data into training and testing datasets based on a user specified percentage. In contrast, the train-test option involved manually inputting two sets of data (i.e., training and testing) separately.

The cross validation option involved using one set of data, which was broken up by a user specified amount of folds. For example, if 10 folds were specified, the software would split up the dataset into 10 sections. The software would then utilize 9 out of the 10 sections for model training and the remaining section for testing. The testing process would be repeated until all 10 sections have been utilized for testing.

Among the three abovementioned options, the train-test method was chosen due to its superior performance compared to the other options (see Table 8).

Table 8. Performance of M5MT for different testing options.

<b>Methods</b>	<b>MAE (mm/d)</b>	<b>RMSE (mm/d)</b>	<b>R<sup>2</sup></b>
Percentage Split	0.2550	0.3422	0.9904
Train-Test	0.2328	0.3189	0.9914
Cross Validation	0.2396	0.3337	0.9906

Presented in Tables 9-12 are the model trees from M5MT1-M5MT4 (left column) and corresponding linear models (right column). To interpret results in Tables 9-12, readers are referred to Appendix A. It is worth mentioning all M5MT models successfully found a relationship between all input variables and  $ET_0$ .

Figures 15-18 show a comparison of  $ET_0$  estimates from the four M5MT models with those from the PM equation for all stations. M5MT1 and M5MT2 yielded  $ET_0$  values closer to the 1:1 line compared to M5MT3 and M5MT4. Figures 19-22 illustrate the time series of estimated  $ET_0$  from the four M5MT models. For comparison, observed  $ET_0$  values from the PM equation are also graphed on the same figures. As shown, M5MT1-M5MT3 underestimated  $ET_0$  in several California stations and M5MT4 overestimated  $ET_0$  for most of the California stations. This is mainly due to measurement errors, and also the fact that no data from the California stations was used in the training process. Nonetheless, the predicted  $ET_0$  values mirrored the daily fluctuations of the observed  $ET_0$  values.

Figure 23 compare the performance of M5MT models using  $MAE$ ,  $RMSE$ , and  $R^2$ . In all stations, M5MT1 performed the best. For California stations, average  $MAE$  of  $ET_0$  estimates from M5MT2, M5MT3, and M5MT4 were respectively 16%, 47%, and 71% greater than that of M5MT1. Also, their average  $RMSE$  values were respectively 17%, 67%, and 93% larger than that of M5MT1. For Iran stations, M5MT1 had the lowest  $MAE$  and  $RMSE$  values (0.38 mm/d and 0.55 mm/d, respectively) and the highest  $R^2$  (0.95). M5MT4 showed better results than M5MT2 and M5MT3 when tested with the Iran stations, with lower  $MAE$  (0.56 mm/d) and  $RMSE$  (0.82 mm/d), and higher  $R^2$  (0.88).



Tables 13 and 14 show the statistical metrics of  $ET_0$  estimates for the four M5MT models. The mean  $MAE$ ,  $RMSE$ , and  $R^2$  for all stations tested with M5MT1 were 0.76 mm/d, 0.94 mm/d, and 0.86, respectively. Average  $MAE$  values from all stations tested with M5MT2, M5MT3, and M5MT4 were respectively, 18%, 49%, and 70% greater than those of M5MT1. Moreover,  $RMSE$  values from all the stations tested with M5MT1 were respectively, 17%, 66%, and 89% less than those of M5MT2, M5MT3, and M5MT4.

Overall, M5MT1 outperformed M5MT2-M5MT4. The results from M5MT1 and M5MT2 tested with California stations showed M5MT to be an effective approach to estimate  $ET_0$ . The outcomes of M5MT2 also demonstrated M5MT's ability to estimate  $ET_0$  with limited climatic data. M5MT4 model performance varied depending on the location of the testing data. M5MT4 performed better than M5MT2 and M5MT3 when tested with data from Iran. While, M5MT4 provided inaccurate  $ET_0$  estimates, compared to M5MT1-M5MT3, when tested with California stations. This may suggest the inputs of M5MT4 to be region dependent.

Table 9. M5MT1 model tree and corresponding linear models.

Rs ≤ 16.271 :	LM num: 1
Tmean ≤ 19.175 :	ET <sub>0</sub> = 0.2167 * W <sub>s</sub> + 0.0057 * RHmean + 0.0523 *
Tmean ≤ 11.65 :	Tmean + 0.0668 * R <sub>s</sub> - 0.7314
W <sub>s</sub> ≤ 1.496 :	
Rs ≤ 11.945 : LM1	LM num: 2
Rs > 11.945 :	ET <sub>0</sub> = 0.2462 * W <sub>s</sub> + 0.0227 * RHmean + 0.049 *
RHmean ≤ 67.641 : LM2	Tmean + 0.1254 * R <sub>s</sub> - 2.4922
RHmean > 67.641 :	
Tmean ≤ 9.1 : LM3	LM num: 3
Tmean > 9.1 :	ET <sub>0</sub> = 0.0174 * W <sub>s</sub> - 0.0002 * RHmean + 0.0772 *
Rs ≤ 13.929 :	Tmean + 0.0423 * R <sub>s</sub> + 0.1846
RHmean ≤ 88.229 : LM4	
RHmean > 88.229 : LM5	LM num: 4
Rs > 13.929 :	ET <sub>0</sub> = -0.025 * W <sub>s</sub> + 0.0089 * RHmean + 0.047 *
Tmean ≤ 9.75 : LM6	Tmean + 0.0736 * R <sub>s</sub> - 0.5938
Tmean > 9.75 : LM7	
W <sub>s</sub> > 1.496 :	LM num: 5
RHmean ≤ 83.058 :	ET <sub>0</sub> = -0.2025 * W <sub>s</sub> + 0.0001 * RHmean + 0.047 *
Tmean ≤ 8.25 :	Tmean + 0.0736 * R <sub>s</sub> + 0.1638
W <sub>s</sub> ≤ 1.846 :	
Rs ≤ 10.086 : LM8	LM num: 6
Rs > 10.086 : LM9	ET <sub>0</sub> = 0.0174 * W <sub>s</sub> + 0.0001 * RHmean + 0.1245
W <sub>s</sub> > 1.846 :	* Tmean + 0.157 * R <sub>s</sub> - 1.7991
RHmean ≤ 65.147 :	
RHmean ≤ 56.173 :	LM num: 7
Rs ≤ 11.305 : LM10	ET <sub>0</sub> = 0.0174 * W <sub>s</sub> + 0.0001 * RHmean + 0.1006
Rs > 11.305 : LM11	* Tmean + 0.1336 * R <sub>s</sub> - 1.1001
RHmean > 56.173 :	
Rs ≤ 11.237 : LM12	LM num: 8
Rs > 11.237 : LM13	ET <sub>0</sub> = 0.0399 * W <sub>s</sub> - 0.0127 * RHmean + 0.0441 *
RHmean > 65.147 : LM14	Tmean + 0.0292 * R <sub>s</sub> + 1.3997
Tmean > 8.25 :	
RHmean ≤ 67.436 :	LM num: 9
RHmean ≤ 59.008 : LM15	ET <sub>0</sub> = 0.0399 * W <sub>s</sub> + 0.0065 * RHmean + 0.0865
RHmean > 59.008 : LM16	* Tmean + 0.0549 * R <sub>s</sub> - 0.4197
RHmean > 67.436 : LM17	
RHmean > 83.058 :	LM num: 10
Rs ≤ 6.679 : LM18	ET <sub>0</sub> = -0.0108 * W <sub>s</sub> - 0.0463 * RHmean + 0.0107
Rs > 6.679 :	* Tmean - 0.0454 * R <sub>s</sub> + 5.1093
Tmean ≤ 8.65 : LM19	
Tmean > 8.65 : LM20	LM num: 11
Tmean > 11.65 :	ET <sub>0</sub> = -0.0108 * W <sub>s</sub> - 0.0463 * RHmean + 0.0107
W <sub>s</sub> ≤ 2.127 :	* Tmean - 0.0454 * R <sub>s</sub> + 5.0685
Rs ≤ 12.346 : LM21	
Rs > 12.346 :	LM num: 12
Rs ≤ 13.707 : LM22	ET <sub>0</sub> = 0.0111 * W <sub>s</sub> - 0.0407 * RHmean + 0.0107 *
Rs > 13.707 :	Tmean - 0.0213 * R <sub>s</sub> + 4.3542
W <sub>s</sub> ≤ 0.625 : LM23	
W <sub>s</sub> > 0.625 :	LM num: 13
RHmean ≤ 80.479 :	ET <sub>0</sub> = 0.0111 * W <sub>s</sub> - 0.0407 * RHmean + 0.0107 *
W <sub>s</sub> ≤ 1.496 : LM24	Tmean - 0.0213 * R <sub>s</sub> + 4.2997
W <sub>s</sub> > 1.496 :	
Tmean ≤ 14.25 : LM25	
Tmean > 14.25 :	

Tmean ≤ 17.45 : LM26	LM num: 14
Tmean > 17.45 : LM27	$ET_0 = 0.1323 * W_s - 0.0062 * RH_{mean} + 0.0107 * T_{mean} + 0.0467 * R_s + 0.9626$
RHmean > 80.479 : LM28	
Ws > 2.127 :	
RHmean ≤ 76.486 : LM29	LM num: 15
RHmean > 76.486 : LM30	$ET_0 = 0.0545 * W_s - 0.0087 * RH_{mean} + 0.2098 * T_{mean} - 0.0576 * R_s + 1.1154$
Tmean > 19.175 :	
RHmean ≤ 15.45 : LM31	
RHmean > 15.45 :	LM num: 16
Tmean ≤ 25.45 :	$ET_0 = 0.2282 * W_s - 0.0069 * RH_{mean} + 0.0368 * T_{mean} + 0.0041 * R_s + 1.4223$
Ws ≤ 2.149 : LM32	
Ws > 2.149 :	
RHmean ≤ 74.723 : LM33	LM num: 17
RHmean > 74.723 : LM34	$ET_0 = 0.1653 * W_s - 0.0242 * RH_{mean} + 0.0474 * T_{mean} + 0.0794 * R_s + 1.7702$
Tmean > 25.45 :	
Ws ≤ 1.66 :	
Ws ≤ 0.898 :	LM num: 18
Rs ≤ 12.007 : LM35	$ET_0 = 0.0111 * W_s - 0.0029 * RH_{mean} + 0.047 * T_{mean} + 0.104 * R_s + 0.2682$
Rs > 12.007 :	
Ws ≤ 0.438 : LM36	
Ws > 0.438 :	LM num: 19
Tmean ≤ 32.65 : LM37	$ET_0 = 0.1052 * W_s - 0.0364 * RH_{mean} + 0.0153 * T_{mean} + 0.0061 * R_s + 3.8513$
Tmean > 32.65 : LM38	
Ws > 0.898 :	
Tmean ≤ 34.75 : LM39	LM num: 20
Tmean > 34.75 :	$ET_0 = 0.0171 * W_s - 0.0049 * RH_{mean} + 0.0151 * T_{mean} + 0.0061 * R_s + 1.6196$
RHmean ≤ 23.35 : LM40	
RHmean > 23.35 :	
Tmean ≤ 1010.35 : LM41	LM num: 21
Tmean > 1010.35 : LM42	$ET_0 = 0.3303 * W_s - 0.0034 * RH_{mean} + 0.0716 * T_{mean} + 0.0718 * R_s - 0.3503$
Ws > 1.66 :	
RHmean ≤ 69.19 :	
RHmean ≤ 23.9 : LM43	LM num: 22
RHmean > 23.9 :	$ET_0 = 0.3061 * W_s - 0.0004 * RH_{mean} + 0.0572 * T_{mean} + 0.0112 * R_s + 0.556$
Ws ≤ 2.999 :	
Tmean ≤ 33.25 : LM44	
Tmean > 33.25 :	LM num: 23
Tmean ≤ 1005.25 : LM45	$ET_0 = 0.2704 * W_s + 0.0136 * RH_{mean} + 0.0413 * T_{mean} + 0.2062 * R_s - 2.7158$
Tmean > 1005.25 : LM46	
Ws > 2.999 :	
Tmean ≤ 32.15 : LM47	LM num: 24
Tmean > 32.15 : LM48	$ET_0 = 0.0434 * W_s - 0.0007 * RH_{mean} + 0.0318 * T_{mean} + 0.0748 * R_s + 0.6326$
RHmean > 69.19 :	
Tmean ≤ 29.45 : LM49	
Tmean > 29.45 :	LM num: 25
RHmean ≤ 81.718 :	$ET_0 = -0.0315 * W_s - 0.0007 * RH_{mean} + 0.0202 * T_{mean} + 0.1944 * R_s - 0.7633$
Ws ≤ 5.061 : LM50	
Ws > 5.061 :	
Tmean ≤ 33.7 : LM51	LM num: 26
Tmean > 33.7 :	$ET_0 = 0.018 * W_s - 0.0007 * RH_{mean} + 0.0094 * T_{mean} + 0.0451 * R_s + 1.7517$
Tmean ≤ 35.3 : LM52	
Tmean > 35.3 : LM53	
RHmean > 81.718 : LM54	LM num: 27
Rs > 16.271 :	$ET_0 = 0.018 * W_s - 0.0007 * RH_{mean} + 0.009 * T_{mean} + 0.1149 * R_s + 0.6364$
Tmean ≤ 28.837 :	
Tmean ≤ 21.15 :	

Tmean ≤ 15.05 :	LM num: 28
Tmean ≤ 10.35 :	ET <sub>0</sub> = -0.1899 * W <sub>s</sub> - 0.024 * RHmean + 0.067 *
RHmean ≤ 75.984 : LM55	Tmean + 0.0233 * R <sub>s</sub> + 3.0864
RHmean > 75.984 : LM56	
Tmean > 10.35 :	LM num: 29
RHmean ≤ 74.45 :	ET <sub>0</sub> = 0.161 * W <sub>s</sub> - 0.0384 * RHmean + 0.0944 *
R <sub>s</sub> ≤ 19.273 : LM57	Tmean + 0.0399 * R <sub>s</sub> + 2.7531
R <sub>s</sub> > 19.273 :	
Tmean ≤ 13.15 : LM58	LM num: 30
Tmean > 13.15 :	ET <sub>0</sub> = 0.0503 * W <sub>s</sub> - 0.0366 * RHmean + 0.0768 *
RHmean ≤ 60.257 : LM59	Tmean + 0.0822 * R <sub>s</sub> + 2.8575
RHmean > 60.257 : LM60	
RHmean > 74.45 : LM61	LM num: 31
Tmean > 15.05 :	ET <sub>0</sub> = 0.2555 * W <sub>s</sub> + 0.0571 * RHmean - 0.005 *
R <sub>s</sub> ≤ 19.827 :	Tmean + 0.1768 * R <sub>s</sub> + 4.1943
W <sub>s</sub> ≤ 2.398 : LM62	
W <sub>s</sub> > 2.398 :	LM num: 32
Tmean ≤ 18.45 :	ET <sub>0</sub> = 0.267 * W <sub>s</sub> - 0.0094 * RHmean + 0.0744 *
RHmean ≤ 78.421 : LM63	Tmean + 0.1143 * R <sub>s</sub> - 0.3165
RHmean > 78.421 : LM64	
Tmean > 18.45 :	LM num: 33
RHmean ≤ 67.942 :	ET <sub>0</sub> = 0.2884 * W <sub>s</sub> - 0.0618 * RHmean + 0.1621 *
RHmean ≤ 59.788 : LM65	Tmean + 0.0723 * R <sub>s</sub> + 2.1154
RHmean > 59.788 : LM66	
RHmean > 67.942 :	LM num: 34
RHmean ≤ 77.224 : LM67	ET <sub>0</sub> = 0.1218 * W <sub>s</sub> - 0.0345 * RHmean + 0.0986 *
RHmean > 77.224 : LM68	Tmean + 0.0842 * R <sub>s</sub> + 1.9539
R <sub>s</sub> > 19.827 :	
RHmean ≤ 75.239 :	LM num: 35
Tmean ≤ 18.25 : LM69	ET <sub>0</sub> = 0.8404 * W <sub>s</sub> - 0.0054 * RHmean - 0.0008 *
Tmean > 18.25 :	Tmean + 0.2178 * R <sub>s</sub> + 0.056
RHmean ≤ 66.375 :	
R <sub>s</sub> ≤ 23.347 : LM70	LM num: 36
R <sub>s</sub> > 23.347 :	ET <sub>0</sub> = 1.1958 * W <sub>s</sub> + 0.0035 * RHmean - 0.0001 *
R <sub>s</sub> ≤ 27.03 : LM71	Tmean + 0.1544 * R <sub>s</sub> + 0.0295
R <sub>s</sub> > 27.03 : LM72	
RHmean > 66.375 : LM73	LM num: 37
RHmean > 75.239 : LM74	ET <sub>0</sub> = 0.7798 * W <sub>s</sub> - 0.0076 * RHmean + 0.0493 *
Tmean > 21.15 :	Tmean + 0.1767 * R <sub>s</sub> - 0.8888
R <sub>s</sub> ≤ 21.308 :	
W <sub>s</sub> ≤ 2.668 :	LM num: 38
Tmean ≤ 26.15 :	ET <sub>0</sub> = 0.5212 * W <sub>s</sub> - 0.0095 * RHmean - 0.0009 *
R <sub>s</sub> ≤ 19.202 :	Tmean + 0.2822 * R <sub>s</sub> - 0.3013
W <sub>s</sub> ≤ 1.66 : LM75	
W <sub>s</sub> > 1.66 : LM76	LM num: 39
R <sub>s</sub> > 19.202 :	ET <sub>0</sub> = 0.6783 * W <sub>s</sub> - 0.0206 * RHmean + 0.0855 *
W <sub>s</sub> ≤ 1.496 :	Tmean + 0.1554 * R <sub>s</sub> - 0.7063
R <sub>s</sub> ≤ 19.854 : LM77	
R <sub>s</sub> > 19.854 : LM78	LM num: 40
W <sub>s</sub> > 1.496 :	ET <sub>0</sub> = 0.7511 * W <sub>s</sub> + 0.0322 * RHmean - 0.0002 *
RHmean ≤ 82.145 : LM79	Tmean + 0.2172 * R <sub>s</sub> - 1.3302
RHmean > 82.145 : LM80	
Tmean > 26.15 : LM81	LM num: 41
W <sub>s</sub> > 2.668 : LM82	ET <sub>0</sub> = 0.9783 * W <sub>s</sub> + 0.0433 * RHmean + 0.0008
R <sub>s</sub> > 21.308 :	* Tmean + 0.3786 * R <sub>s</sub> - 4.775
RHmean ≤ 70.957 :	

Tmean ≤ 26.288 : LM83	LM num: 42
Tmean > 26.288 : LM84	ET <sub>0</sub> = 0.6124 * W <sub>s</sub> + 0.0428 * RHmean + 0.0002
RHmean > 70.957 :	* Tmean + 0.2783 * R <sub>s</sub> - 2.2927
RHmean ≤ 78.741 :	
Ws ≤ 2.55 :	LM num: 43
Tmean ≤ 24.55 : LM85	ET <sub>0</sub> = 0.4624 * W <sub>s</sub> + 0.0703 * RHmean - 0 *
Tmean > 24.55 : LM86	Tmean + 0.237 * R <sub>s</sub> - 2.0476
Ws > 2.55 : LM87	
RHmean > 78.741 : LM88	LM num: 44
Tmean > 28.837 :	ET <sub>0</sub> = 0.7394 * W <sub>s</sub> - 0.0112 * RHmean + 0.0922 *
RHmean ≤ 71.067 :	Tmean + 0.2297 * R <sub>s</sub> - 2.3566
Ws ≤ 4.171 :	
Rs ≤ 22.693 :	LM num: 45
RHmean ≤ 22 : LM89	ET <sub>0</sub> = 0.7531 * W <sub>s</sub> + 0.0445 * RHmean + 0.0007
RHmean > 22 :	* Tmean + 0.4069 * R <sub>s</sub> - 4.7047
Ws ≤ 2.263 :	
Ws ≤ 1.389 :	LM num: 46
Tmean ≤ 31.05 :	ET <sub>0</sub> = 0.6017 * W <sub>s</sub> + 0.0852 * RHmean + 0.0001
Ws ≤ 0.58 : LM90	* Tmean + 0.2535 * R <sub>s</sub> - 2.7791
Ws > 0.58 :	
RHmean ≤ 64.179 : LM91	LM num: 47
RHmean > 64.179 : LM92	ET <sub>0</sub> = 0.3706 * W <sub>s</sub> - 0.0487 * RHmean + 0.0918 *
Tmean > 31.05 :	Tmean + 0.1721 * R <sub>s</sub> + 1.9976
RHmean ≤ 30.05 : LM93	
RHmean > 30.05 :	LM num: 48
Tmean ≤ 32.1 : LM94	ET <sub>0</sub> = 0.5979 * W <sub>s</sub> + 0.0523 * RHmean + 0.0006
Tmean > 32.1 : LM95	* Tmean + 0.3101 * R <sub>s</sub> - 3.2486
Ws > 1.389 :	
Tmean ≤ 31.65 : LM96	LM num: 49
Tmean > 31.65 :	ET <sub>0</sub> = 0.219 * W <sub>s</sub> - 0.0398 * RHmean + 0.0967 *
RHmean ≤ 29.45 : LM97	Tmean + 0.0755 * R <sub>s</sub> + 2.3572
RHmean > 29.45 : LM98	
Ws > 2.263 :	LM num: 50
RHmean ≤ 27.95 : LM99	ET <sub>0</sub> = 0.2434 * W <sub>s</sub> - 0.0577 * RHmean + 0.1472 *
RHmean > 27.95 :	Tmean + 0.066 * R <sub>s</sub> + 2.4549
Tmean ≤ 33.15 : LM100	
Tmean > 33.15 :	LM num: 51
RHmean ≤ 55.235 : LM101	ET <sub>0</sub> = -0.0261 * W <sub>s</sub> - 0.0626 * RHmean + 0.1712
RHmean > 55.235 : LM102	* Tmean + 0.0201 * R <sub>s</sub> + 4.5152
Rs > 22.693 :	
Tmean ≤ 32.05 :	LM num: 52
RHmean ≤ 62.829 : LM103	ET <sub>0</sub> = 0.013 * W <sub>s</sub> - 0.0635 * RHmean + 0.303 *
RHmean > 62.829 : LM104	Tmean + 0.0201 * R <sub>s</sub> + 0.1058
Tmean > 32.05 :	
RHmean ≤ 27.75 : LM105	LM num: 53
RHmean > 27.75 :	ET <sub>0</sub> = 0.013 * W <sub>s</sub> - 0.0541 * RHmean + 0.3177 *
Tmean ≤ 35.05 :	Tmean + 0.0201 * R <sub>s</sub> - 1.0526
RHmean ≤ 64.141 :	
Ws ≤ 1.988 : LM106	LM num: 54
Ws > 1.988 :	ET <sub>0</sub> = 0.1058 * W <sub>s</sub> - 0.0645 * RHmean + 0.1375 *
Rs ≤ 24.46 : LM107	Tmean + 0.1678 * R <sub>s</sub> + 2.2579
Rs > 24.46 : LM108	
RHmean > 64.141 : LM109	LM num: 55
Tmean > 35.05 :	ET <sub>0</sub> = 0.0133 * W <sub>s</sub> + 0.0123 * RHmean + 0.1286
Ws ≤ 2.398 :	* Tmean + 0.067 * R <sub>s</sub> - 1.0262
Rs ≤ 25.646 :	

<p> <math>RH_{mean} \leq 51.456</math> : LM110  <math>RH_{mean} &gt; 51.456</math> : LM111  <math>Rs &gt; 25.646</math> :  <math>Ws \leq 1.496</math> : LM112  <math>Ws &gt; 1.496</math> :  <math>RH_{mean} \leq 52.578</math> :  <math>RH_{mean} \leq 31.3</math> :  <math>Rs \leq 28.414</math> : LM113  <math>Rs &gt; 28.414</math> : LM114  <math>RH_{mean} &gt; 31.3</math> : LM115  <math>RH_{mean} &gt; 52.578</math> :  <math>T_{mean} \leq 36.85</math> : LM116  <math>T_{mean} &gt; 36.85</math> : LM117  <math>Ws &gt; 2.398</math> :  <math>Rs \leq 27.227</math> :  <math>RH_{mean} \leq 30.6</math> : LM118  <math>RH_{mean} &gt; 30.6</math> :  <math>T_{mean} \leq 36.45</math> :  <math>RH_{mean} \leq 64.476</math> : LM119  <math>RH_{mean} &gt; 64.476</math> : LM120  <math>T_{mean} &gt; 36.45</math> :  <math>Rs \leq 24.248</math> :  <math>Ws \leq 2.974</math> :  <math>Rs \leq 23.444</math> : LM121  <math>Rs &gt; 23.444</math> : LM122  <math>Ws &gt; 2.974</math> :  <math>T_{mean} \leq 38.05</math> :  <math>RH_{mean} \leq 61.445</math> : LM123  <math>RH_{mean} &gt; 61.445</math> : LM124  <math>T_{mean} &gt; 38.05</math> : LM125  <math>Rs &gt; 24.248</math> :  <math>Ws \leq 3.266</math> :  <math>T_{mean} \leq 37.55</math> : LM126  <math>T_{mean} &gt; 37.55</math> : LM127  <math>Ws &gt; 3.266</math> :  <math>T_{mean} \leq 37.75</math> : LM128  <math>T_{mean} &gt; 37.75</math> : LM129  <math>Rs &gt; 27.227</math> :  <math>RH_{mean} \leq 62.978</math> :  <math>RH_{mean} \leq 53.18</math> : LM130  <math>RH_{mean} &gt; 53.18</math> : LM131  <math>RH_{mean} &gt; 62.978</math> : LM132  <math>Ws &gt; 4.171</math> :  <math>T_{mean} \leq 33.35</math> : LM133  <math>T_{mean} &gt; 33.35</math> :  <math>Rs \leq 23.814</math> :  <math>RH_{mean} \leq 27.25</math> : LM134  <math>RH_{mean} &gt; 27.25</math> :  <math>Ws \leq 5.415</math> :  <math>Rs \leq 19.656</math> :  <math>RH_{mean} \leq 30.05</math> :  <math>T_{mean} \leq 1012.6</math> : LM135  <math>T_{mean} &gt; 1012.6</math> : LM136  <math>RH_{mean} &gt; 30.05</math> :  <math>T_{mean} \leq 37</math> :  <math>RH_{mean} \leq 66.567</math> : LM137 </p>	<p> LM num: 56  <math>ET_0 = -0.113 * W_s - 0.0373 * RH_{mean} + 0.065 * T_{mean} + 0.0107 * R_s + 4.1903</math>   LM num: 57  <math>ET_0 = 0.1103 * W_s + 0.0218 * RH_{mean} + 0.1029 * T_{mean} + 0.1756 * R_s - 3.3612</math>   LM num: 58  <math>ET_0 = 0.102 * W_s + 0.0146 * RH_{mean} + 0.1241 * T_{mean} + 0.0225 * R_s - 0.0746</math>   LM num: 59  <math>ET_0 = -0.11 * W_s + 0.0081 * RH_{mean} + 0.0363 * T_{mean} + 0.1703 * R_s - 1.4371</math>   LM num: 60  <math>ET_0 = 0.0825 * W_s - 0.019 * RH_{mean} + 0.0363 * T_{mean} + 0.0276 * R_s + 3.4704</math>   LM num: 61  <math>ET_0 = 0.12 * W_s - 0.0665 * RH_{mean} + 0.0881 * T_{mean} - 0.0322 * R_s + 6.9019</math>   LM num: 62  <math>ET_0 = 0.1382 * W_s - 0.0021 * RH_{mean} + 0.057 * T_{mean} + 0.1808 * R_s - 1.3575</math>   LM num: 63  <math>ET_0 = 0.1033 * W_s - 0.008 * RH_{mean} + 0.0196 * T_{mean} + 0.1781 * R_s + 0.0866</math>   LM num: 64  <math>ET_0 = 0.0491 * W_s - 0.0792 * RH_{mean} + 0.1192 * T_{mean} + 0.062 * R_s + 6.1645</math>   LM num: 65  <math>ET_0 = 0.5904 * W_s - 0.0106 * RH_{mean} + 0.121 * T_{mean} + 0.1415 * R_s - 2.0452</math>   LM num: 66  <math>ET_0 = 0.2287 * W_s - 0.0106 * RH_{mean} + 0.1932 * T_{mean} + 0.2354 * R_s - 4.1627</math>   LM num: 67  <math>ET_0 = 0.1294 * W_s - 0.009 * RH_{mean} + 0.0268 * T_{mean} + 0.172 * R_s + 0.1761</math>   LM num: 68  <math>ET_0 = 0.0467 * W_s - 0.0746 * RH_{mean} + 0.0351 * T_{mean} + 0.0581 * R_s + 7.6209</math>   LM num: 69  <math>ET_0 = 0.1472 * W_s + 0.0099 * RH_{mean} + 0.0882 * T_{mean} + 0.0532 * R_s + 0.2453</math> </p>
---	--

<p> RHmean &gt; 66.567 : LM138    Tmean &gt; 37 : LM139    Rs &gt; 19.656 :      RHmean ≤ 65.868 : LM140      RHmean &gt; 65.868 : LM141      Ws &gt; 5.415 :        RHmean ≤ 61.8 : LM142        RHmean &gt; 61.8 : LM143      Rs &gt; 23.814 :        Tmean ≤ 35.95 :          RHmean ≤ 65.888 : LM144          RHmean &gt; 65.888 : LM145        Tmean &gt; 35.95 :          RHmean ≤ 54.875 :            RHmean ≤ 27.35 : LM146            RHmean &gt; 27.35 :            Ws ≤ 5.9 :              Rs ≤ 29.123 : LM147              Rs &gt; 29.123 : LM148            Ws &gt; 5.9 : LM149        RHmean &gt; 54.875 : LM150  RHmean &gt; 71.067 :      Rs ≤ 20.615 :        Rs ≤ 17.99 :          Ws ≤ 4.029 :            Ws ≤ 2.263 : LM151            Ws &gt; 2.263 : LM152          Ws &gt; 4.029 :            RHmean ≤ 81.631 :              RHmean ≤ 76.841 : LM153              RHmean &gt; 76.841 : LM154            RHmean &gt; 81.631 : LM155        Rs &gt; 17.99 :          Ws ≤ 3.343 : LM156          Ws &gt; 3.343 : LM157  Rs &gt; 20.615 :      Rs ≤ 23.848 :        Ws ≤ 2.668 :          Tmean ≤ 31.95 :            Tmean ≤ 29.85 :              Ws ≤ 2.075 : LM158              Ws &gt; 2.075 : LM159            Tmean &gt; 29.85 :              Rs ≤ 22.335 :                RHmean ≤ 79.56 :                  Ws ≤ 1.653 : LM160                  Ws &gt; 1.653 : LM161                RHmean &gt; 79.56 : LM162              Rs &gt; 22.335 : LM163            Tmean &gt; 31.95 :              RHmean ≤ 74.167 : LM164              RHmean &gt; 74.167 : LM165          Ws &gt; 2.668 :            RHmean ≤ 80.022 :              Ws ≤ 3.926 : LM166            Ws &gt; 3.926 : </p>	<p> LM num: 70  <math>ET_0 = 0.2585 * W_s - 0.0001 * RH_{mean} + 0.023 * T_{mean} + 0.026 * R_s + 2.6351</math> </p> <p> LM num: 71  <math>ET_0 = 0.1391 * W_s - 0.0027 * RH_{mean} + 0.1912 * T_{mean} + 0.0048 * R_s + 0.895</math> </p> <p> LM num: 72  <math>ET_0 = 0.04 * W_s - 0.0027 * RH_{mean} + 0.0701 * T_{mean} - 0.0126 * R_s + 3.6056</math> </p> <p> LM num: 73  <math>ET_0 = 0.0956 * W_s - 0.0372 * RH_{mean} + 0.1832 * T_{mean} + 0.0126 * R_s + 2.659</math> </p> <p> LM num: 74  <math>ET_0 = 0.0149 * W_s - 0.0911 * RH_{mean} + 0.1625 * T_{mean} - 0.0586 * R_s + 8.7415</math> </p> <p> LM num: 75  <math>ET_0 = 0.2068 * W_s + 0.0058 * RH_{mean} + 0.0754 * T_{mean} + 0.1604 * R_s - 2.0667</math> </p> <p> LM num: 76  <math>ET_0 = 0.2567 * W_s - 0.0337 * RH_{mean} + 0.0652 * T_{mean} + 0.1668 * R_s + 1.0009</math> </p> <p> LM num: 77  <math>ET_0 = 0.0831 * W_s - 0.0052 * RH_{mean} + 0.0252 * T_{mean} + 0.074 * R_s + 1.7807</math> </p> <p> LM num: 78  <math>ET_0 = 0.0733 * W_s - 0.0052 * RH_{mean} + 0.0221 * T_{mean} + 0.0601 * R_s + 2.3334</math> </p> <p> LM num: 79  <math>ET_0 = 0.0554 * W_s - 0.0098 * RH_{mean} + 0.0257 * T_{mean} + 0.206 * R_s - 0.0295</math> </p> <p> LM num: 80  <math>ET_0 = 0.0554 * W_s - 0.0986 * RH_{mean} + 0.0406 * T_{mean} + 0.0758 * R_s + 9.3159</math> </p> <p> LM num: 81  <math>ET_0 = 0.3841 * W_s - 0.0397 * RH_{mean} + 0.117 * T_{mean} + 0.1742 * R_s - 0.129</math> </p> <p> LM num: 82  <math>ET_0 = 0.2215 * W_s - 0.0565 * RH_{mean} + 0.168 * T_{mean} + 0.1601 * R_s + 0.6541</math> </p> <p> LM num: 83  <math>ET_0 = 0.1957 * W_s - 0.0409 * RH_{mean} + 0.1334 * T_{mean} + 0.063 * R_s + 2.6507</math> </p>
---	---

<p> <math>RH_{mean} \leq 73.779</math> : LM167  <math>RH_{mean} &gt; 73.779</math> :  <math>W_s \leq 5.693</math> : LM168  <math>W_s &gt; 5.693</math> :  <math>RH_{mean} \leq 74.971</math> : LM169  <math>RH_{mean} &gt; 74.971</math> : LM170  <math>RH_{mean} &gt; 80.022</math> : LM171  <math>R_s &gt; 23.848</math> : LM172 </p>	<p> LM num: 84  <math>ET_0 = 0.3402 * W_s - 0.0628 * RH_{mean} + 0.1113 * T_{mean} + 0.0844 * R_s + 3.9393</math> </p> <p> LM num: 85  <math>ET_0 = 0.0204 * W_s - 0.0565 * RH_{mean} + 0.1196 * T_{mean} + 0.0084 * R_s + 5.5466</math> </p> <p> LM num: 86  <math>ET_0 = 0.1251 * W_s - 0.0382 * RH_{mean} + 0.013 * T_{mean} + 0.0559 * R_s + 5.7266</math> </p> <p> LM num: 87  <math>ET_0 = 0.0847 * W_s - 0.0805 * RH_{mean} + 0.1937 * T_{mean} + 0.0054 * R_s + 5.6192</math> </p> <p> LM num: 88  <math>ET_0 = 0.258 * W_s - 0.1163 * RH_{mean} + 0.1343 * T_{mean} + 0.0047 * R_s + 9.4738</math> </p> <p> LM num: 89  <math>ET_0 = 0.5067 * W_s + 0.0948 * RH_{mean} - 0.017 * T_{mean} + 0.1804 * R_s + 15.5606</math> </p> <p> LM num: 90  <math>ET_0 = 1.0375 * W_s - 0.0361 * RH_{mean} + 0.0544 * T_{mean} + 0.0958 * R_s + 2.5772</math> </p> <p> LM num: 91  <math>ET_0 = 0.8072 * W_s - 0.0216 * RH_{mean} + 0.065 * T_{mean} + 0.1451 * R_s + 0.6261</math> </p> <p> LM num: 92  <math>ET_0 = 0.5511 * W_s - 0.0271 * RH_{mean} + 0.0684 * T_{mean} + 0.1631 * R_s + 0.5841</math> </p> <p> LM num: 93  <math>ET_0 = 0.876 * W_s + 0.0328 * RH_{mean} - 0.0004 * T_{mean} + 0.2212 * R_s - 1.0178</math> </p> <p> LM num: 94  <math>ET_0 = 0.8708 * W_s - 0.0033 * RH_{mean} - 0.0004 * T_{mean} + 0.2095 * R_s + 0.5698</math> </p> <p> LM num: 95  <math>ET_0 = 0.9232 * W_s - 0.013 * RH_{mean} - 0.0009 * T_{mean} + 0.1473 * R_s + 2.6076</math> </p> <p> LM num: 96  <math>ET_0 = 0.6604 * W_s - 0.0644 * RH_{mean} + 0.1063 * T_{mean} + 0.1957 * R_s + 1.1989</math> </p> <p> LM num: 97  <math>ET_0 = 0.891 * W_s + 0.0586 * RH_{mean} - 0.0005 * T_{mean} + 0.2091 * R_s - 1.2995</math> </p>
---	---



	<p>LM num: 98  <math>ET_0 = 0.9545 * W_s - 0 * RH_{mean} - 0.0005 * T_{mean} + 0.1792 * R_s + 1.1961</math></p> <p>LM num: 99  <math>ET_0 = 0.6077 * W_s + 0.1068 * RH_{mean} - 0.0247 * T_{mean} + 0.2308 * R_s + 22.145</math></p> <p>LM num: 100  <math>ET_0 = 0.5196 * W_s - 0.0834 * RH_{mean} + 0.1717 * T_{mean} + 0.2024 * R_s + 0.5766</math></p> <p>LM num: 101  <math>ET_0 = 0.6241 * W_s + 0.018 * RH_{mean} - 0.0003 * T_{mean} + 0.1982 * R_s + 0.8349</math></p> <p>LM num: 102  <math>ET_0 = 0.6998 * W_s - 0.0353 * RH_{mean} + 0.1858 * T_{mean} + 0.243 * R_s - 4.0606</math></p> <p>LM num: 103  <math>ET_0 = 0.5068 * W_s - 0.0292 * RH_{mean} + 0.1963 * T_{mean} + 0.1273 * R_s - 1.5246</math></p> <p>LM num: 104  <math>ET_0 = 0.3723 * W_s - 0.1054 * RH_{mean} + 0.2285 * T_{mean} + 0.059 * R_s + 4.1711</math></p> <p>LM num: 105  <math>ET_0 = 0.6272 * W_s + 0.1496 * RH_{mean} - 0.0002 * T_{mean} + 0.245 * R_s - 4.2355</math></p> <p>LM num: 106  <math>ET_0 = 0.6572 * W_s - 0.0159 * RH_{mean} + 0.1886 * T_{mean} + 0.2318 * R_s - 4.895</math></p> <p>LM num: 107  <math>ET_0 = 0.6852 * W_s - 0.0511 * RH_{mean} + 0.2737 * T_{mean} + 0.0593 * R_s - 1.6114</math></p> <p>LM num: 108  <math>ET_0 = 0.2844 * W_s - 0.064 * RH_{mean} + 0.2575 * T_{mean} + 0.0748 * R_s + 0.8417</math></p> <p>LM num: 109  <math>ET_0 = 0.4477 * W_s - 0.1174 * RH_{mean} + 0.1342 * T_{mean} + 0.0892 * R_s + 7.2201</math></p> <p>LM num: 110  <math>ET_0 = 0.919 * W_s + 0.0151 * RH_{mean} - 0.0007 * T_{mean} + 0.2179 * R_s + 0.2842</math></p> <p>LM num: 111  <math>ET_0 = 0.7666 * W_s - 0.0206 * RH_{mean} + 0.1461 * T_{mean} + 0.1984 * R_s - 2.3622</math></p>
--	---

	<p>LM num: 112  <math>ET_0 = 0.7622 * W_s - 0.0124 * RH_{mean} - 0.0014 * T_{mean} + 0.1568 * R_s + 3.9728</math></p>
	<p>LM num: 113  <math>ET_0 = 0.4364 * W_s + 0.0499 * RH_{mean} - 0.0015 * T_{mean} + 0.1601 * R_s + 2.7322</math></p>
	<p>LM num: 114  <math>ET_0 = 0.4364 * W_s + 0.0233 * RH_{mean} - 0.0015 * T_{mean} + 0.179 * R_s + 3.0575</math></p>
	<p>LM num: 115  <math>ET_0 = 0.5333 * W_s - 0.0266 * RH_{mean} - 0.0016 * T_{mean} + 0.1976 * R_s + 4.0839</math></p>
	<p>LM num: 116  <math>ET_0 = 0.6503 * W_s - 0.0744 * RH_{mean} + 0.1572 * T_{mean} + 0.1431 * R_s + 2.131</math></p>
	<p>LM num: 117  <math>ET_0 = 0.726 * W_s - 0.0355 * RH_{mean} + 0.1324 * T_{mean} + 0.1809 * R_s - 0.2315</math></p>
	<p>LM num: 118  <math>ET_0 = 0.7315 * W_s - 0.0197 * RH_{mean} - 0.0505 * T_{mean} + 0.2936 * R_s + 50.0822</math></p>
	<p>LM num: 119  <math>ET_0 = 0.6211 * W_s - 0.0602 * RH_{mean} + 0.1865 * T_{mean} + 0.2142 * R_s - 1.4676</math></p>
	<p>LM num: 120  <math>ET_0 = 0.3365 * W_s - 0.1772 * RH_{mean} + 0.0835 * T_{mean} + 0.1837 * R_s + 11.5674</math></p>
	<p>LM num: 121  <math>ET_0 = 0.4137 * W_s - 0.0213 * RH_{mean} - 0.001 * T_{mean} + 0.304 * R_s + 1.6544</math></p>
	<p>LM num: 122  <math>ET_0 = 0.4137 * W_s - 0.0206 * RH_{mean} - 0.001 * T_{mean} + 0.2882 * R_s + 2.0119</math></p>
	<p>LM num: 123  <math>ET_0 = 0.3953 * W_s - 0.0249 * RH_{mean} + 0.041 * T_{mean} + 0.2461 * R_s + 1.8676</math></p>
	<p>LM num: 124  <math>ET_0 = 0.3953 * W_s - 0.0269 * RH_{mean} + 0.041 * T_{mean} + 0.2356 * R_s + 2.2118</math></p>
	<p>LM num: 125  <math>ET_0 = 0.3953 * W_s - 0.0142 * RH_{mean} + 0.055 * T_{mean} + 0.212 * R_s + 1.5143</math></p>

	<p>LM num: 126  <math>ET_0 = 0.6104 * W_s - 0.0176 * RH_{mean} - 0.0011 * T_{mean} + 0.2472 * R_s + 2.2277</math></p> <p>LM num: 127  <math>ET_0 = 0.5014 * W_s - 0.008 * RH_{mean} - 0.001 * T_{mean} + 0.1791 * R_s + 3.8758</math></p> <p>LM num: 128  <math>ET_0 = 0.4234 * W_s - 0.0314 * RH_{mean} - 0.0009 * T_{mean} + 0.141 * R_s + 6.4235</math></p> <p>LM num: 129  <math>ET_0 = 0.2873 * W_s - 0.0176 * RH_{mean} - 0.0011 * T_{mean} + 0.1635 * R_s + 5.6695</math></p> <p>LM num: 130  <math>ET_0 = 0.791 * W_s - 0.007 * RH_{mean} - 0.001 * T_{mean} + 0.252 * R_s + 0.8494</math></p> <p>LM num: 131  <math>ET_0 = 0.5896 * W_s - 0.0522 * RH_{mean} + 0.1433 * T_{mean} + 0.1189 * R_s + 2.5565</math></p> <p>LM num: 132  <math>ET_0 = 0.2251 * W_s - 0.2206 * RH_{mean} + 0.2509 * T_{mean} + 0.0675 * R_s + 11.9312</math></p> <p>LM num: 133  <math>ET_0 = 0.28 * W_s - 0.132 * RH_{mean} + 0.2253 * T_{mean} + 0.1073 * R_s + 5.2344</math></p> <p>LM num: 134  <math>ET_0 = 0.4782 * W_s + 0.1608 * RH_{mean} - 0.0004 * T_{mean} + 0.2276 * R_s - 3.2895</math></p> <p>LM num: 135  <math>ET_0 = 0.4884 * W_s + 0.0527 * RH_{mean} - 0.0332 * T_{mean} + 0.0554 * R_s + 36.5765</math></p> <p>LM num: 136  <math>ET_0 = 0.3571 * W_s + 0.0835 * RH_{mean} - 0.0504 * T_{mean} + 0.0554 * R_s + 53.5042</math></p> <p>LM num: 137  <math>ET_0 = 0.4414 * W_s - 0.045 * RH_{mean} + 0.0489 * T_{mean} + 0.0554 * R_s + 6.418</math></p> <p>LM num: 138  <math>ET_0 = 0.4414 * W_s - 0.0485 * RH_{mean} + 0.0723 * T_{mean} + 0.0554 * R_s + 5.7604</math></p> <p>LM num: 139  <math>ET_0 = 0.6744 * W_s - 0.0197 * RH_{mean} - 0.001 * T_{mean} + 0.0554 * R_s + 5.6781</math></p>
--	---

	<p>LM num: 140  <math>ET_0 = 0.5315 * W_s - 0.0195 * RH_{mean} - 0.0012 * T_{mean} + 0.1101 * R_s + 5.5081</math></p>
	<p>LM num: 141  <math>ET_0 = 0.334 * W_s - 0.0348 * RH_{mean} + 0.1638 * T_{mean} + 0.049 * R_s + 2.4769</math></p>
	<p>LM num: 142  <math>ET_0 = 0.4318 * W_s - 0.0433 * RH_{mean} - 0.0017 * T_{mean} + 0.194 * R_s + 6.097</math></p>
	<p>LM num: 143  <math>ET_0 = 0.3588 * W_s - 0.0898 * RH_{mean} + 0.1942 * T_{mean} + 0.1902 * R_s + 2.1411</math></p>
	<p>LM num: 144  <math>ET_0 = 0.5453 * W_s - 0.1068 * RH_{mean} + 0.3348 * T_{mean} + 0.1179 * R_s - 1.072</math></p>
	<p>LM num: 145  <math>ET_0 = 0.5404 * W_s - 0.05 * RH_{mean} + 0.0721 * T_{mean} + 0.0446 * R_s + 5.5416</math></p>
	<p>LM num: 146  <math>ET_0 = 0.7004 * W_s + 0.171 * RH_{mean} - 0.0019 * T_{mean} + 0.218 * R_s - 2.6384</math></p>
	<p>LM num: 147  <math>ET_0 = 0.5496 * W_s - 0.021 * RH_{mean} - 0.0021 * T_{mean} + 0.1798 * R_s + 4.8873</math></p>
	<p>LM num: 148  <math>ET_0 = 0.6089 * W_s - 0.0312 * RH_{mean} - 0.0019 * T_{mean} + 0.1864 * R_s + 5.0853</math></p>
	<p>LM num: 149  <math>ET_0 = 0.6014 * W_s - 0.0207 * RH_{mean} + 0.0932 * T_{mean} + 0.1956 * R_s + 0.6233</math></p>
	<p>LM num: 150  <math>ET_0 = 0.4919 * W_s - 0.0899 * RH_{mean} + 0.2203 * T_{mean} + 0.1914 * R_s + 0.3419</math></p>
	<p>LM num: 151  <math>ET_0 = 0.276 * W_s + 0.0028 * RH_{mean} + 0.0645 * T_{mean} + 0.2458 * R_s - 2.759</math></p>
	<p>LM num: 152  <math>ET_0 = 0.1123 * W_s - 0.0461 * RH_{mean} + 0.1522 * T_{mean} + 0.1697 * R_s + 0.1263</math></p>
	<p>LM num: 153  <math>ET_0 = 0.1741 * W_s - 0.0963 * RH_{mean} + 0.236 * T_{mean} + 0.1166 * R_s + 2.2372</math></p>

	<p>LM num: 154  <math>ET_0 = 0.1133 * W_s - 0.0358 * RH_{mean} + 0.0953 * T_{mean} + 0.224 * R_s + 0.4526</math></p>
	<p>LM num: 155  <math>ET_0 = 0.129 * W_s - 0.0867 * RH_{mean} + 0.0977 * T_{mean} + 0.1845 * R_s + 5.0296</math></p>
	<p>LM num: 156  <math>ET_0 = 0.2182 * W_s - 0.0318 * RH_{mean} + 0.1415 * T_{mean} + 0.1871 * R_s - 1.2798</math></p>
	<p>LM num: 157  <math>ET_0 = 0.1192 * W_s - 0.0797 * RH_{mean} + 0.1243 * T_{mean} + 0.1793 * R_s + 3.6845</math></p>
	<p>LM num: 158  <math>ET_0 = 0.1582 * W_s - 0.0411 * RH_{mean} + 0.0575 * T_{mean} + 0.0421 * R_s + 4.9139</math></p>
	<p>LM num: 159  <math>ET_0 = 0.1947 * W_s - 0.0229 * RH_{mean} + 0.0575 * T_{mean} + 0.0906 * R_s + 2.6421</math></p>
	<p>LM num: 160  <math>ET_0 = 0.2179 * W_s - 0.0527 * RH_{mean} + 0.1239 * T_{mean} + 0.0636 * R_s + 3.4265</math></p>
	<p>LM num: 161  <math>ET_0 = 0.1829 * W_s - 0.0319 * RH_{mean} + 0.101 * T_{mean} + 0.0636 * R_s + 2.7614</math></p>
	<p>LM num: 162  <math>ET_0 = 0.1936 * W_s - 0.0911 * RH_{mean} + 0.0998 * T_{mean} + 0.0636 * R_s + 7.3623</math></p>
	<p>LM num: 163  <math>ET_0 = 0.2265 * W_s - 0.0228 * RH_{mean} + 0.1132 * T_{mean} + 0.198 * R_s - 1.3752</math></p>
	<p>LM num: 164  <math>ET_0 = 0.3288 * W_s - 0.0201 * RH_{mean} + 0.2536 * T_{mean} + 0.06 * R_s - 3.2182</math></p>
	<p>LM num: 165  <math>ET_0 = 0.1895 * W_s - 0.0316 * RH_{mean} + 0.1148 * T_{mean} + 0.1564 * R_s + 0.344</math></p>
	<p>LM num: 166  <math>ET_0 = 0.025 * W_s - 0.0633 * RH_{mean} + 0.117 * T_{mean} + 0.1582 * R_s + 3.3244</math></p>
	<p>LM num: 167  <math>ET_0 = 0.0489 * W_s - 0.0293 * RH_{mean} + 0.1146 * T_{mean} + 0.0348 * R_s + 4.0607</math></p>

	<p>LM num: 168  <math>ET_0 = 0.0448 * W_s - 0.0458 * RH_{mean} + 0.106 * T_{mean} + 0.1142 * R_s + 3.4281</math></p> <p>LM num: 169  <math>ET_0 = 0.1742 * W_s - 0.0252 * RH_{mean} + 0.2516 * T_{mean} + 0.1498 * R_s - 4.2065</math></p> <p>LM num: 170  <math>ET_0 = 0.1226 * W_s - 0.0252 * RH_{mean} + 0.0888 * T_{mean} + 0.1029 * R_s + 2.3879</math></p> <p>LM num: 171  <math>ET_0 = 0.0986 * W_s - 0.0648 * RH_{mean} + 0.1221 * T_{mean} + 0.1429 * R_s + 3.3768</math></p> <p>LM num: 172  <math>ET_0 = 0.2209 * W_s - 0.0449 * RH_{mean} + 0.1599 * T_{mean} + 0.1714 * R_s - 0.5402</math></p>
--	--

Table 10. M5MT2 model tree and corresponding linear models.

Rs ≤ 16.271 :	LM num: 1
Tmean ≤ 19.175 :	ET <sub>0</sub> = 0.055 * Tmean + 0.0452 * Rs + 0.2615
Tmean ≤ 11.05 :	
Tmean ≤ 8.55 : LM1	LM num: 2
Tmean > 8.55 :	ET <sub>0</sub> = 0.1191 * Tmean + 0.0465 * Rs - 0.3114
Rs ≤ 12.768 : LM2	
Rs > 12.768 : LM3	LM num: 3
Tmean > 11.05 : LM4	ET <sub>0</sub> = 0.1244 * Tmean + 0.1536 * Rs - 1.614
Tmean > 19.175 :	
Rs ≤ 12.217 :	LM num: 4
Tmean ≤ 1014.05 :	ET <sub>0</sub> = 0.0898 * Tmean + 0.0948 * Rs - 0.3844
Tmean ≤ 24.15 : LM5	
Tmean > 24.15 :	LM num: 5
Tmean ≤ 517.85 : LM6	ET <sub>0</sub> = 0.0907 * Tmean + 0.0095 * Rs + 0.5308
Tmean > 517.85 : LM7	
Tmean > 1014.05 :	LM num: 6
Rs ≤ 9.683 : LM8	ET <sub>0</sub> = 0.1668 * Tmean - 0.0826 * Rs - 0.102
Rs > 9.683 : LM9	
Rs > 12.217 :	LM num: 7
Tmean ≤ 29.55 : LM10	ET <sub>0</sub> = -0.0286 * Tmean + 0.25 * Rs + 28.9016
Tmean > 29.55 :	
Tmean ≤ 1011.65 :	LM num: 8
Tmean ≤ 34.35 :	ET <sub>0</sub> = -0.0245 * Tmean + 0.1368 * Rs + 25.4375
Rs ≤ 14.749 : LM11	
Rs > 14.749 : LM12	LM num: 9
Tmean > 34.35 :	ET <sub>0</sub> = -0.0545 * Tmean + 0.3132 * Rs + 54.5032
Tmean ≤ 1000.2 :	
Tmean ≤ 35.75 : LM13	LM num: 10
Tmean > 35.75 : LM14	ET <sub>0</sub> = 0.1099 * Tmean + 0.1697 * Rs - 1.8084
Tmean > 1000.2 : LM15	
Tmean > 1011.65 : LM16	LM num: 11
Rs > 16.271 :	ET <sub>0</sub> = 0.261 * Tmean + 0.0237 * Rs - 4.6786
Tmean ≤ 28.837 :	
Tmean ≤ 21.15 :	LM num: 12
Tmean ≤ 15.05 : LM17	ET <sub>0</sub> = 0.0068 * Tmean + 0.2225 * Rs + 0.698
Tmean > 15.05 :	
Rs ≤ 19.827 : LM18	LM num: 13
Rs > 19.827 :	ET <sub>0</sub> = 0.2878 * Tmean - 0.0926 * Rs - 3.5999
Tmean ≤ 18.35 : LM19	
Tmean > 18.35 :	LM num: 14
Rs ≤ 23.345 : LM20	ET <sub>0</sub> = -0.0001 * Tmean + 0.2954 * Rs + 1.6971
Rs > 23.345 : LM21	
Tmean > 21.15 :	LM num: 15
Rs ≤ 21.308 : LM22	ET <sub>0</sub> = -0.0001 * Tmean + 0.358 * Rs - 0.6375
Rs > 21.308 : LM23	
Tmean > 28.837 :	LM num: 16
Rs ≤ 23.821 :	ET <sub>0</sub> = -0.0709 * Tmean + 0.3143 * Rs + 71.2821
Tmean ≤ 35.05 :	
Rs ≤ 20.573 : LM24	LM num: 17
Rs > 20.573 : LM25	ET <sub>0</sub> = 0.1549 * Tmean + 0.0758 * Rs - 0.6739
Tmean > 35.05 :	
Tmean ≤ 1010.65 :	LM num: 18
Tmean ≤ 998.4 :	ET <sub>0</sub> = 0.1129 * Tmean + 0.1528 * Rs - 1.5611
Tmean ≤ 36.25 : LM26	

Tmean > 36.25 : LM27	LM num: 19
Tmean > 998.4 : LM28	$ET_0 = 0.0816 * Tmean + 0.007 * Rs + 2.0797$
Tmean > 1010.65 : LM29	
Rs > 23.821 :	LM num: 20
Tmean ≤ 33.362 : LM30	$ET_0 = 0.017 * Tmean + 0.0118 * Rs + 3.3481$
Tmean > 33.362 :	
Tmean ≤ 996.5 :	LM num: 21
Tmean ≤ 35.85 :	$ET_0 = 0.0177 * Tmean - 0.06 * Rs + 5.7062$
Rs ≤ 25.269 : LM31	
Rs > 25.269 : LM32	LM num: 22
Tmean > 35.85 :	$ET_0 = 0.1283 * Tmean + 0.1361 * Rs - 1.5961$
Rs ≤ 26.667 : LM33	
Rs > 26.667 :	LM num: 23
Tmean ≤ 36.65 : LM34	$ET_0 = 0.1468 * Tmean + 0.0942 * Rs - 0.9974$
Tmean > 36.65 : LM35	
Tmean > 996.5 :	LM num: 24
Tmean ≤ 1012.65 : LM36	$ET_0 = 0.0936 * Tmean + 0.2272 * Rs - 2.175$
Tmean > 1012.65 : LM37	
	LM num: 25
	$ET_0 = 0.2001 * Tmean + 0.3041 * Rs - 7.1203$
	LM num: 26
	$ET_0 = -0 * Tmean + 0.4277 * Rs - 2.3509$
	LM num: 27
	$ET_0 = -0 * Tmean + 0.2871 * Rs + 2.3509$
	LM num: 28
	$ET_0 = -0 * Tmean + 0.2247 * Rs + 1.9173$
	LM num: 29
	$ET_0 = -0.1221 * Tmean + 0.1748 * Rs + 125.6793$
	LM num: 30
	$ET_0 = 0.3013 * Tmean + 0.1504 * Rs - 6.4609$
	LM num: 31
	$ET_0 = 0.2893 * Tmean + 0.033 * Rs - 3.3114$
	LM num: 32
	$ET_0 = 0.5463 * Tmean + 0.1636 * Rs - 14.7396$
	LM num: 33
	$ET_0 = 0.3421 * Tmean + 0.2588 * Rs - 9.9582$
	LM num: 34
	$ET_0 = -0 * Tmean + 0.0182 * Rs + 9.3817$
	LM num: 35
	$ET_0 = -0 * Tmean + 0.0182 * Rs + 10.0524$
	LM num: 36
	$ET_0 = -0.0407 * Tmean + 0.2123 * Rs + 43.2007$
	LM num: 37
	$ET_0 = -0.1143 * Tmean + 0.3193 * Rs + 114.1612$



Table 11. M5MT3 model tree and corresponding linear models

Tmean ≤ 23.85 :	LM num: 1
Tmean ≤ 13.85 :	ET <sub>0</sub> = 0.1051 * Tmean - 0.0117 * RHmean + 1.3417
Tmean ≤ 10.25 :	
RHmean ≤ 83.795 : LM1	LM num: 2
RHmean > 83.795 : LM2	ET <sub>0</sub> = 0.0582 * Tmean - 0.0316 * RHmean + 3.3931
Tmean > 10.25 : LM3	
Tmean > 13.85 :	LM num: 3
Tmean ≤ 19.488 :	ET <sub>0</sub> = 0.1463 * Tmean - 0.0296 * RHmean + 2.3315
RHmean ≤ 74.667 :	
RHmean ≤ 70.126 :	LM num: 4
Tmean ≤ 18.35 : LM4	ET <sub>0</sub> = 0.1123 * Tmean - 0.0012 * RHmean + 1.1801
Tmean > 18.35 : LM5	
RHmean > 70.126 : LM6	LM num: 5
RHmean > 74.667 : LM7	ET <sub>0</sub> = 0.0105 * Tmean - 0.0469 * RHmean + 6.2457
Tmean > 19.488 :	
RHmean ≤ 72.906 : LM8	LM num: 6
RHmean > 72.906 : LM9	ET <sub>0</sub> = 0.1001 * Tmean - 0.0013 * RHmean + 1.0823
Tmean > 23.85 :	
RHmean ≤ 69.416 :	LM num: 7
RHmean ≤ 18.65 :	ET <sub>0</sub> = 0.0876 * Tmean - 0.0484 * RHmean + 4.7497
RHmean ≤ 11.55 :	
RHmean ≤ 7.75 : LM10	LM num: 8
RHmean > 7.75 : LM11	ET <sub>0</sub> = 0.184 * Tmean - 0.0374 * RHmean + 2.3942
RHmean > 11.55 : LM12	
RHmean > 18.65 :	LM num: 9
Tmean ≤ 31.85 :	ET <sub>0</sub> = 0.1588 * Tmean - 0.0546 * RHmean + 3.9712
Tmean ≤ 28.15 : LM13	
Tmean > 28.15 :	LM num: 10
RHmean ≤ 63.534 :	ET <sub>0</sub> = -0.002 * Tmean + 0.1192 * RHmean + 2.8914
RHmean ≤ 58.207 : LM14	
RHmean > 58.207 : LM15	LM num: 11
RHmean > 63.534 : LM16	ET <sub>0</sub> = -0.0393 * Tmean + 0.0066 * RHmean + 42.0496
Tmean > 31.85 :	
RHmean ≤ 30.15 : LM17	LM num: 12
RHmean > 30.15 :	ET <sub>0</sub> = -0.0766 * Tmean + 0.1929 * RHmean + 78.2035
Tmean ≤ 34.55 : LM18	
Tmean > 34.55 :	LM num: 13
RHmean ≤ 60.804 :	ET <sub>0</sub> = 0.2032 * Tmean + 0.0003 * RHmean - 0.2284
RHmean ≤ 58.384 :	
RHmean ≤ 53.392 :	LM num: 14
RHmean ≤ 31.35 : LM19	ET <sub>0</sub> = 0.0169 * Tmean + 0.006 * RHmean + 4.4895
RHmean > 31.35 :	
Tmean ≤ 36.85 : LM20	LM num: 15
Tmean > 36.85 : LM21	ET <sub>0</sub> = 0.0157 * Tmean + 0.0053 * RHmean + 5.187
RHmean > 53.392 : LM22	
RHmean > 58.384 : LM23	LM num: 16
RHmean > 60.804 : LM24	ET <sub>0</sub> = 0.3194 * Tmean - 0.1013 * RHmean + 3.2813
RHmean > 69.416 :	
Tmean ≤ 29.45 : LM25	LM num: 17
Tmean > 29.45 :	ET <sub>0</sub> = -0.1276 * Tmean + 0.1691 * RHmean + 130.7925
RHmean ≤ 80.109 :	
Tmean ≤ 31.65 : LM26	LM num: 18
Tmean > 31.65 : LM27	ET <sub>0</sub> = 0.5543 * Tmean + 0.0176 * RHmean - 12.079
RHmean > 80.109 :	

	RHmean ≤ 84.591 : LM28	LM num: 19
	RHmean > 84.591 :	ET <sub>0</sub> = -0.001 * Tmean - 0.0147 * RHmean + 8.9144
	RHmean ≤ 87.71 :	
	Tmean ≤ 34.35 :	LM num: 20
	Tmean ≤ 32.85 :	ET <sub>0</sub> = -0.001 * Tmean - 0.0147 * RHmean + 10.0672
	Tmean ≤ 31.05 : LM29	
	Tmean > 31.05 : LM30	LM num: 21
	Tmean > 32.85 : LM31	ET <sub>0</sub> = -0.001 * Tmean + 0.0393 * RHmean + 8.3204
	Tmean > 34.35 : LM32	
	RHmean > 87.71 :	LM num: 22
	Tmean ≤ 34.15 : LM33	ET <sub>0</sub> = 0.2932 * Tmean - 0.2086 * RHmean + 10.5241
	Tmean > 34.15 : LM34	
		LM num: 23
		ET <sub>0</sub> = -0.0003 * Tmean + 0.2264 * RHmean - 4.4997
		LM num: 24
		ET <sub>0</sub> = -0.0002 * Tmean - 0.0386 * RHmean + 11.1191
		LM num: 25
		ET <sub>0</sub> = 0.1596 * Tmean - 0.0872 * RHmean + 6.7334
		LM num: 26
		ET <sub>0</sub> = 0.308 * Tmean - 0.1028 * RHmean + 3.7017
		LM num: 27
		ET <sub>0</sub> = 0.2144 * Tmean - 0.1418 * RHmean + 9.7024
		LM num: 28
		ET <sub>0</sub> = 0.1908 * Tmean - 0.1033 * RHmean + 7.3385
		LM num: 29
		ET <sub>0</sub> = -0.017 * Tmean - 0.0187 * RHmean + 6.8232
		LM num: 30
		ET <sub>0</sub> = -0.0013 * Tmean - 0.0187 * RHmean + 6.0764
		LM num: 31
		ET <sub>0</sub> = 0.012 * Tmean - 0.1332 * RHmean + 15.7479
		LM num: 32
		ET <sub>0</sub> = 0.1253 * Tmean - 0.1232 * RHmean + 11.1369
		LM num: 33
		ET <sub>0</sub> = -0.0308 * Tmean - 0.1851 * RHmean + 21.6473
		LM num: 34
		ET <sub>0</sub> = 0.2421 * Tmean - 0.0438 * RHmean - 0.0308

Table 12. M5MT4 model tree and corresponding linear models.

Tmean ≤ 23.85 :	LM num: 1
Tmax ≤ 19.587 :	ET <sub>0</sub> = -0.0039 * Tmean + 0.0309 * Tmax + 0.0191 * Tmin + 0.2201 * Ra - 0.9325
Ra ≤ 7.791 : LM1	
Ra > 7.791 :	LM num: 2
Ra ≤ 12.399 : LM2	ET <sub>0</sub> = -0.0021 * Tmean + 0.0789 * Tmax + 0.0108 * Tmin + 0.1327 * Ra - 0.7615
Ra > 12.399 :	LM num: 3
Tmax ≤ 14.15 : LM3	ET <sub>0</sub> = -0.0091 * Tmean + 0.1988 * Tmax - 0.0971 * Tmin + 0.1157 * Ra - 1.3236
Tmax > 14.15 :	LM num: 4
Tmin ≤ 9.3 : LM4	ET <sub>0</sub> = -0.0051 * Tmean + 0.112 * Tmax - 0.0014 * Tmin + 0.2485 * Ra - 2.4605
Tmin > 9.3 :	LM num: 5
Tmin ≤ 12.5 : LM5	ET <sub>0</sub> = -0.0051 * Tmean + 0.1719 * Tmax - 0.0007 * Tmin + 0.0169 * Ra - 0.4506
Tmin > 12.5 : LM6	LM num: 6
Tmax > 19.587 :	ET <sub>0</sub> = -0.0051 * Tmean + 0.0289 * Tmax - 0.0007 * Tmin + 0.0169 * Ra + 2.1989
Ra ≤ 11.661 :	LM num: 7
Ra ≤ 8.569 :	ET <sub>0</sub> = -0.0005 * Tmean + 0.0862 * Tmax + 0.0005 * Tmin + 0.1569 * Ra - 1.244
Tmean ≤ 18.85 : LM7	LM num: 8
Tmean > 18.85 : LM8	ET <sub>0</sub> = 0.1201 * Tmean + 0.0091 * Tmax + 0.0017 * Tmin - 0.3511 * Ra + 2.5801
Ra > 8.569 : LM9	LM num: 9
Ra > 11.661 :	ET <sub>0</sub> = 0.2238 * Tmean + 0.0017 * Tmax - 0.1357 * Tmin + 0.2132 * Ra - 1.8172
Tmax ≤ 25.55 : LM10	LM num: 10
Tmax > 25.55 :	ET <sub>0</sub> = -0.0001 * Tmean + 0.1657 * Tmax - 0.056 * Tmin + 0.1742 * Ra - 2.0785
Ra ≤ 13.463 : LM11	LM num: 11
Ra > 13.463 :	ET <sub>0</sub> = -0.0001 * Tmean + 0.158 * Tmax - 0.0402 * Tmin + 0.261 * Ra - 3.1174
Tmax ≤ 28.325 :	LM num: 12
Tmin ≤ 15.1 :	ET <sub>0</sub> = -0.0151 * Tmean + 0.05 * Tmax + 0.0649 * Tmin + 0.0764 * Ra + 1.2339
Ra ≤ 16.043 : LM12	LM num: 13
Ra > 16.043 : LM13	ET <sub>0</sub> = -0.0151 * Tmean + 0.1279 * Tmax - 0.0018 * Tmin + 0.5828 * Ra - 7.6865
Tmin > 15.1 :	
Ra ≤ 16.527 : LM14	
Ra > 16.527 : LM15	
Tmax > 28.325 :	
Ra ≤ 15.671 : LM16	
Ra > 15.671 : LM17	
Tmean > 23.85 :	
Tmax ≤ 39.938 :	
Ra ≤ 11.752 :	
Tmin ≤ 9.25 :	
Ra ≤ 7.646 : LM18	
Ra > 7.646 : LM19	
Tmin > 9.25 :	
Ra ≤ 9.879 :	
Tmax ≤ 29.1 :	
Tmean ≤ 26.4 :	
Ra ≤ 9.265 : LM20	
Ra > 9.265 : LM21	
Tmean > 26.4 :	
Tmean ≤ 1014.85 :	
Ra ≤ 9.01 : LM22	
Ra > 9.01 :	
Tmean ≤ 1011.05 : LM23	
Tmean > 1011.05 : LM24	
Tmean > 1014.85 : LM25	
Tmax > 29.1 :	
Tmin ≤ 22.15 : LM26	

<p>           Tmin &gt; 22.15 : LM27            Ra &gt; 9.879 :            Tmax ≤ 34.55 :            Tmin ≤ 19.45 :            Tmax ≤ 0.05 : LM28            Tmax &gt; 0.05 :            Tmax ≤ 33.35 :            Ra ≤ 10.824 : LM29            Ra &gt; 10.824 : LM30            Tmax &gt; 33.35 : LM31            Tmin &gt; 19.45 : LM32            Tmax &gt; 34.55 : LM33  Ra &gt; 11.752 :            Tmax ≤ 28.35 :            Tmax ≤ 0.05 : LM34            Tmax &gt; 0.05 :            Ra ≤ 14.666 :            Tmin ≤ 2.25 : LM35            Tmin &gt; 2.25 : LM36            Ra &gt; 14.666 :            Tmax ≤ 21.1 :            Tmin ≤ 1.15 : LM37            Tmin &gt; 1.15 : LM38            Tmax &gt; 21.1 : LM39  Tmax &gt; 28.35 :            Tmax ≤ 36.487 :            Ra ≤ 14.109 :            Tmax ≤ 31.45 : LM40            Tmax &gt; 31.45 :            Tmax ≤ 35.45 : LM41            Tmax &gt; 35.45 :            Tmin ≤ 24.675 :            Ra ≤ 12.339 : LM42            Ra &gt; 12.339 : LM43            Tmin &gt; 24.675 : LM44  Ra &gt; 14.109 :            Tmax ≤ 32.15 : LM45            Tmax &gt; 32.15 :            Tmin ≤ 28.9 : LM46            Tmin &gt; 28.9 :            Ra ≤ 15.744 : LM47            Ra &gt; 15.744 :            Tmin ≤ 30.3 :            Tmax ≤ 35.3 :            Tmin ≤ 29.9 : LM48            Tmin &gt; 29.9 :            Ra ≤ 16.289 : LM49            Ra &gt; 16.289 : LM50            Tmax &gt; 35.3 : LM51            Tmin &gt; 30.3 :            Ra ≤ 16.196 : LM52            Ra &gt; 16.196 : LM53  Tmax &gt; 36.487 :            Tmin ≤ 29.35 :            Ra ≤ 14.918 :            Tmin ≤ 24.45 : LM54 </p>	<p> LM num: 14  <math>ET_0 = -0.0154 * T_{mean} + 0.192 * T_{max} - 0.0018 * T_{min} + 0.1251 * Ra - 2.3983</math>    LM num: 15  <math>ET_0 = -0.1479 * T_{mean} + 0.2579 * T_{max} - 0.0018 * T_{min} + 0.0141 * Ra + 0.2144</math>    LM num: 16  <math>ET_0 = 0.0857 * T_{mean} + 0.1059 * T_{max} - 0.0018 * T_{min} + 0.0307 * Ra - 0.7997</math>    LM num: 17  <math>ET_0 = 0.3503 * T_{mean} + 0.0337 * T_{max} - 0.3052 * T_{min} + 0.0281 * Ra + 0.5695</math>    LM num: 18  <math>ET_0 = -0.0486 * T_{mean} + 0.001 * T_{max} + 0.0812 * T_{min} + 0.3109 * Ra + 48.6714</math>    LM num: 19  <math>ET_0 = -0.0758 * T_{mean} + 0.001 * T_{max} + 0.1685 * T_{min} + 0.3623 * Ra + 75.7266</math>    LM num: 20  <math>ET_0 = 0.0003 * T_{mean} + 0.0061 * T_{max} + 0.0055 * T_{min} + 0.1567 * Ra + 1.0434</math>    LM num: 21  <math>ET_0 = 0.0003 * T_{mean} + 0.0061 * T_{max} + 0.0055 * T_{min} + 0.1714 * Ra + 1.1579</math>    LM num: 22  <math>ET_0 = -0.0047 * T_{mean} + 0.0061 * T_{max} - 0.2973 * T_{min} + 0.3694 * Ra + 7.7452</math>    LM num: 23  <math>ET_0 = -0.0051 * T_{mean} + 0.0061 * T_{max} - 0.3195 * T_{min} + 0.3951 * Ra + 8.5883</math>    LM num: 24  <math>ET_0 = -0.0051 * T_{mean} + 0.0061 * T_{max} - 0.3195 * T_{min} + 0.3951 * Ra + 8.4212</math>    LM num: 25  <math>ET_0 = -0.0365 * T_{mean} + 0.0061 * T_{max} - 0.0845 * T_{min} + 0.301 * Ra + 38.3346</math>    LM num: 26  <math>ET_0 = 0.0424 * T_{mean} + 0.0034 * T_{max} + 0.0061 * T_{min} + 0.2371 * Ra - 0.0379</math>    LM num: 27  <math>ET_0 = 0.0001 * T_{mean} + 0.0034 * T_{max} + 0.2073 * T_{min} + 0.0336 * Ra - 1.5949</math> </p>
---	--

<p>           Tmin &gt; 24.45 : LM55            Ra &gt; 14.918 :            Tmin ≤ 27.45 : LM56            Tmin &gt; 27.45 : LM57            Tmin &gt; 29.35 : LM58  Tmax &gt; 39.938 :    Ra ≤ 12.546 :      Ra ≤ 8.482 :        Ra ≤ 7.87 : LM59        Ra &gt; 7.87 : LM60      Ra &gt; 8.482 :        Tmin ≤ 28.1 : LM61        Tmin &gt; 28.1 : LM62  Ra &gt; 12.546 :    Tmax ≤ 42.55 :      Tmin ≤ 29.7 : LM63      Tmin &gt; 29.7 : LM64  Tmax &gt; 42.55 :    Ra ≤ 16.185 : LM65    Ra &gt; 16.185 :      Tmax ≤ 45.3 :        Ra ≤ 16.39 : LM66        Ra &gt; 16.39 : LM67        Tmax &gt; 45.3 : LM68 </p>	<p> LM num: 28  <math>ET_0 = -0.0748 * T_{mean} + 0.0009 * T_{max} - 0.0036 * T_{min} + 0.5039 * Ra + 75.1206</math>   LM num: 29  <math>ET_0 = 0.0001 * T_{mean} + 0.0145 * T_{max} - 0.054 * T_{min} - 0.0947 * Ra + 5.4603</math>   LM num: 30  <math>ET_0 = -0.0002 * T_{mean} + 0.0105 * T_{max} - 0.0701 * T_{min} - 0.1344 * Ra + 6.0692</math>   LM num: 31  <math>ET_0 = 0.1156 * T_{mean} + 0.0507 * T_{max} - 0.0309 * T_{min} - 0.0478 * Ra + 0.7195</math>   LM num: 32  <math>ET_0 = 0.3243 * T_{mean} + 0.0009 * T_{max} - 0.1955 * T_{min} + 0.1093 * Ra - 1.8256</math>   LM num: 33  <math>ET_0 = 0 * T_{mean} + 0.1537 * T_{max} - 0.0009 * T_{min} + 0.029 * Ra - 1.1669</math>   LM num: 34  <math>ET_0 = -0.0979 * T_{mean} + 0.0007 * T_{max} + 0.1843 * T_{min} + 0.4766 * Ra + 96.568</math>   LM num: 35  <math>ET_0 = -0.0762 * T_{mean} - 0.0368 * T_{max} + 0.0126 * T_{min} + 0.0842 * Ra + 79.3077</math>   LM num: 36  <math>ET_0 = 0.0001 * T_{mean} - 0.0106 * T_{max} - 0.0416 * T_{min} + 0.4334 * Ra - 1.147</math>   LM num: 37  <math>ET_0 = -0.0163 * T_{mean} - 0.0502 * T_{max} + 0.0549 * T_{min} + 1.3162 * Ra + 0.1336</math>   LM num: 38  <math>ET_0 = -0.1242 * T_{mean} - 0.0136 * T_{max} + 0.147 * T_{min} + 0.1487 * Ra + 128.616</math>   LM num: 39  <math>ET_0 = 0.001 * T_{mean} + 0.1975 * T_{max} + 0.0227 * T_{min} + 0.1202 * Ra - 3.8525</math>   LM num: 40  <math>ET_0 = 0.2844 * T_{mean} + 0.0201 * T_{max} - 0.282 * T_{min} + 0.5213 * Ra - 4.8537</math>   LM num: 41  <math>ET_0 = -0.0055 * T_{mean} + 0.2207 * T_{max} - 0.0975 * T_{min} + 0.0859 * Ra - 1.5875</math> </p>
---	---

	<p>LM num: 42  <math>ET_0 = -0.0136 * T_{mean} + 0.7841 * T_{max} - 0.0632 * T_{min} + 0.0141 * Ra - 20.8525</math></p> <p>LM num: 43  <math>ET_0 = -0.0136 * T_{mean} + 0.2076 * T_{max} - 0.0506 * T_{min} + 0.2595 * Ra - 4.085</math></p> <p>LM num: 44  <math>ET_0 = -0.0136 * T_{mean} + 0.1934 * T_{max} - 0.1409 * T_{min} + 0.1364 * Ra + 0.3336</math></p> <p>LM num: 45  <math>ET_0 = 0 * T_{mean} + 0.2035 * T_{max} - 0.0994 * T_{min} + 0.0074 * Ra + 0.5209</math></p> <p>LM num: 46  <math>ET_0 = 0 * T_{mean} + 0.3293 * T_{max} - 0.0974 * T_{min} + 0.2211 * Ra - 6.8822</math></p> <p>LM num: 47  <math>ET_0 = 0 * T_{mean} + 0.4095 * T_{max} - 0.253 * T_{min} + 0.1368 * Ra - 4.4634</math></p> <p>LM num: 48  <math>ET_0 = 0 * T_{mean} + 0.1253 * T_{max} - 0.0608 * T_{min} + 0.0945 * Ra + 0.7244</math></p> <p>LM num: 49  <math>ET_0 = 0 * T_{mean} + 0.1253 * T_{max} - 0.0608 * T_{min} + 0.0945 * Ra + 0.8233</math></p> <p>LM num: 50  <math>ET_0 = 0 * T_{mean} + 0.1253 * T_{max} - 0.0608 * T_{min} - 2.4711 * Ra + 42.8921</math></p> <p>LM num: 51  <math>ET_0 = 0 * T_{mean} + 0.1126 * T_{max} - 0.3299 * T_{min} + 0.0945 * Ra + 9.4554</math></p> <p>LM num: 52  <math>ET_0 = 0 * T_{mean} + 0.325 * T_{max} - 0.252 * T_{min} + 0.265 * Ra - 3.4958</math></p> <p>LM num: 53  <math>ET_0 = 0 * T_{mean} + 0.106 * T_{max} - 0.0976 * T_{min} + 1.5975 * Ra - 21.89</math></p> <p>LM num: 54  <math>ET_0 = -0.0041 * T_{mean} + 0.3827 * T_{max} + 0.0555 * T_{min} + 0.1906 * Ra - 11.7983</math></p> <p>LM num: 55  <math>ET_0 = -0.0041 * T_{mean} + 0.3576 * T_{max} - 0.0977 * T_{min} + 0.2136 * Ra - 8.0507</math></p>
--	---

	<p>LM num: 56  <math>ET_0 = -0.0041 * T_{mean} + 0.2525 * T_{max} - 0.0312 * T_{min} + 0.0171 * Ra - 2.0945</math></p> <p>LM num: 57  <math>ET_0 = 0.4947 * T_{mean} + 0.0262 * T_{max} - 0.4129 * T_{min} + 0.2685 * Ra - 3.6808</math></p> <p>LM num: 58  <math>ET_0 = -0.0055 * T_{mean} + 0.3603 * T_{max} - 0.2839 * T_{min} + 0.3018 * Ra - 3.9747</math></p> <p>LM num: 59  <math>ET_0 = 0.0048 * T_{mean} + 0.0159 * T_{max} + 0.2523 * T_{min} + 1.8181 * Ra - 16.5588</math></p> <p>LM num: 60  <math>ET_0 = 0.0003 * T_{mean} - 0.1337 * T_{max} + 0.1811 * T_{min} + 0.2034 * Ra + 5.0849</math></p> <p>LM num: 61  <math>ET_0 = -0.0001 * T_{mean} + 0.1697 * T_{max} + 0.1427 * T_{min} + 0.3542 * Ra - 8.5106</math></p> <p>LM num: 62  <math>ET_0 = -0.0001 * T_{mean} + 0.019 * T_{max} + 0.0101 * T_{min} + 0.6059 * Ra - 0.1704</math></p> <p>LM num: 63  <math>ET_0 = -0.0002 * T_{mean} + 0.4438 * T_{max} - 0.0993 * T_{min} + 0.4252 * Ra - 14.507</math></p> <p>LM num: 64  <math>ET_0 = -0.0002 * T_{mean} + 0.4729 * T_{max} - 0.2464 * T_{min} + 0.7366 * Ra - 16.6866</math></p> <p>LM num: 65  <math>ET_0 = -0.0002 * T_{mean} + 0.2871 * T_{max} - 0.0013 * T_{min} + 0.2557 * Ra - 7.6575</math></p> <p>LM num: 66  <math>ET_0 = -0.0014 * T_{mean} + 0.06 * T_{max} - 0.075 * T_{min} + 0.7214 * Ra - 2.9764</math></p> <p>LM num: 67  <math>ET_0 = -0.0037 * T_{mean} + 0.0547 * T_{max} + 0.1074 * T_{min} - 4.0612 * Ra + 71.9315</math></p> <p>LM num: 68  <math>ET_0 = -0.0005 * T_{mean} + 0.1471 * T_{max} + 0.0922 * T_{min} + 1.7732 * Ra - 27.6132</math></p>
--	---

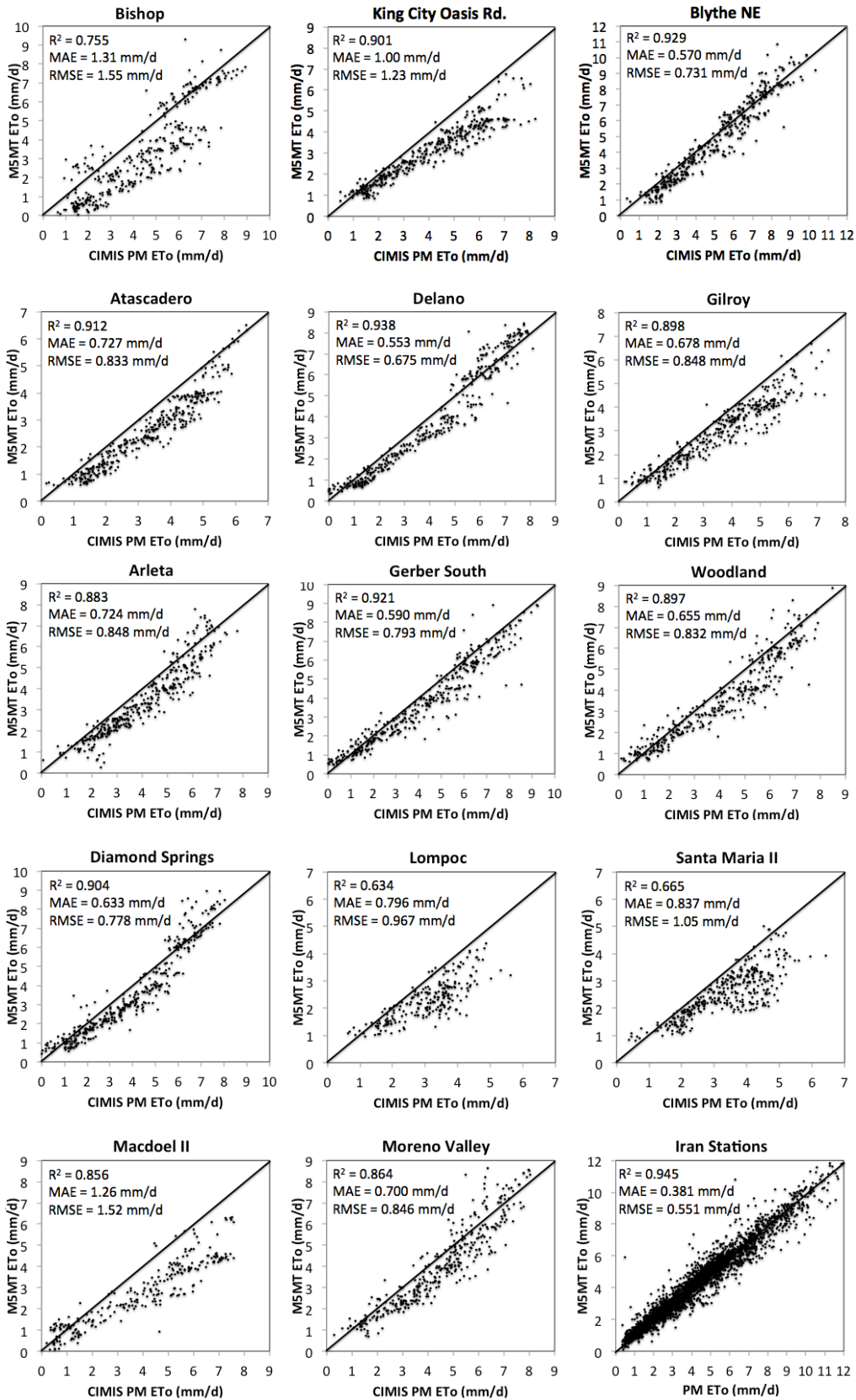


Figure 15. Estimated  $ET_0$  values from M5MT1 versus observations.



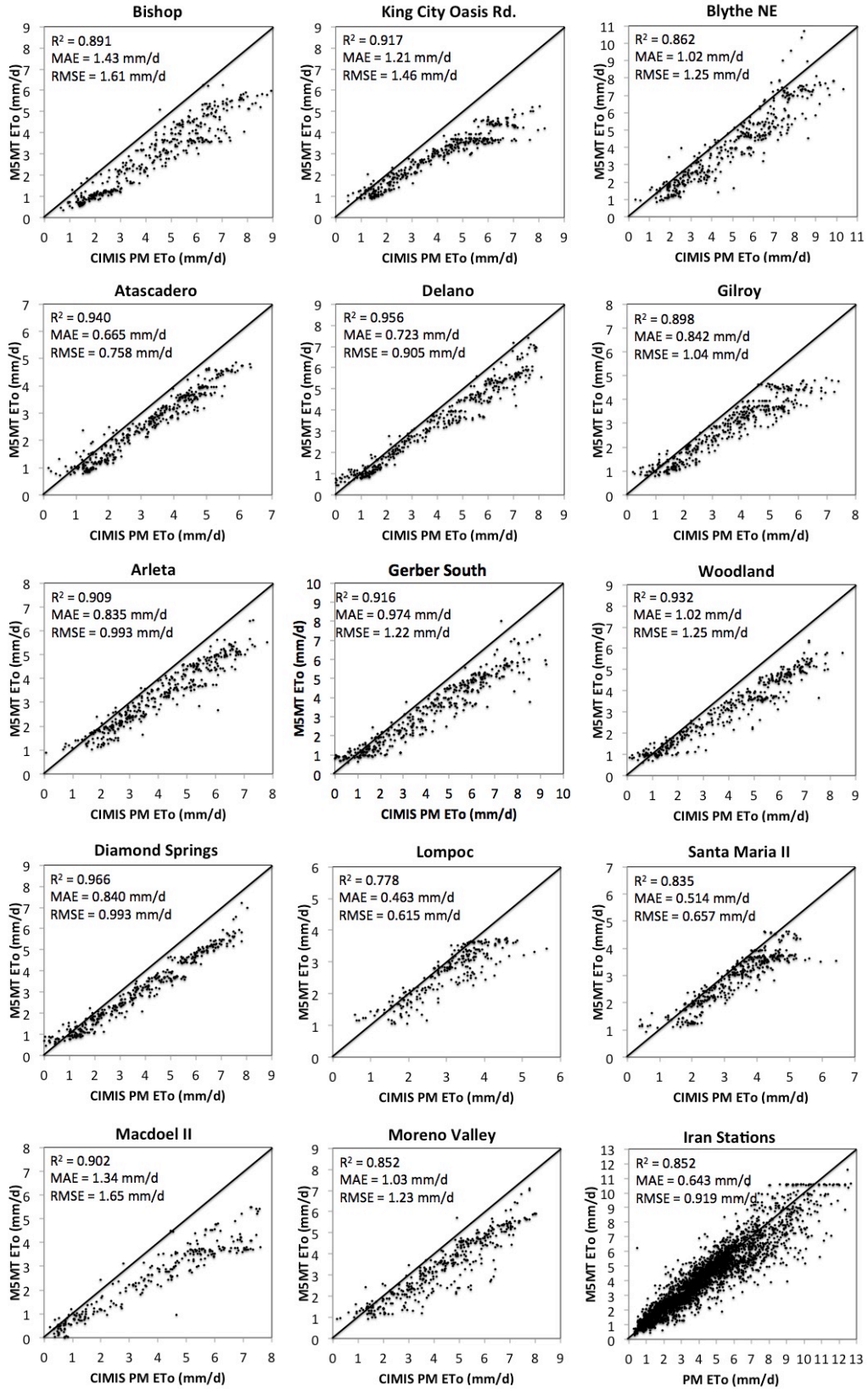


Figure 16. Estimated  $ET_0$  values from M5MT2 versus observations.

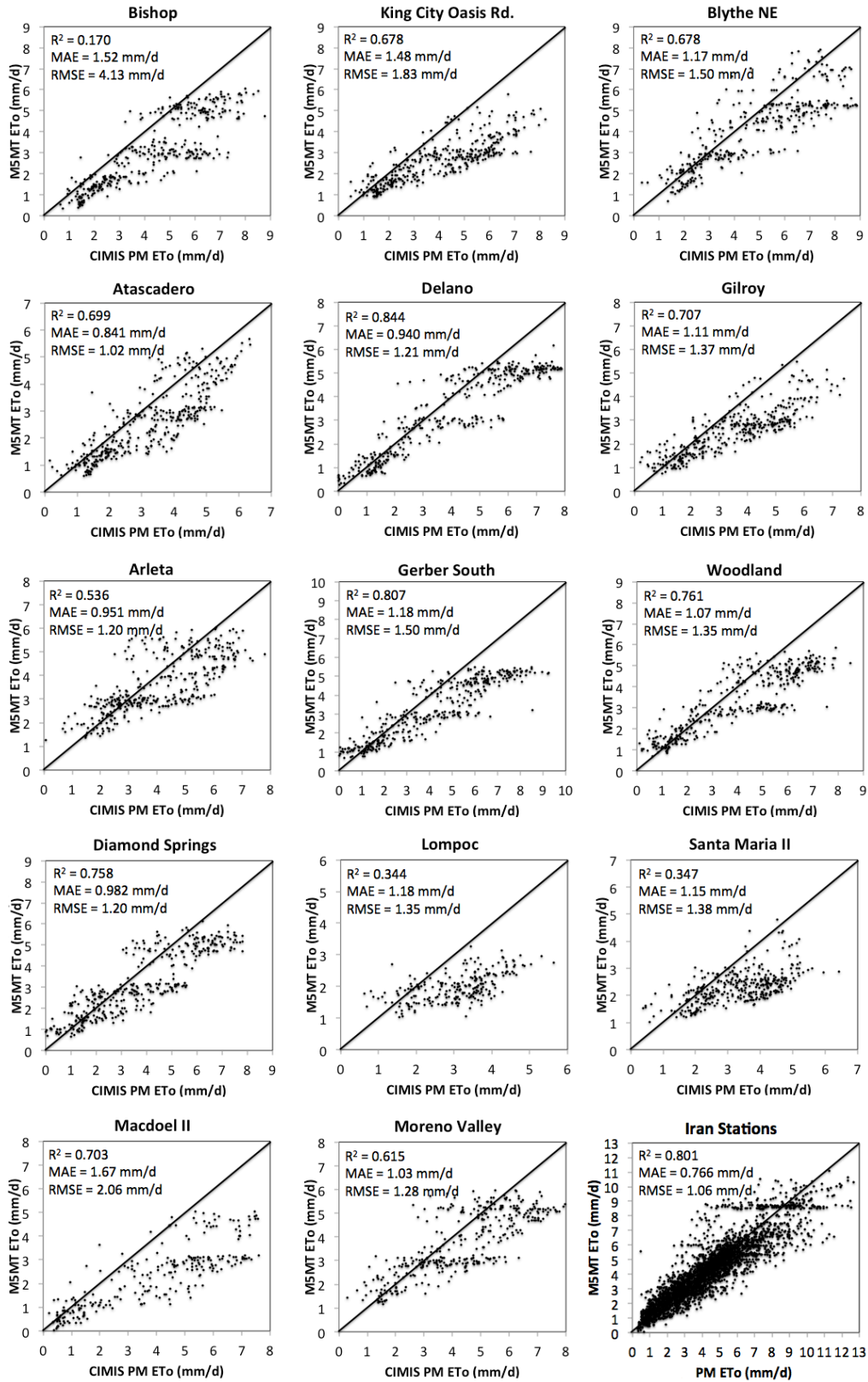


Figure 17. Estimated  $ET_0$  values from M5MT3 versus observations.

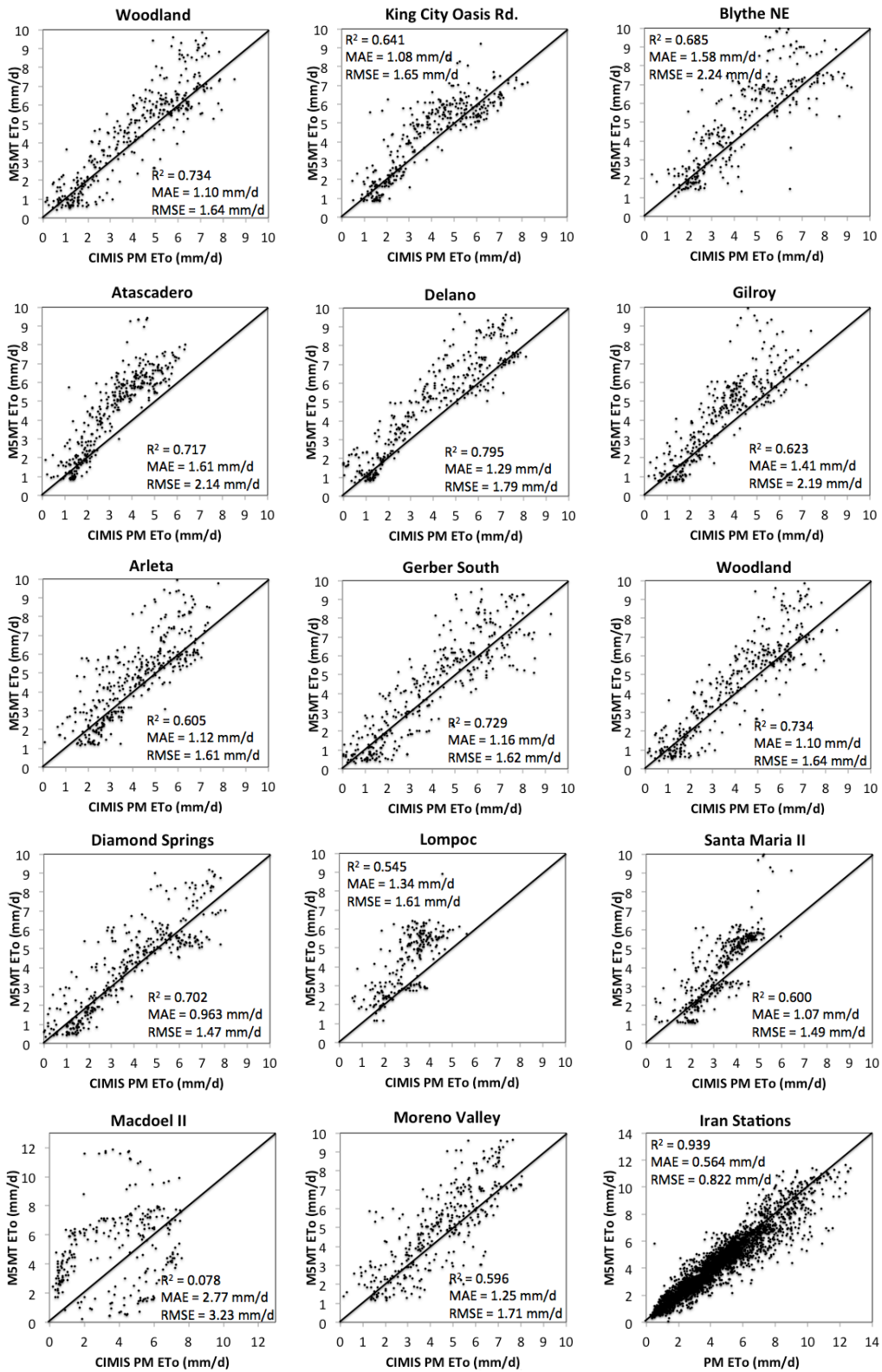
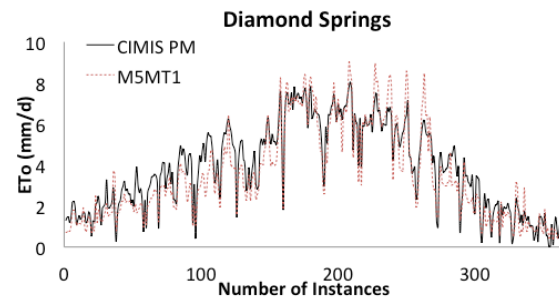
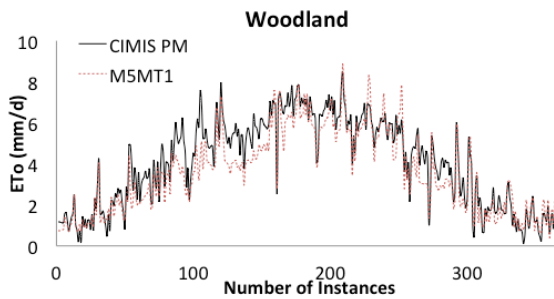
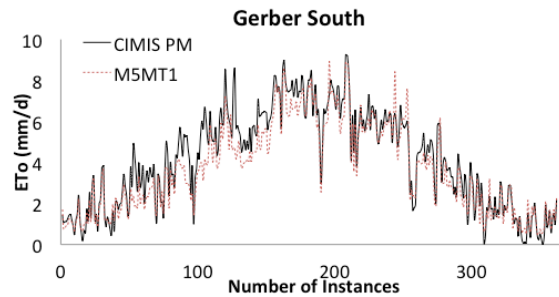
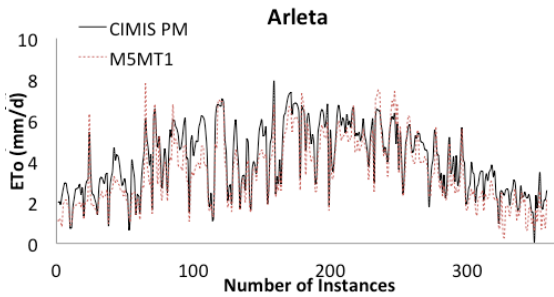
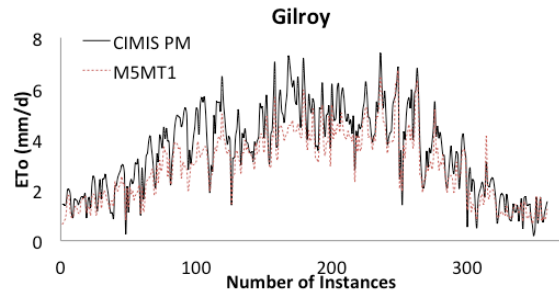
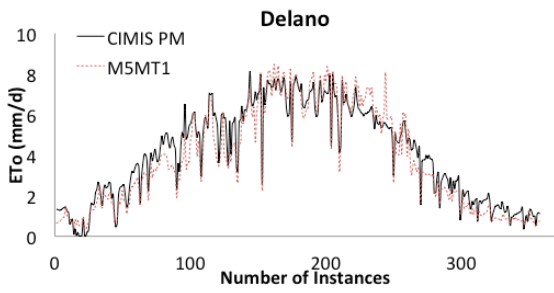
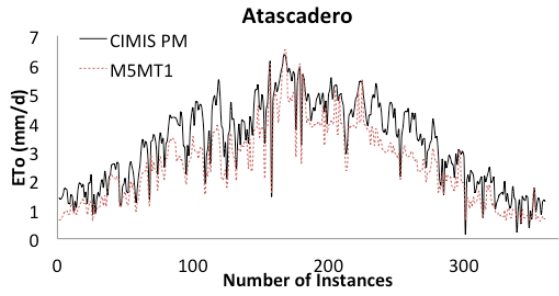
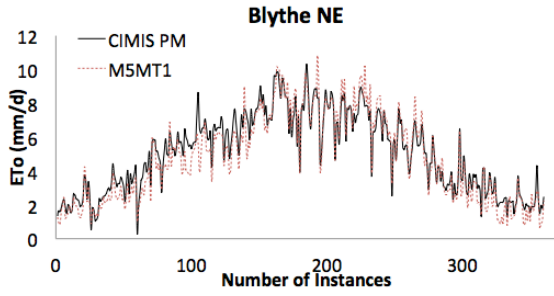
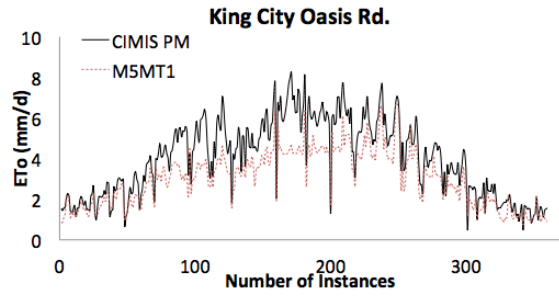
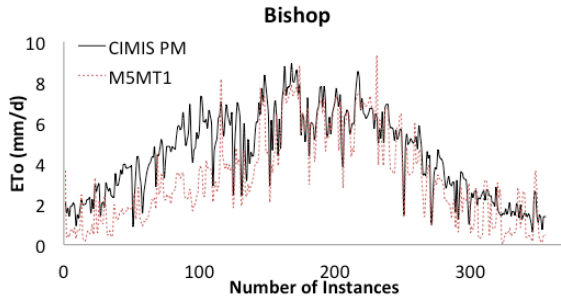


Figure 18. Estimated  $ET_0$  values from M5MT4 versus observations.



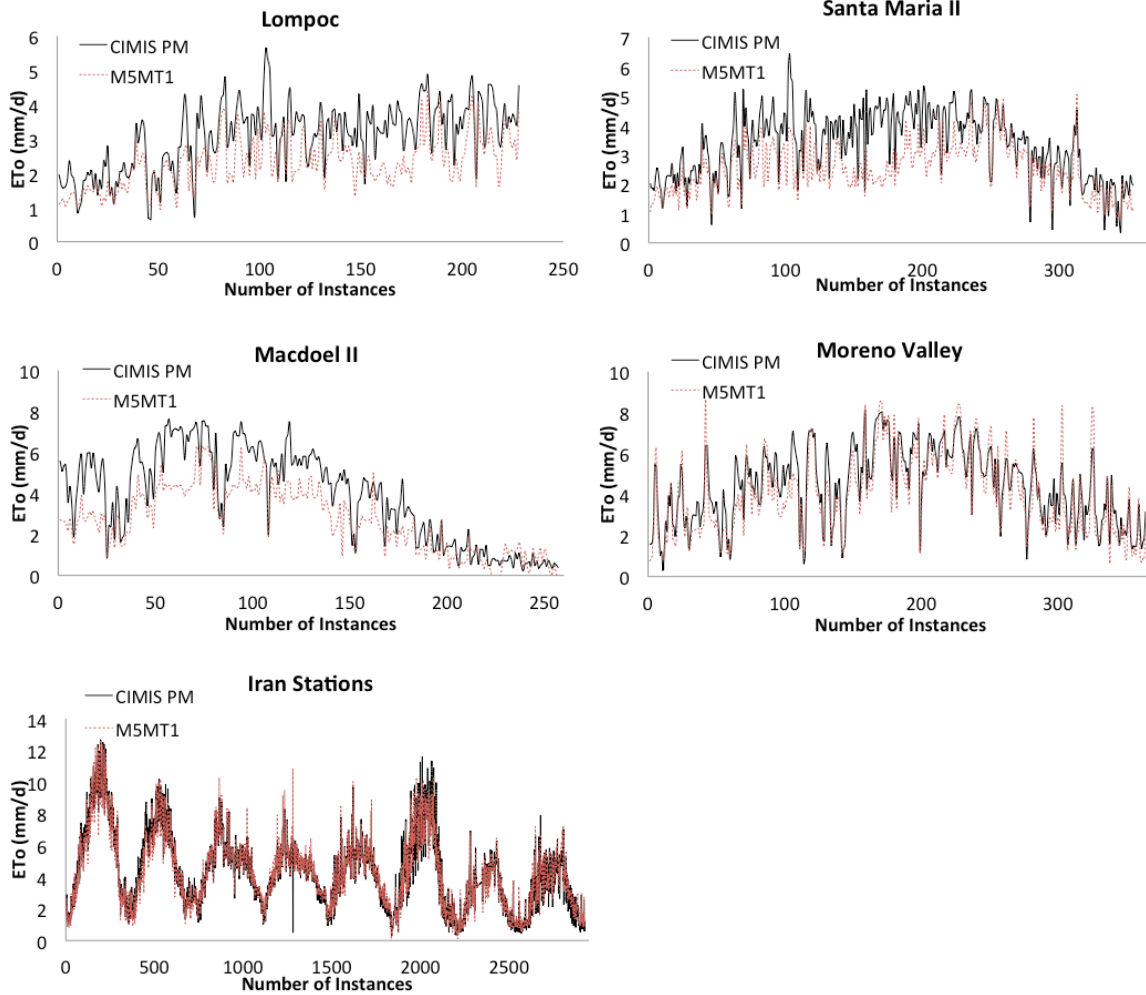
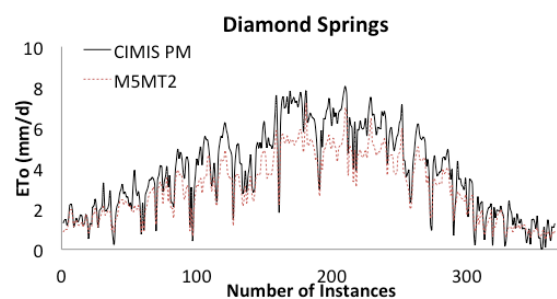
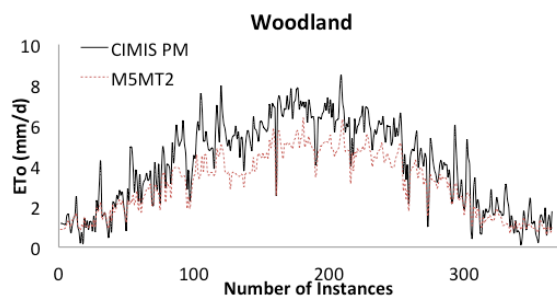
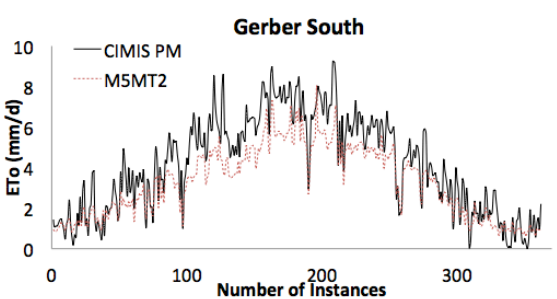
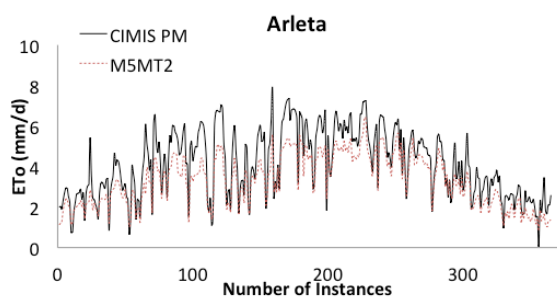
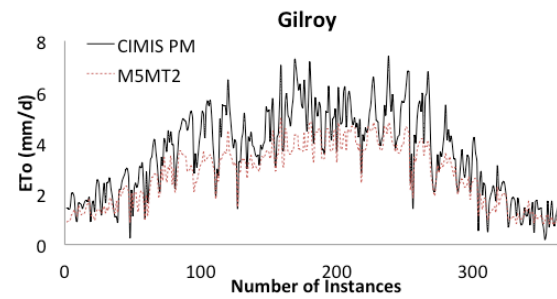
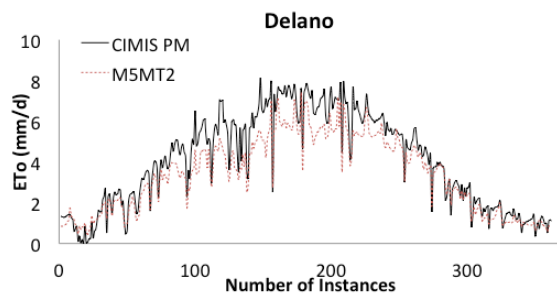
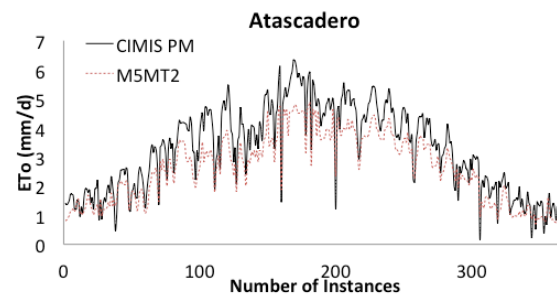
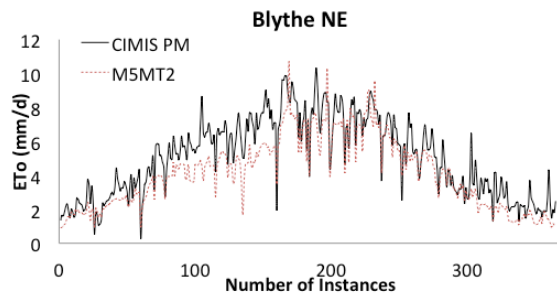
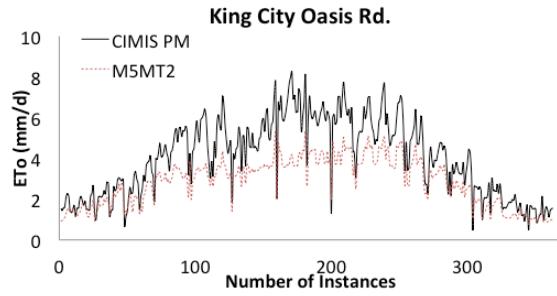
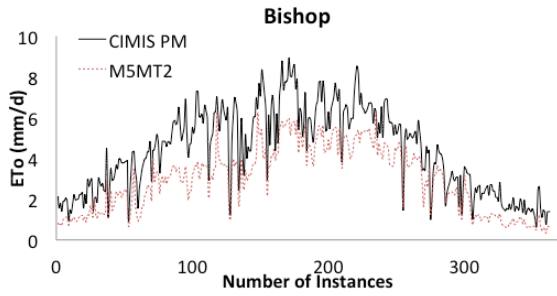


Figure 19. Time series of observed and estimated  $ET_0$  values from M5MT1.



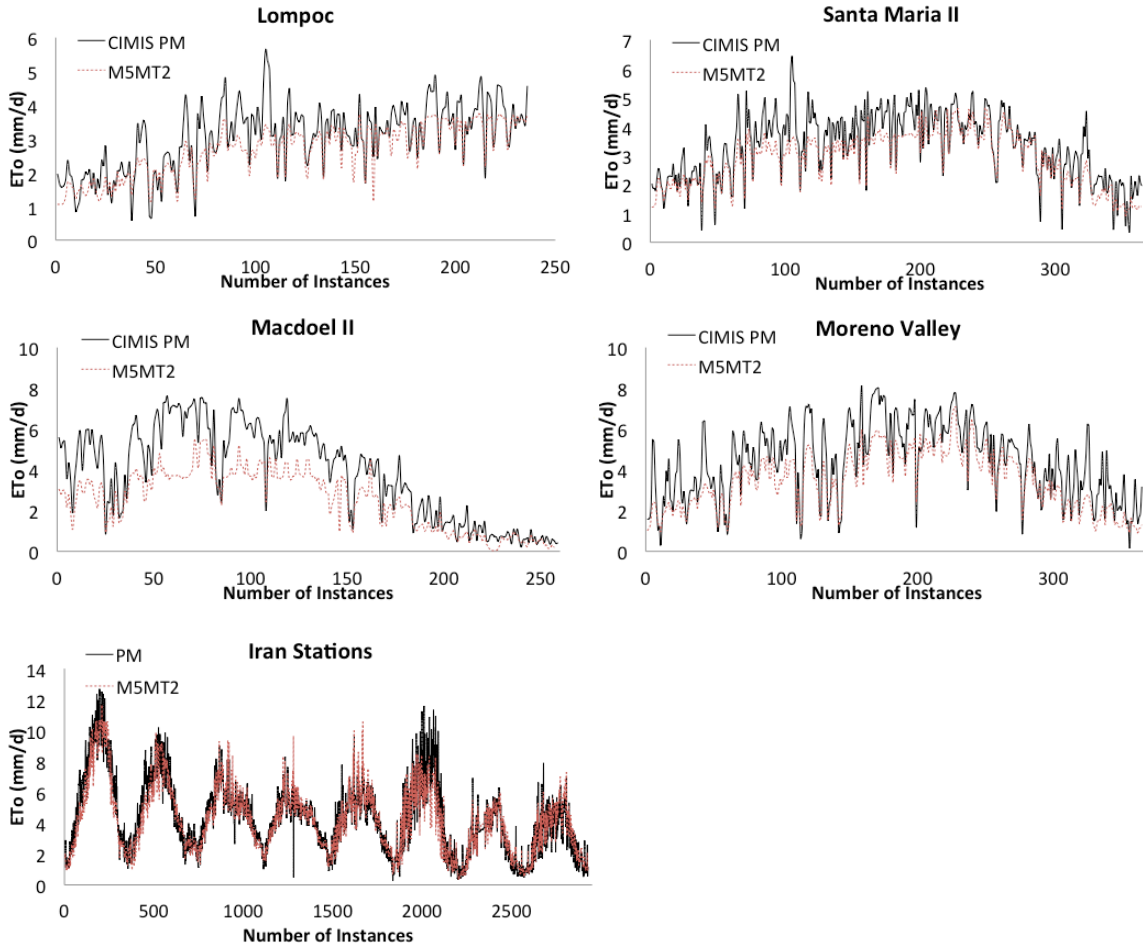
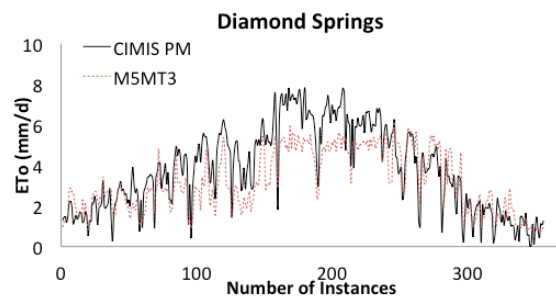
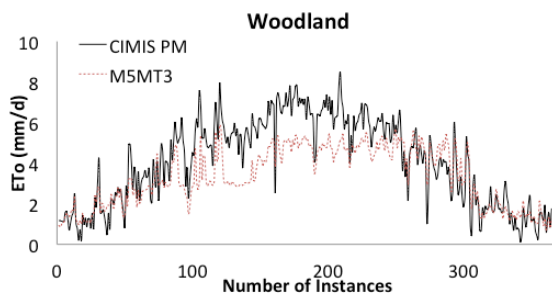
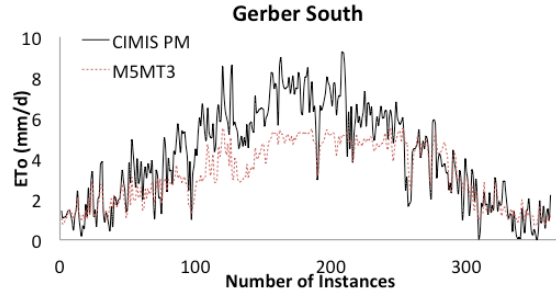
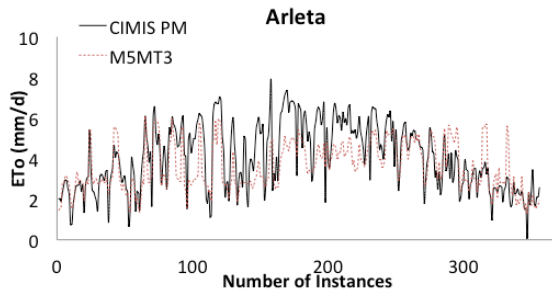
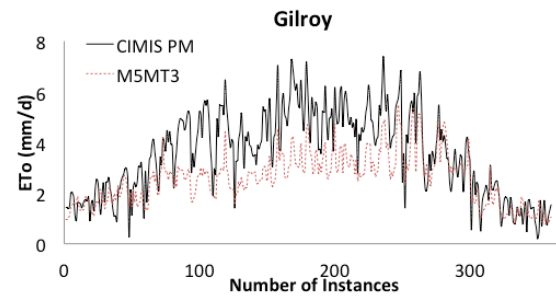
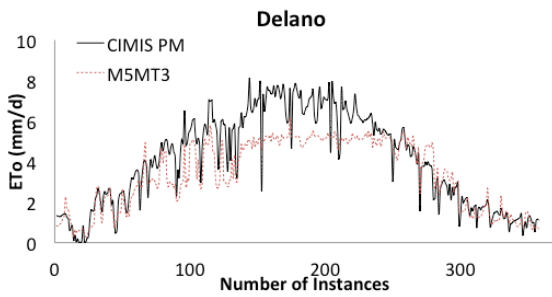
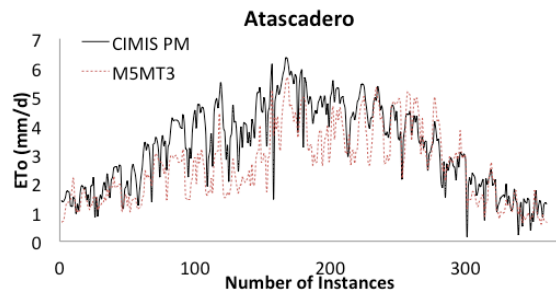
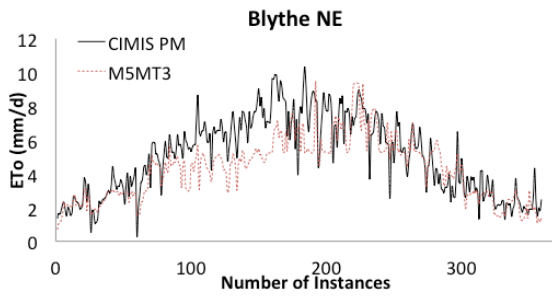
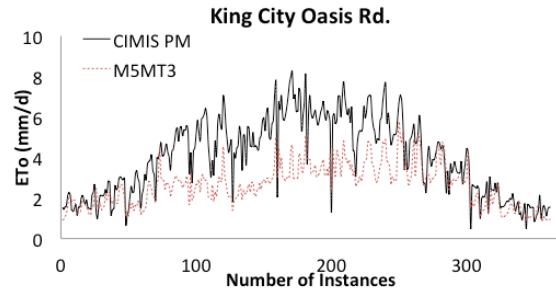
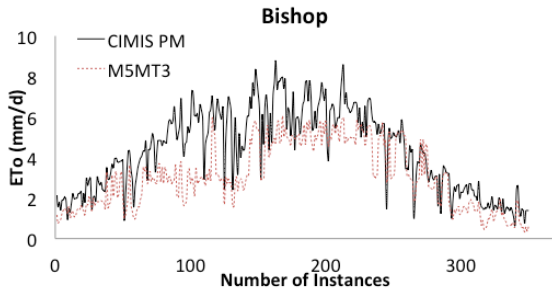


Figure 20. Time series of observed and estimated  $ET_0$  values from M5MT2.





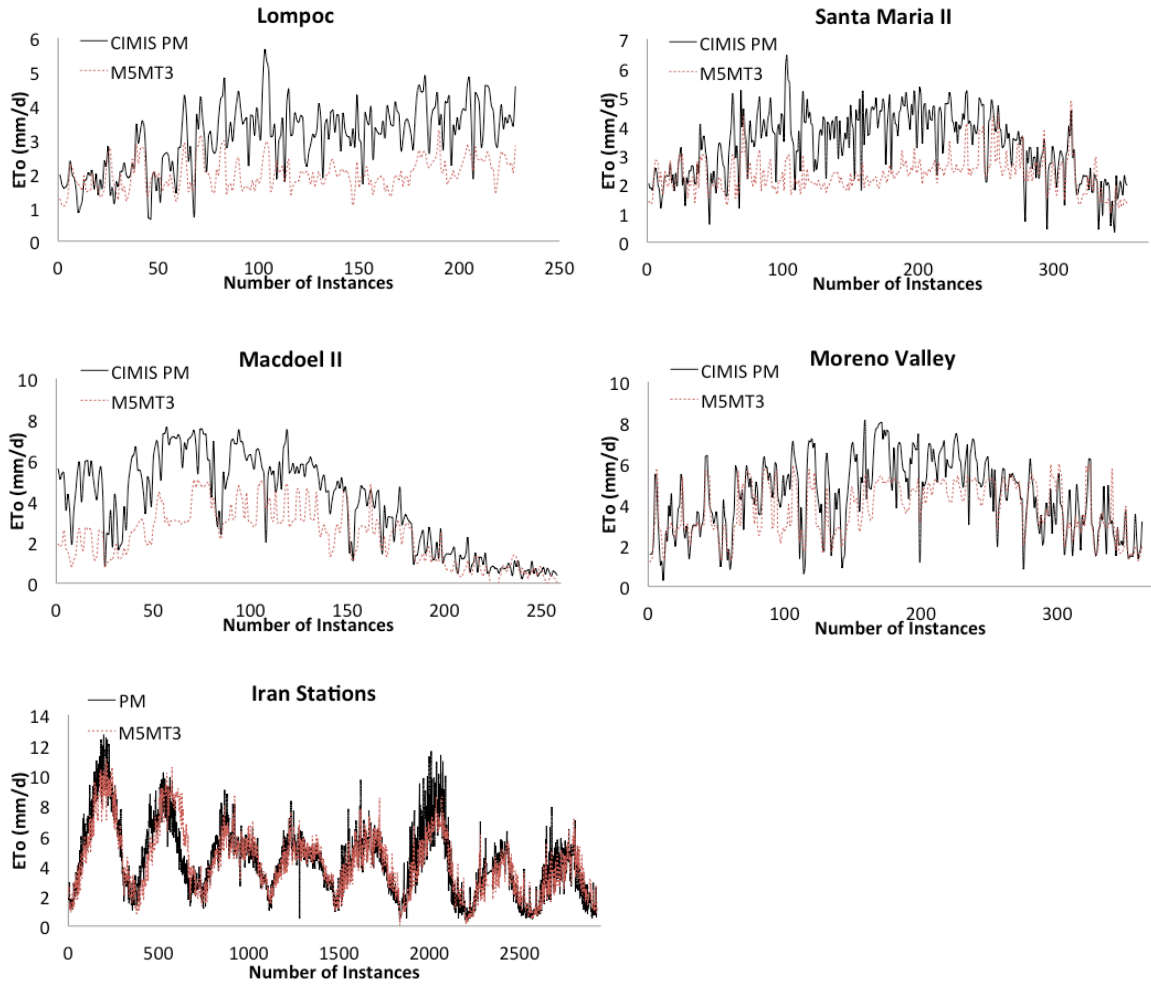
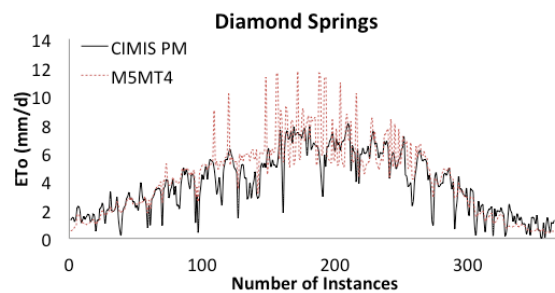
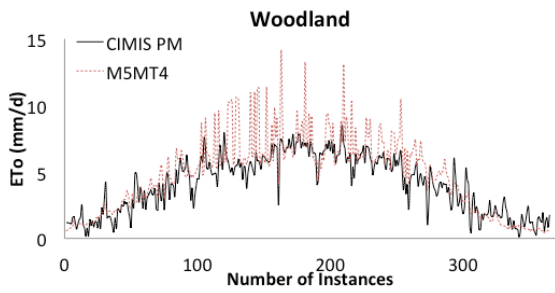
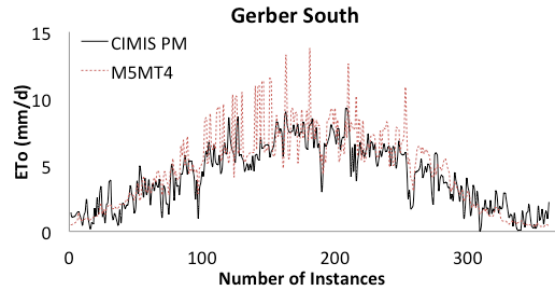
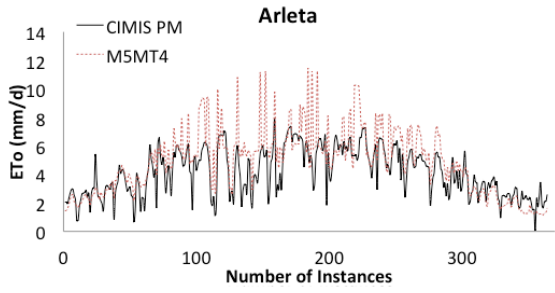
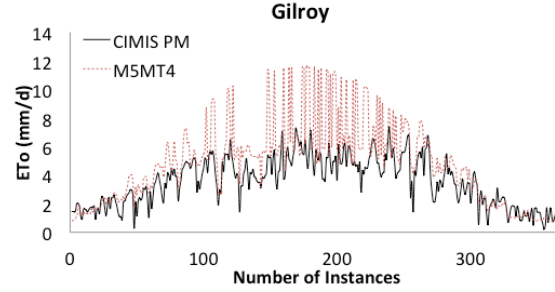
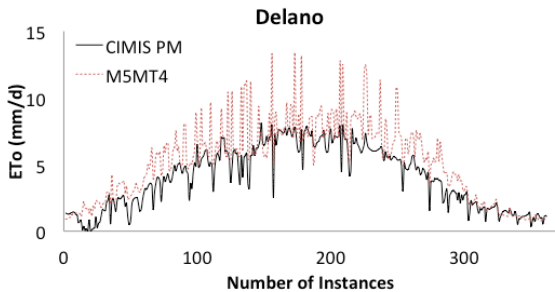
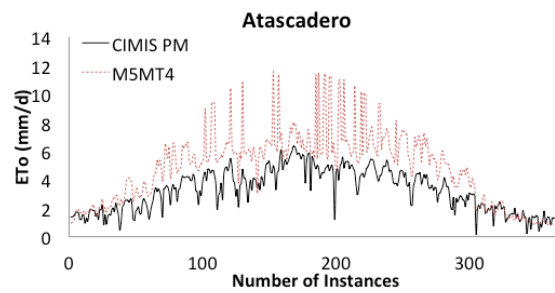
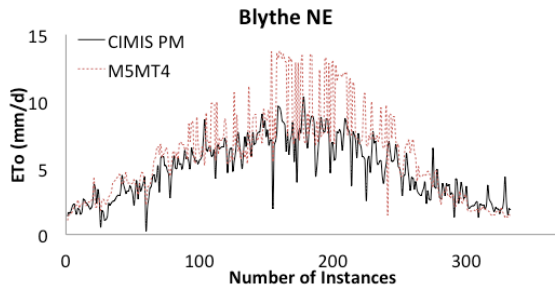
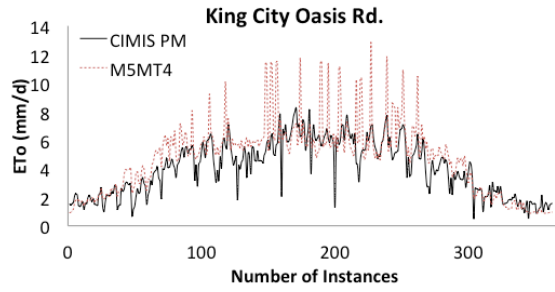
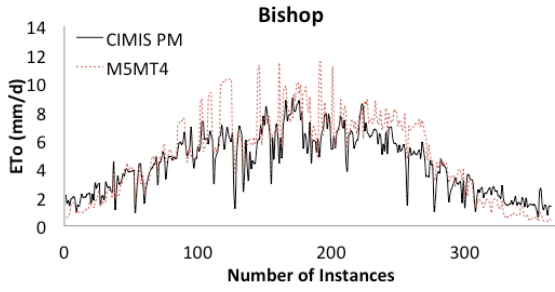


Figure 21. Time series of observed and estimated  $ET_0$  values from M5MT3.



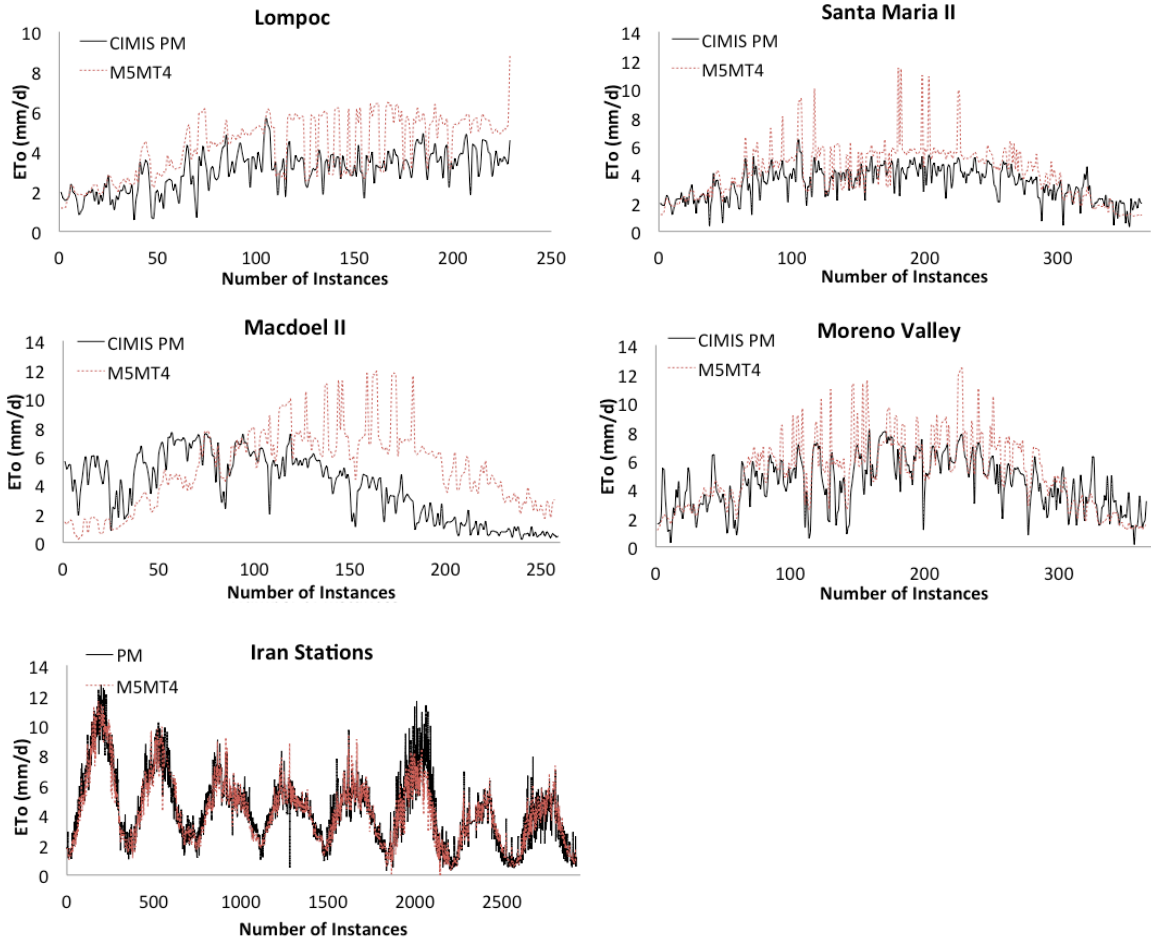


Figure 22. Time series of observed and estimated  $ET_0$  values from M5MT4.

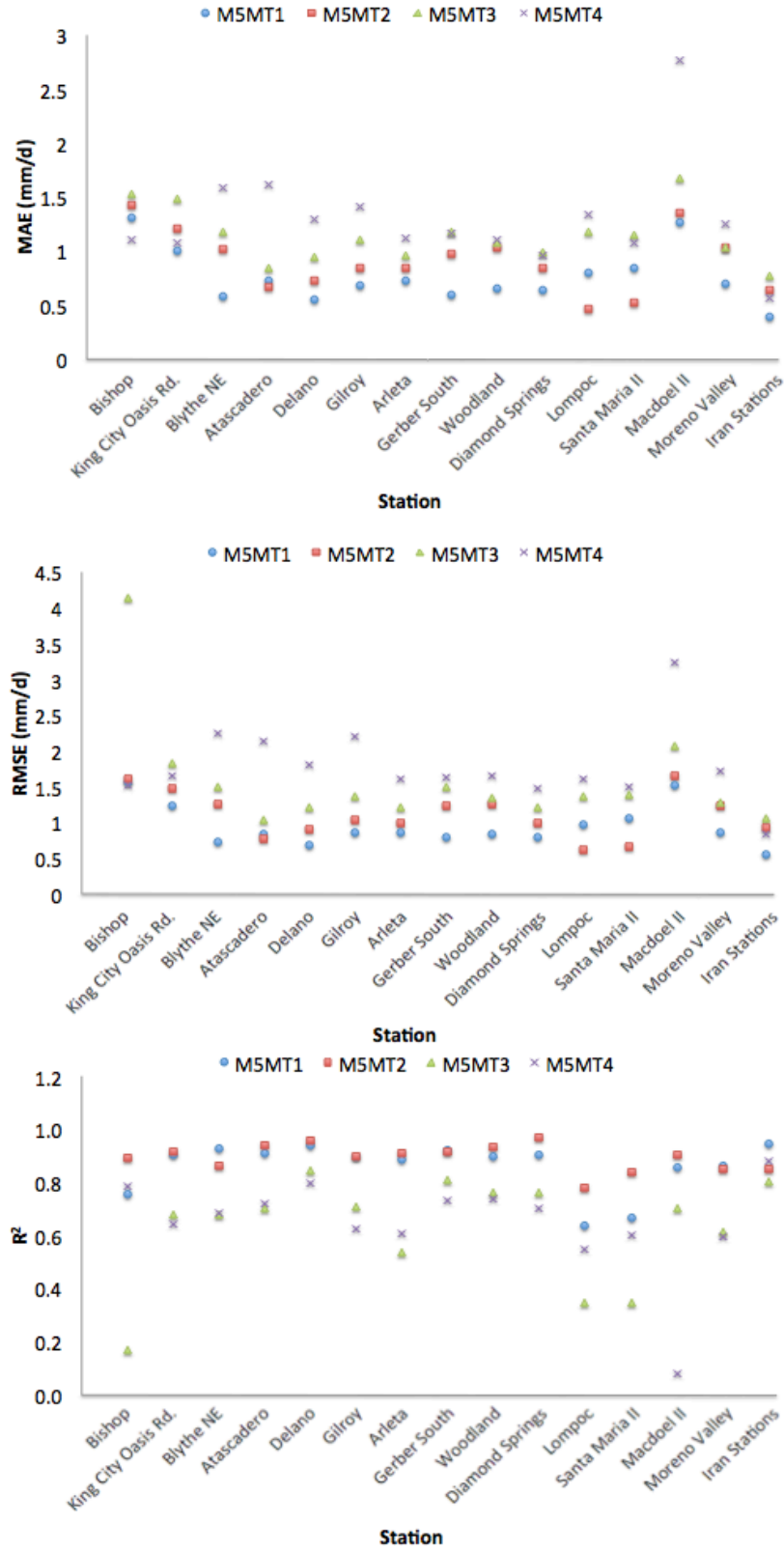


Figure 23. Comparing performance of M5MT models in different stations.

Table 13. Statistical metrics of  $ET_0$  estimates from M5MT1 and M5MT2.

<b>Model</b>	<b>Station</b>	<b>MAE (mm/d)</b>	<b>RMSE (mm/d)</b>	<b>R<sup>2</sup></b>
M5MT1	Bishop	1.31	1.55	0.75
	King City Oasis Rd.	1.00	1.23	0.90
	Blythe NE	0.57	0.73	0.93
	Atascadero	0.73	0.83	0.91
	Delano	0.55	0.68	0.94
	Gilroy	0.68	0.85	0.90
	Arleta	0.72	0.85	0.88
	Gerber South	0.59	0.79	0.92
	Woodland	0.66	0.83	0.90
	Diamond Springs	0.63	0.78	0.90
	Lompoc	0.80	0.97	0.63
	Santa Maria II	0.84	1.05	0.66
	Macdoel II	1.26	1.52	0.86
	Moreno Valley	0.70	0.85	0.86
	All Iran Stations	0.38	0.55	0.94
M5MT2	Bishop	1.43	1.61	0.89
	King City Oasis Rd.	1.21	1.46	0.92
	Blythe NE	1.02	1.25	0.86
	Atascadero	0.67	0.76	0.94
	Delano	0.72	0.90	0.96
	Gilroy	0.84	1.04	0.90
	Arleta	0.84	0.99	0.91
	Gerber South	0.97	1.22	0.92
	Woodland	1.02	1.25	0.93
	Diamond Springs	0.84	0.99	0.97
	Lompoc	0.46	0.61	0.78
	Santa Maria II	0.51	0.66	0.84
	Macdoel II	1.34	1.65	0.90
	Moreno Valley	1.03	1.23	0.85
	All Iran Stations	0.64	0.92	0.85

Table 14. Statistical metrics of  $ET_0$  estimates from M5MT3 and M5MT4.

<b>Model</b>	<b>Station</b>	<b>MAE (mm/d)</b>	<b>RMSE (mm/d)</b>	<b>R<sup>2</sup></b>
M5MT3	Bishop	1.52	4.13	0.17
	King City Oasis Rd.	1.48	1.83	0.68
	Blythe NE	1.17	1.50	0.68
	Atascadero	0.84	1.02	0.70
	Delano	0.94	1.21	0.84
	Gilroy	1.11	1.37	0.71
	Arleta	0.95	1.20	0.54
	Gerber South	1.18	1.50	0.81
	Woodland	1.07	1.35	0.76
	Diamond Springs	0.98	1.20	0.76
	Lompoc	1.18	1.35	0.34
	Santa Maria II	1.15	1.38	0.35
	Macdoel II	1.67	2.06	0.70
	Moreno Valley	1.03	1.28	0.61
All Iran Stations	0.77	1.06	0.80	
M5MT4	Bishop	1.10	1.53	0.78
	King City Oasis Rd.	1.08	1.65	0.64
	Blythe NE	1.58	2.24	0.68
	Atascadero	1.61	2.14	0.72
	Delano	1.29	1.79	0.79
	Gilroy	1.41	2.19	0.62
	Arleta	1.12	1.61	0.60
	Gerber South	1.16	1.62	0.73
	Woodland	1.10	1.64	0.73
	Diamond Springs	0.96	1.47	0.70
	Lompoc	1.34	1.61	0.55
	Santa Maria II	1.07	1.49	0.60
	Macdoel II	2.77	3.23	0.08
	Moreno Valley	1.25	1.71	0.60
All Iran Stations	0.56	0.82	0.88	

### 4.3 GEP

The GeneXpro program was used to create a GEP model for each input combination. The parameters that were specified by the user were terminal and function sets, the head size, the number of chromosomes, the number of genes, and the linking function.

The terminal and function sets were specified to create the genes of the chromosomes. The terminal function set consisted of  $W_s$ ,  $RH_{mean}$ ,  $T_{mean}$ ,  $T_{max}$ ,  $T_{min}$ ,  $R_s$ , and  $R_a$ . The function set consisted of the following arithmetic functions: +, -, x, /, square root, exponential, natural log,  $x^2$ ,  $x^3$ ,  $x^{1/3}$ , sine, cosine, and arctangent. Next, the length of the head and the number of genes per chromosome were specified. The head size dictated the amount of terminal and functional symbols used in each chromosome and the number of genes determined how many sub-expression trees would be generated in the model.

In this study, the head size was set to a default value of seven. 30 chromosomes and three genes were used (Ferreira, 2001; Emamgolizadeh et al., 2015). The addition mathematical operator was utilized as the linking function (Zakaria et al., 2010; Hashmi et al., 2011; Azamathulla and Ahmad, 2012; Azamathulla and Jarrett, 2013). Lastly, RMSE was used as the fitness function. The applied parameters are summarized in Table 15.

Table 15. Summary of GEP model parameters.

Parameter	Parameter Setting
Terminal set	$W_s$ , $RH_{mean}$ , $T_{mean}$ , $T_{max}$ , $T_{min}$ , $R_s$ , and $R_a$
Function set	+, -, x, /, sqrt, exp, ln, $x^2$ , $x^3$ , $x^{1/3}$ , sin, cos, and arctan
Head size	7
Number of chromosomes	30
Number of genes	3
Linking function	Addition

Table 16 presents the  $ET_0$  mathematical expressions generated by the four GEP models. GEP1-GEP3 models successfully determined a relationship between all input variables and  $ET_0$ . The GEP4 model, however, was not able to establish a relationship between all input variables ( $T_{mean}$ ,  $T_{min}$ ,  $T_{max}$ , and  $R_a$ ) and  $ET_0$ , resulting in the omission  $T_{min}$ .

Figures 24-27 show a comparison between  $ET_0$  estimates from the four GEP models and those from the PM equation for all stations. As indicated, it was observed that the majority of the  $ET_0$  estimates from GEP1 and GEP2 conformed to the 45-degree line better than those from GEP3 and GEP4. Figures 28-31 indicate the time series of the calculated  $ET_0$  values from the four GEP models. For comparison, the estimated  $ET_0$  values from the PM equation were also plotted on the same figures. Underestimation of  $ET_0$  was observed from GEP2 and GEP3, while GEP1 and GEP4 mostly overestimated  $ET_0$ . The under- and overestimation is most likely attributed to measurement errors and the exclusion of California stations from the training process. However, most of the  $ET_0$  estimates from the GEP models coincided with the daily variations in observed  $ET_0$  values.

The performance of GEP models in different stations was compared in Figure 32 using  $MAE$ ,  $RMSE$ , and  $R^2$ . GEP1 provided the best results in all stations. Pertaining to the California stations, average  $MAE$  of  $ET_0$  estimates from GEP2, GEP3, and GEP4 were respectively, 31%, 91%, and 139% higher than those from GEP1. Also, their average  $RMSE$  were respectively 22%, 79%, and 125% greater than the average  $RMSE$  value of GEP1. When tested with data from Iran, GEP1 resulted in the lowest  $MAE$  and  $RMSE$  values (0.81 mm/d and 1.06 mm/d, respectively) and the highest  $R^2$  (0.81). Performances of GEP2 and GEP4 tested with Iran stations were comparable, with similar  $MAE$ ,  $RMSE$ , and  $R^2$  values. This indicates GEP may be a plausible approach to estimate  $ET_0$  for areas where only air temperature is available.



Tables 17 and 18 present statistical metrics of  $ET_0$  estimates from the four GEP models. The average *MAE* for all stations tested with GEP2, GEP3, and GEP4 were respectively, 28%, 91%, and 126% greater than that of GEP1. Also, average *RMSE* values for all stations tested with GEP2, GEP3, and GEP4 were respectively, 20%, 75%, and 111% greater than that of GEP1.

Generally, results showed GEP1 to be the most accurate model, followed by GEP2. The results from GEP1 and GEP2 tested with California stations indicated GEP to be a viable approach to estimate  $ET_0$ . Metrics from GEP2 further showed GEP's capability to successfully estimate  $ET_0$  with limited climatic data. GEP4 model performance varied when tested with data from different locations. GEP4 performed comparably to GEP2 when tested with Iran stations, while GEP4 performed not as good as GEP1-GEP3 when tested with California stations. This may indicate the inputs of GEP4 to be region dependent.

Table 16. GEP equations corresponding to each model.

Model	Equation
GEP1	$ET_0 = \frac{(W_s + (W_s + 3.66)) + ((\frac{RH_{mean}}{9.42} - R_s))}{-3.66} + \arctan \left( \sqrt{\exp \left( \left( \frac{RH_{mean}}{4.15} \right)^2 - ((W_s + 4.15) + 4.15) \right)} \right)$ $+ W_s - \cos \left( \arctan(R_s - 9.23) - \frac{T_{mean}}{9.82} \right)$
GEP2	$ET_0 = \left[ \sin \left( \frac{(7.63 - T_{mean}) - 8.14}{8.14} \right) \right]^3 + \arctan \left[ \cos \left( 3.23 + \left( \frac{T_{mean} - 9.07}{12.3} \right) \right) \right]$ $+ R_s \left[ \cos \left( \arctan((R_s - 3.4) - R_s) \right) \right]$
GEP3	$ET_0 = [\arctan(T_{mean})]^3 + 2\cos[0.03(T_{mean}\arctan(T_{mean}) - (RH_{mean} + 3.14))]$
GEP4	$ET_0 = \frac{R_a}{5.81 + \cos \left( \arctan(T_{max}) + \frac{T_{mean}}{-7.76} \right)} + \frac{R_a}{\exp \left[ \frac{R_a + 6.02}{T_{max} - 5.47} \right] + 5.47}$ $+ \left[ \arctan \left( \cos(19.06(e^{T_{max}} - 16.84)) \right) \right]^3$

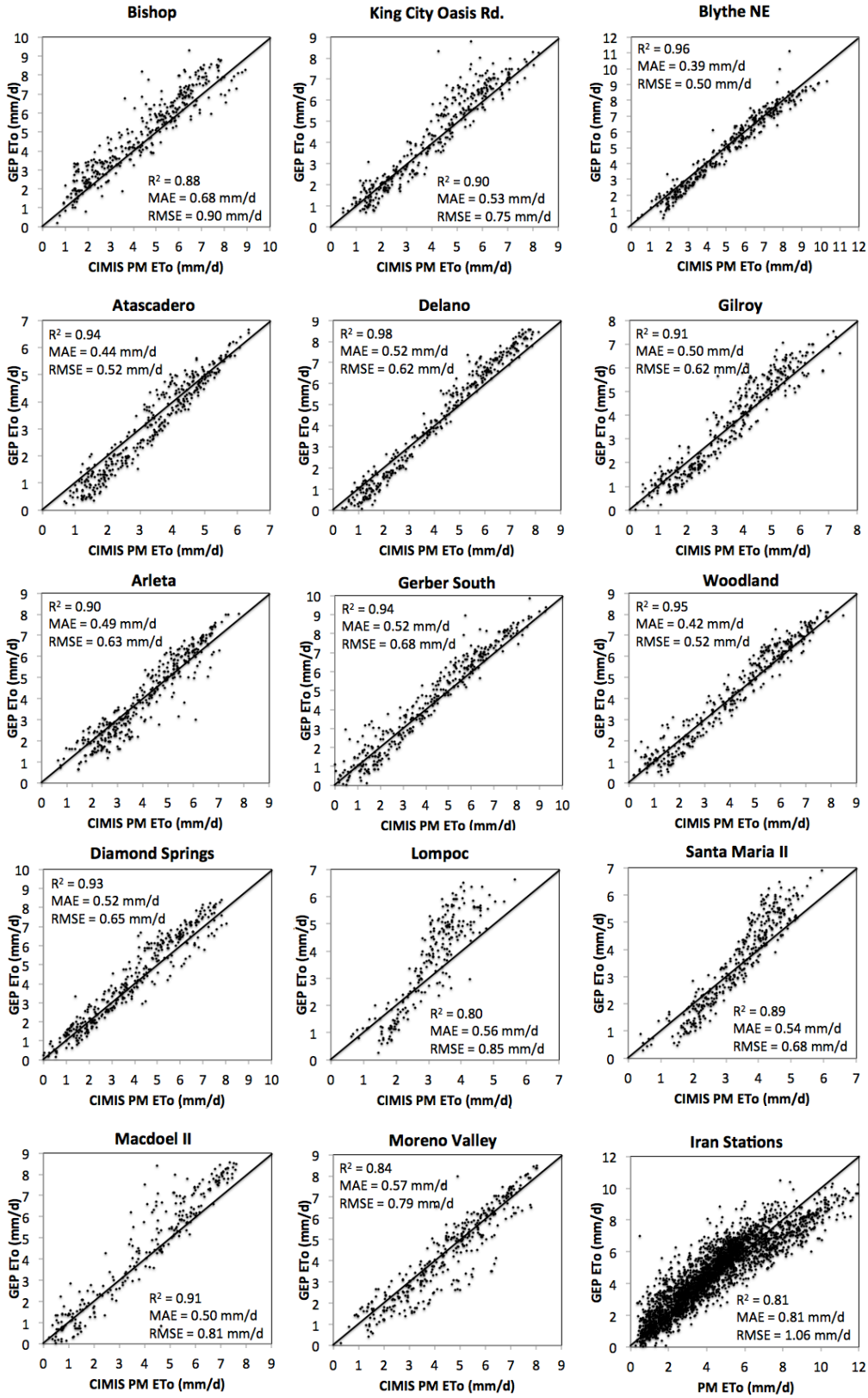


Figure 24. Estimated  $ET_0$  values from GEP1 versus observations.

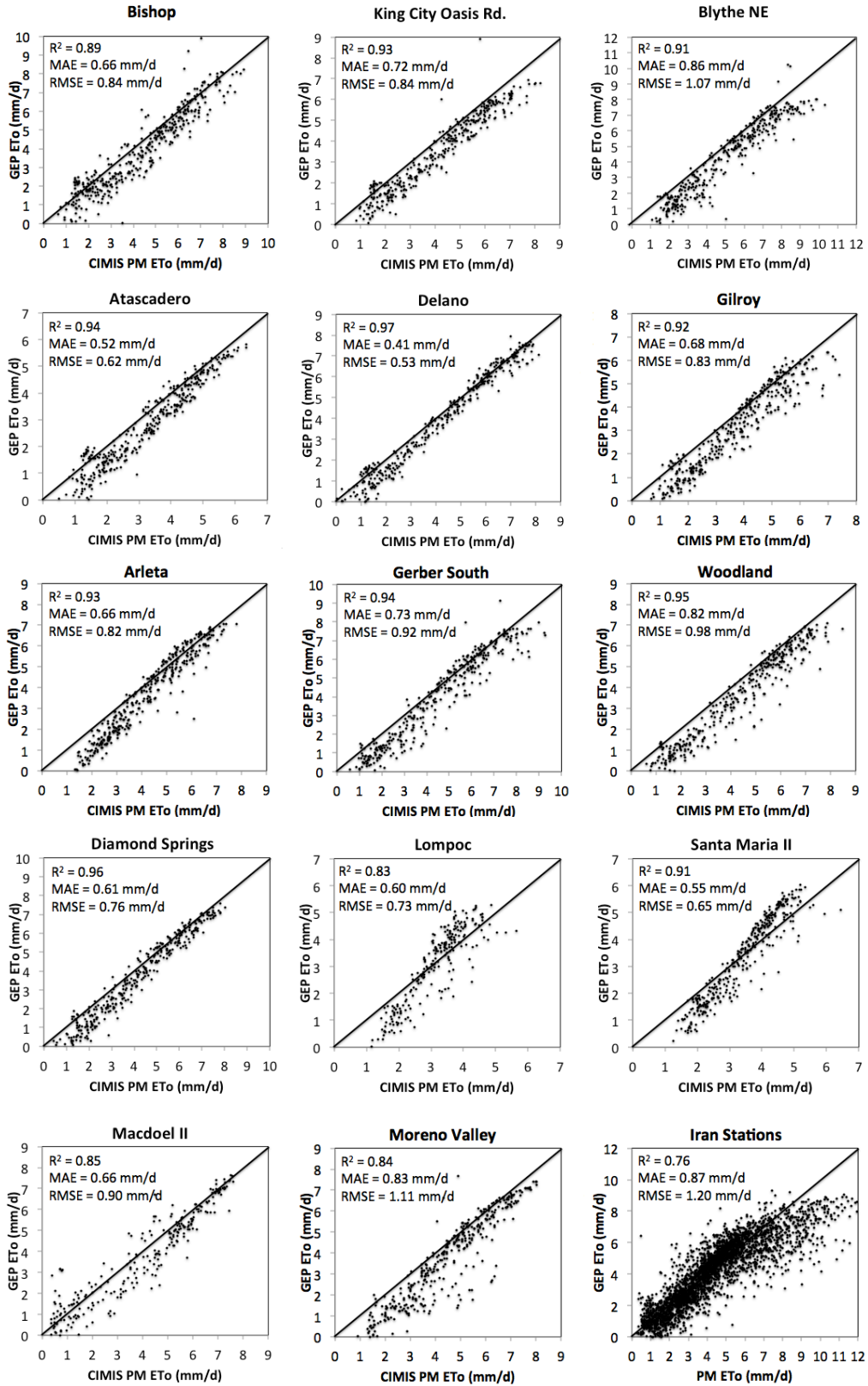


Figure 25. Estimated  $ET_0$  values from GEP2 versus observations.

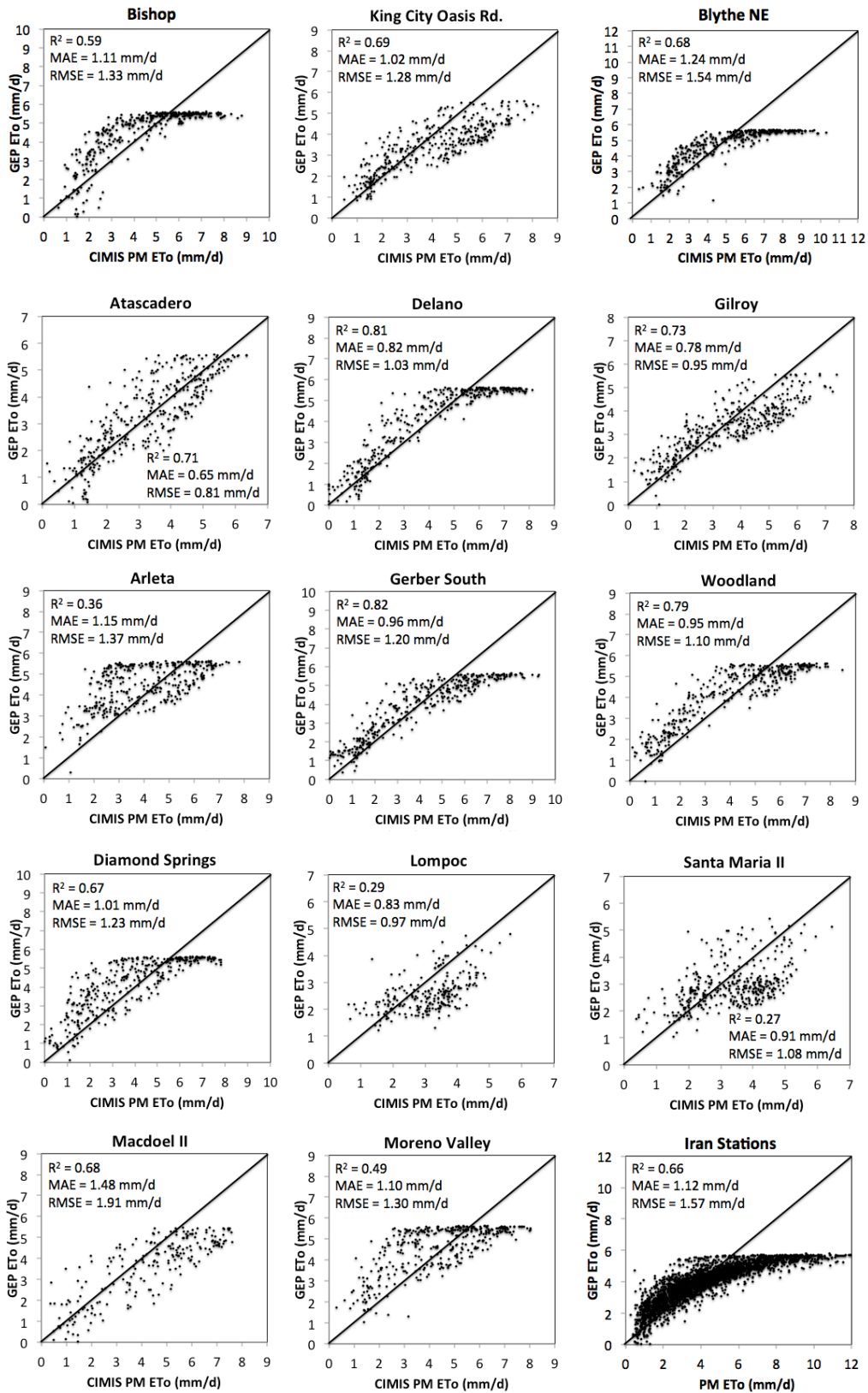


Figure 26. Estimated  $ET_0$  values from GEP3 versus observations.

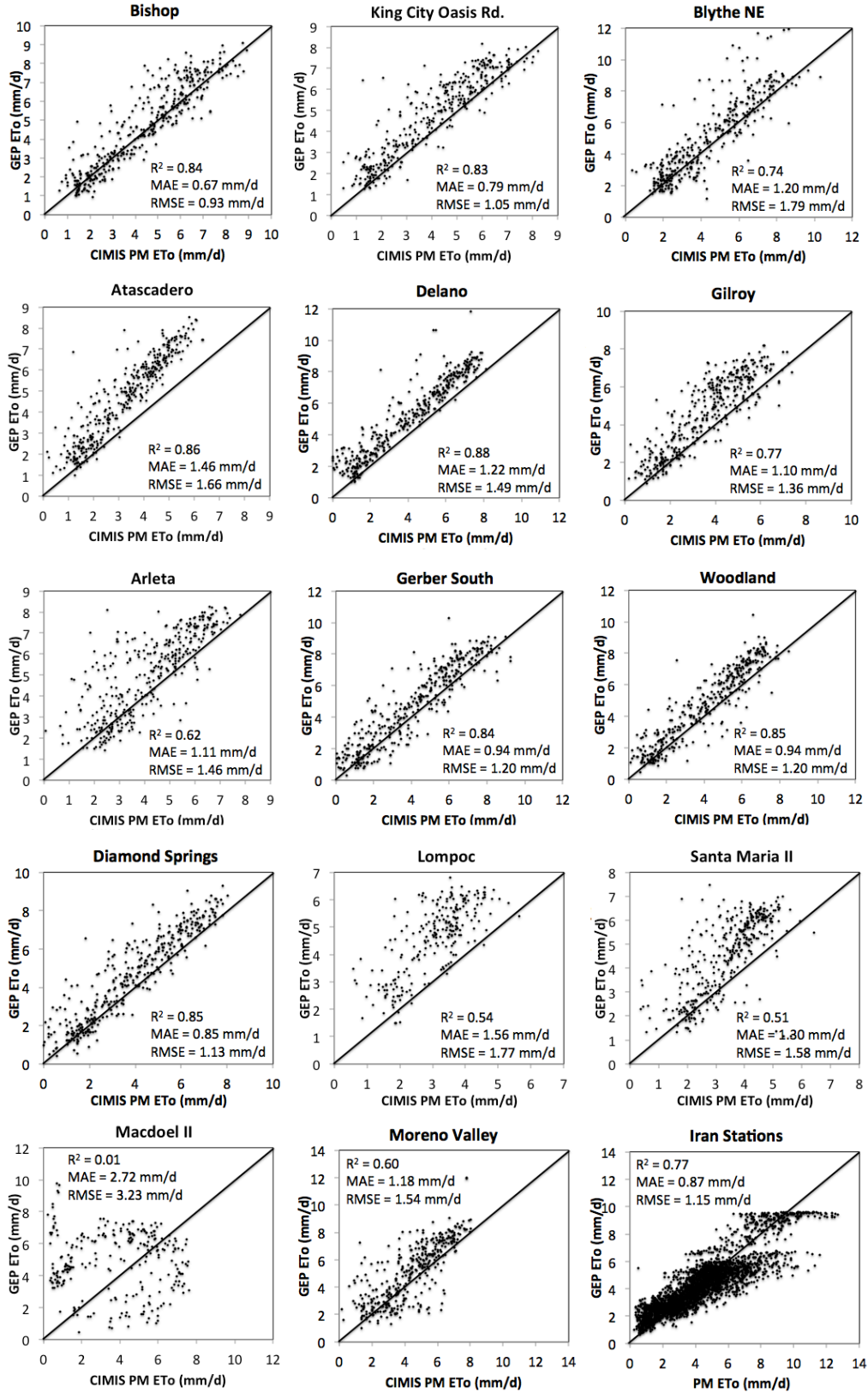
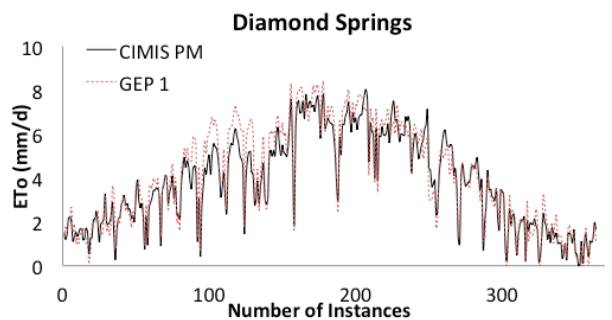
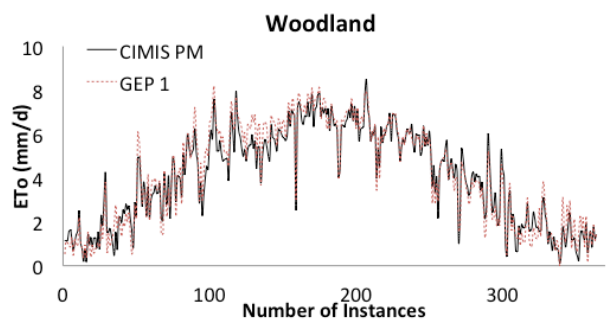
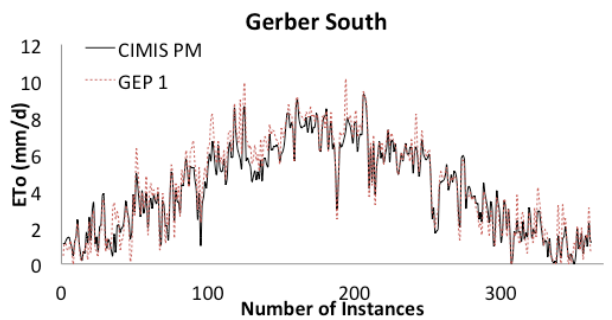
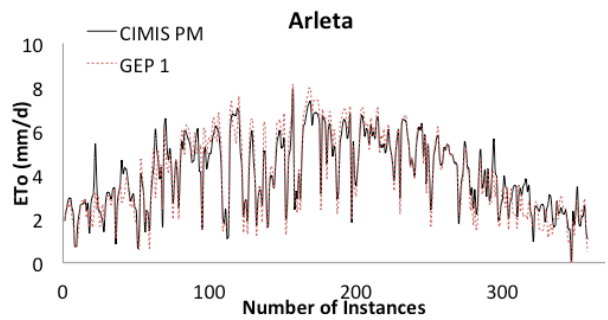
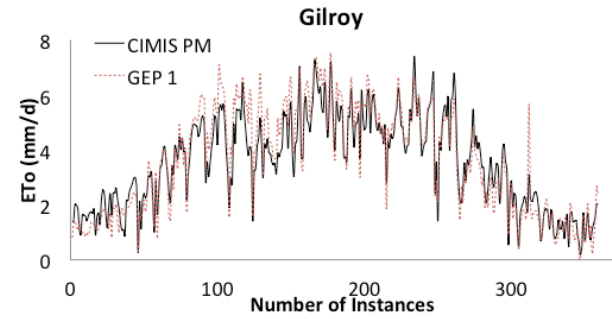
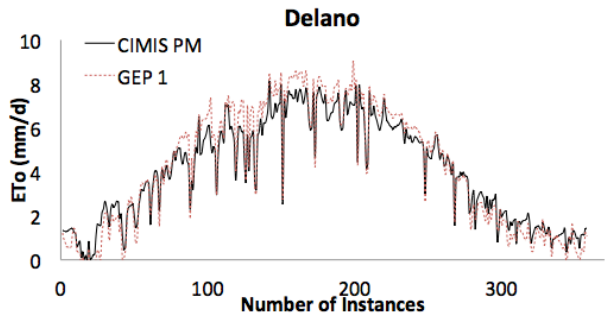
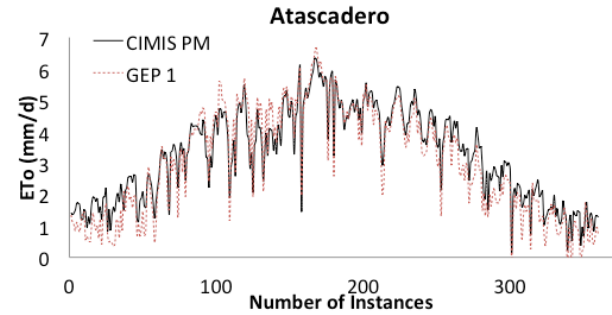
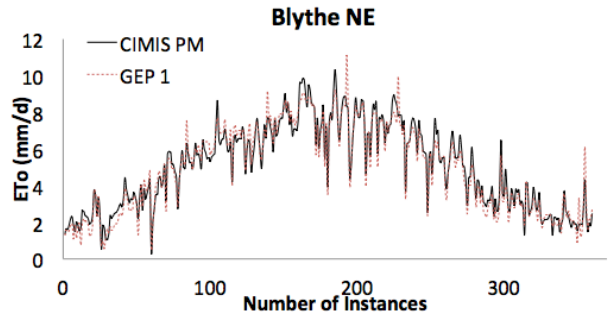
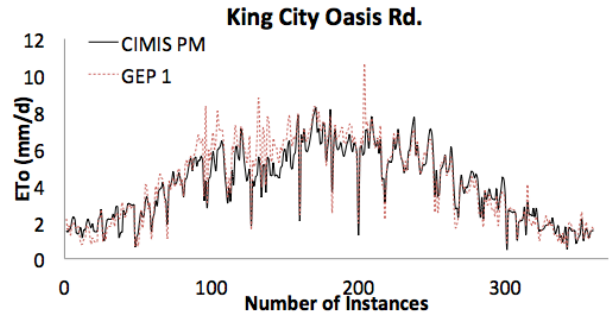
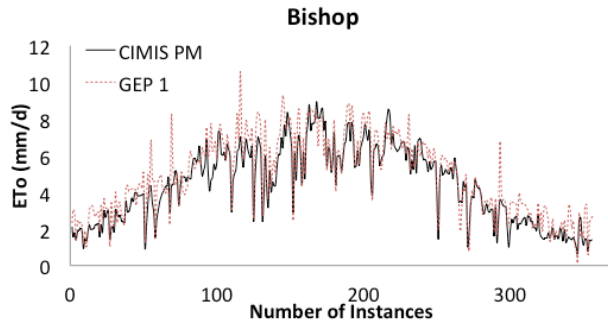


Figure 27. Estimated  $ET_0$  values from GEP4 versus observations.



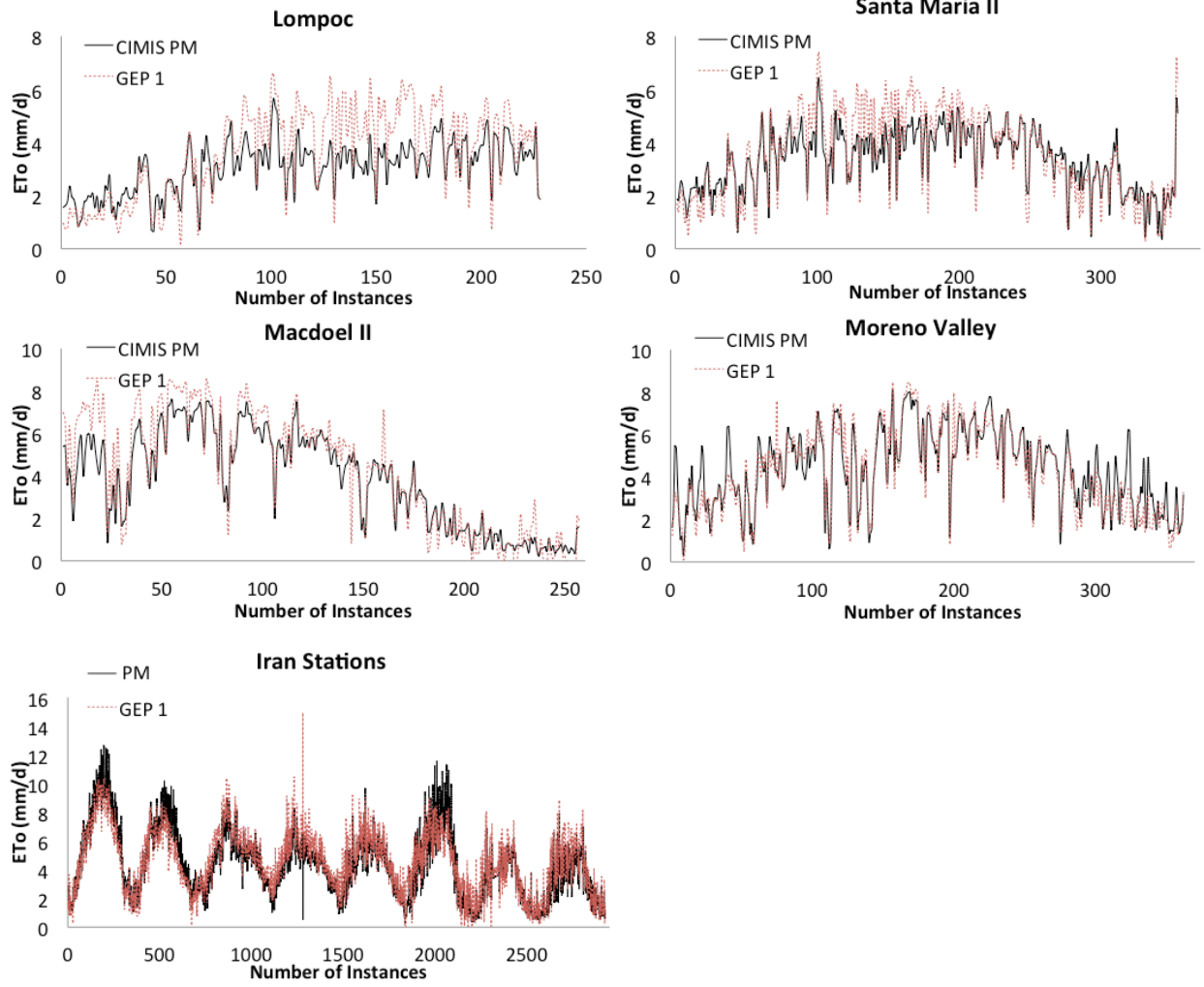
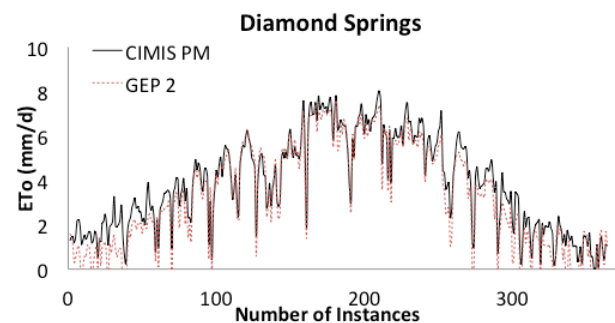
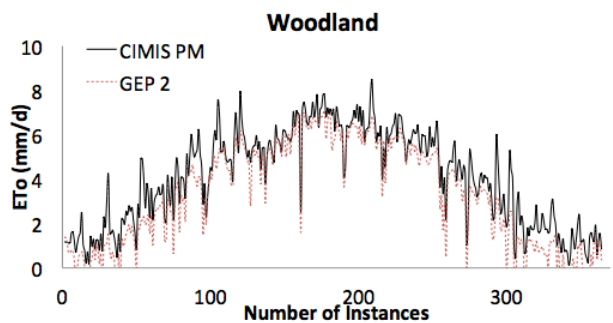
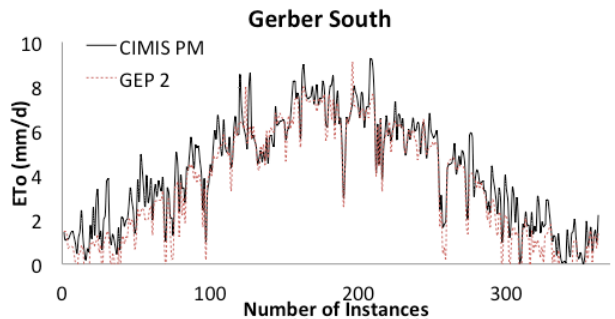
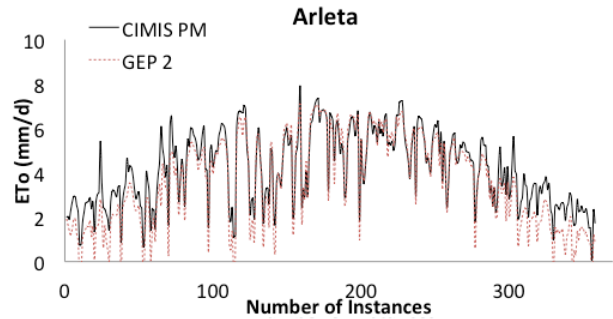
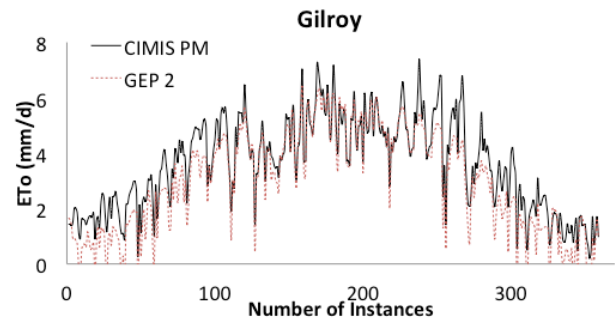
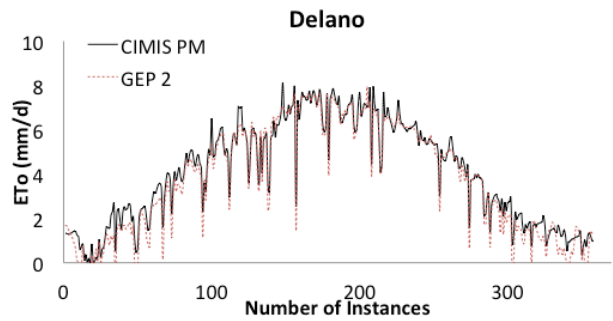
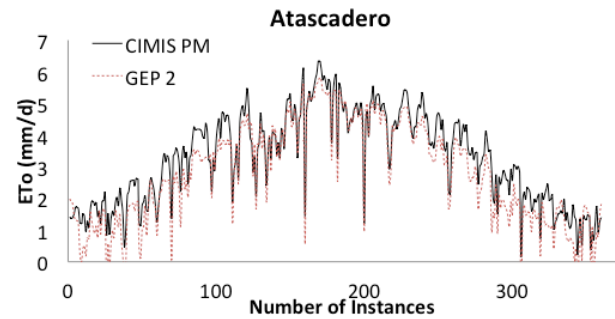
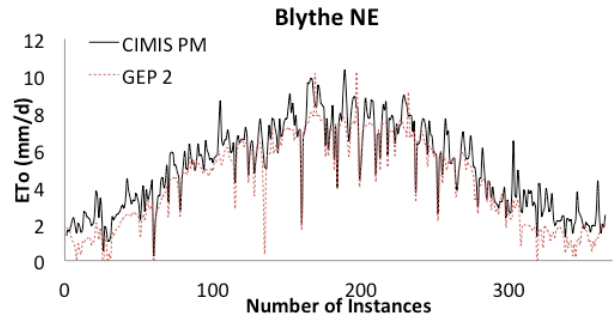
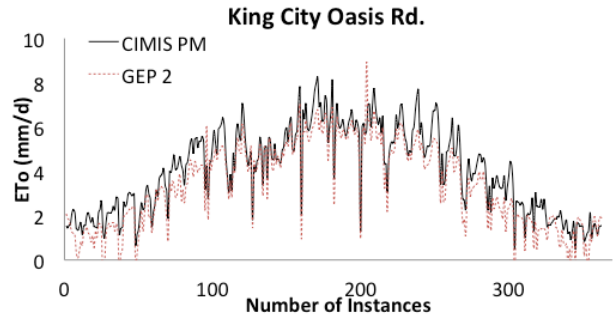
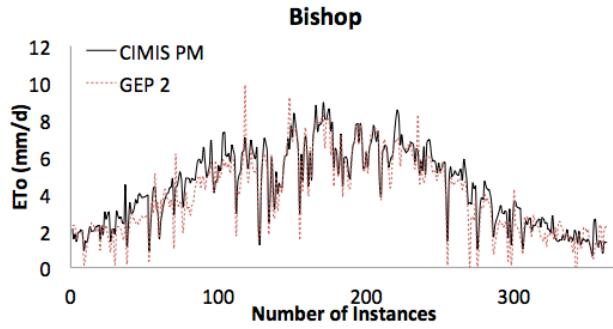


Figure 28. Time series of observed and estimated  $ET_0$  values from GEP1.





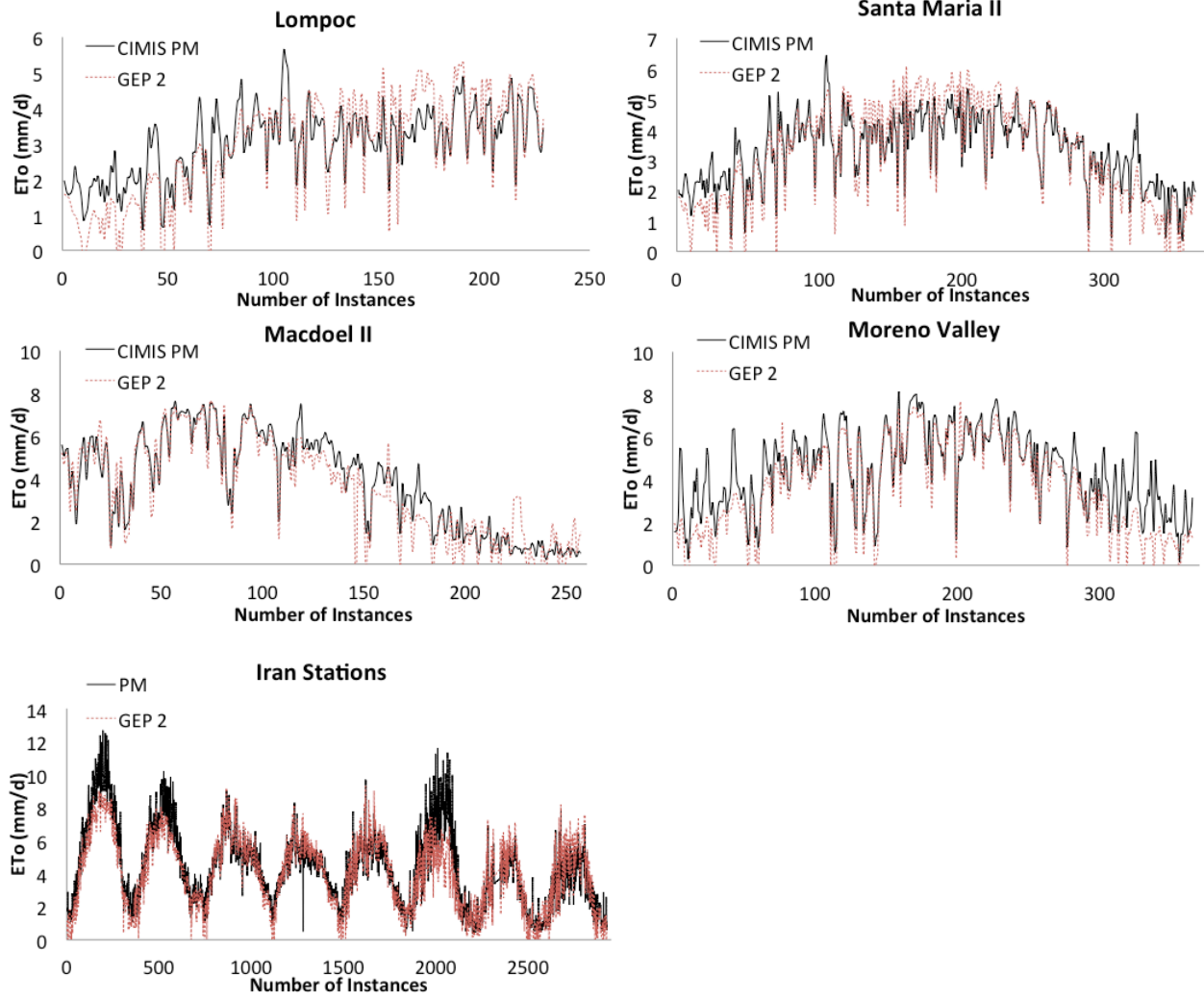
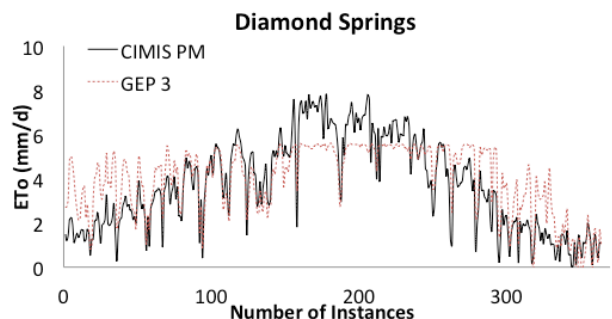
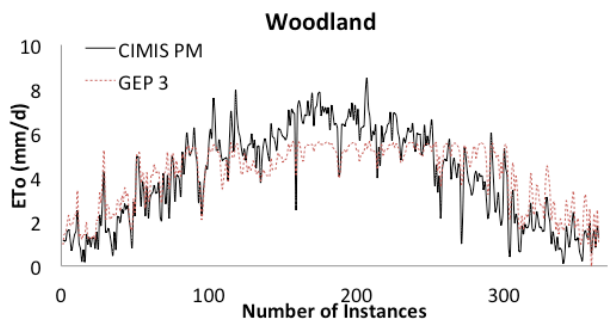
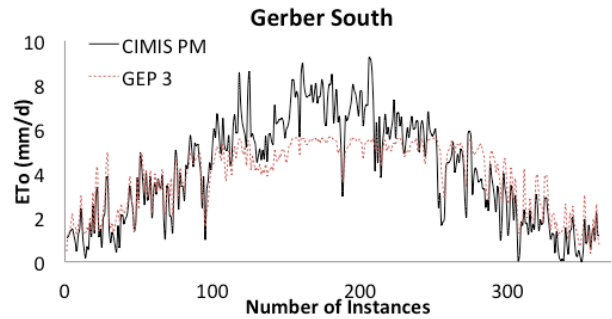
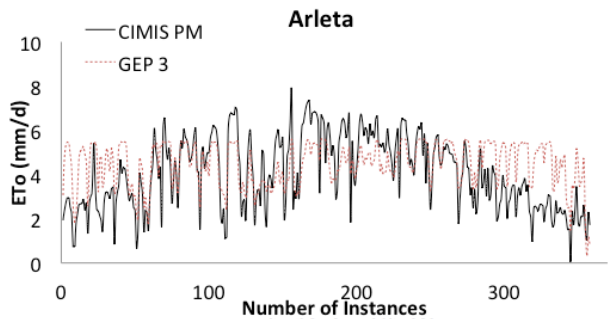
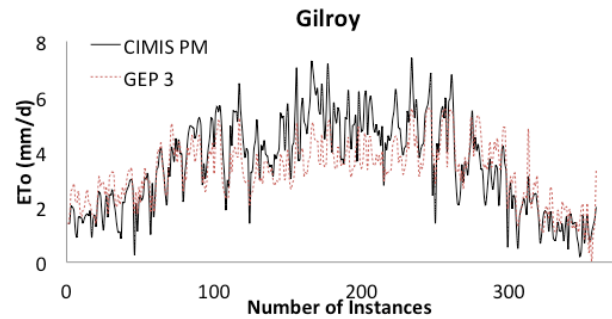
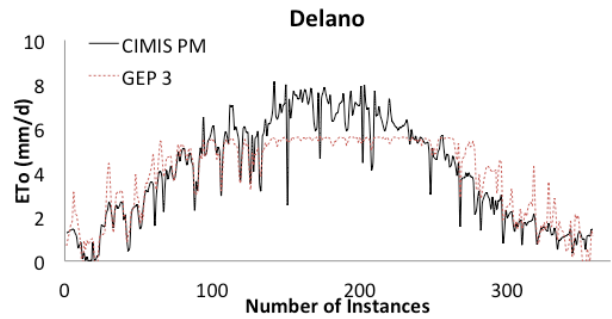
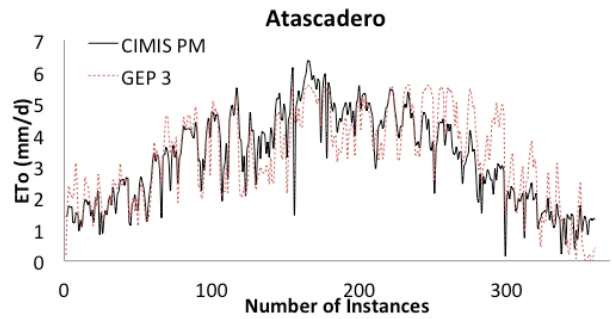
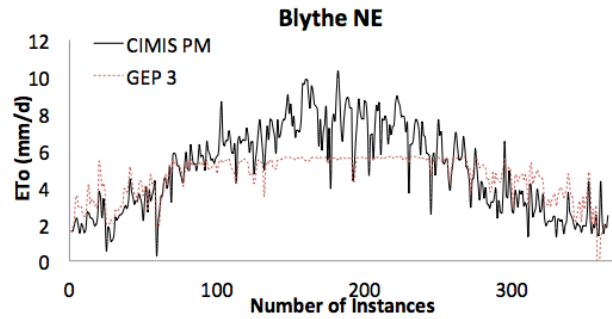
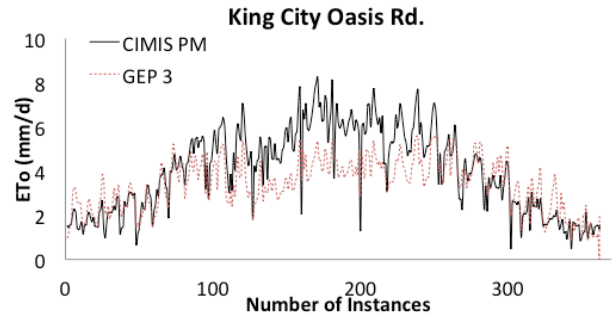
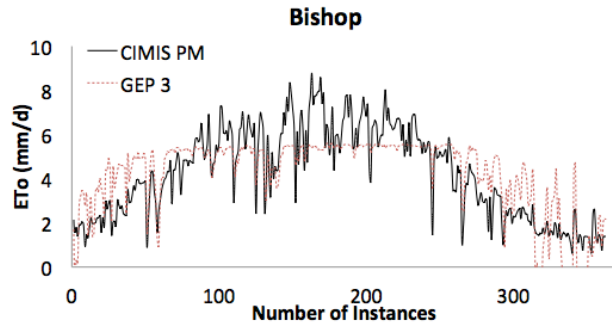


Figure 29. Time series of observed and estimated  $ET_0$  values from GEP2.



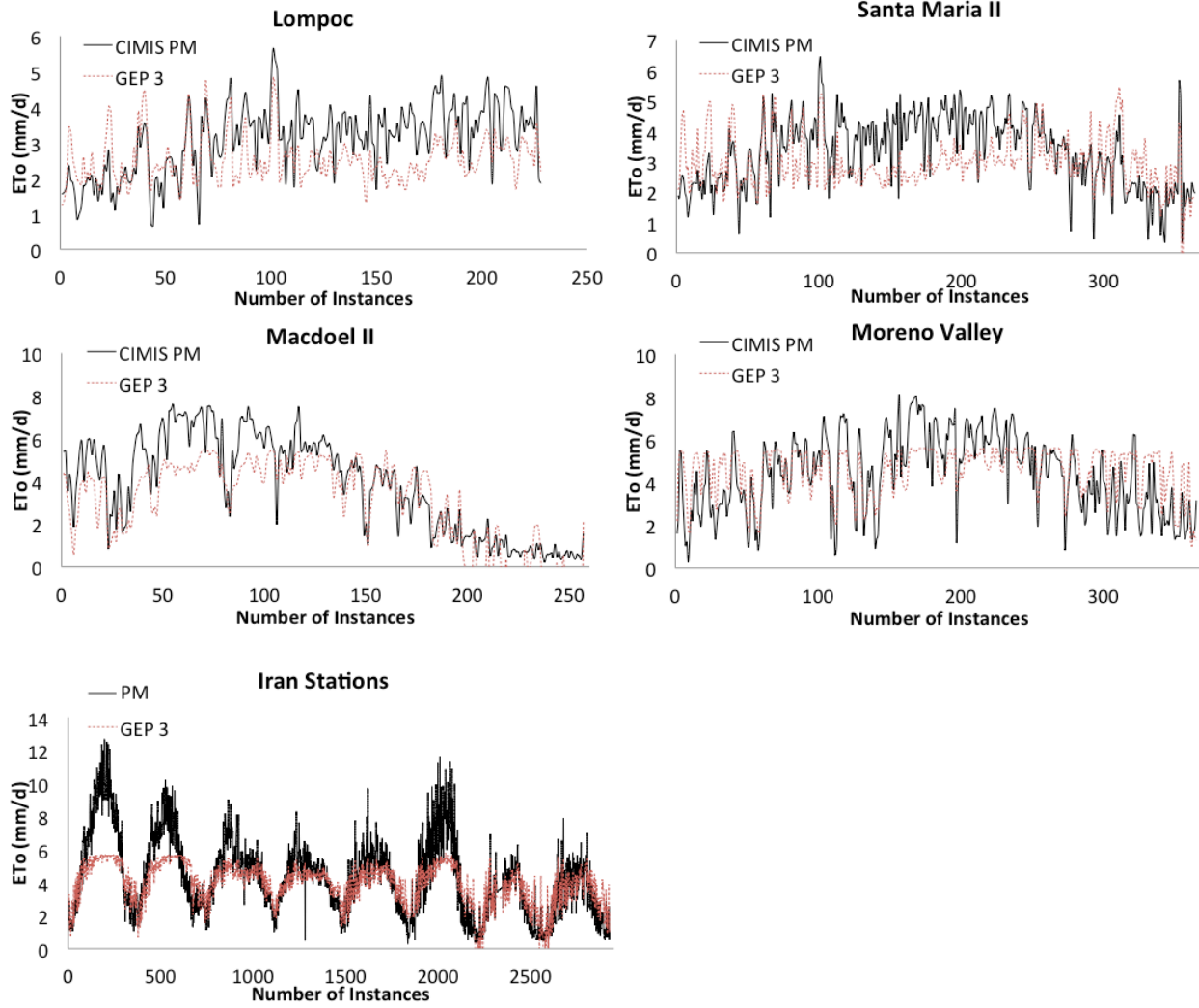
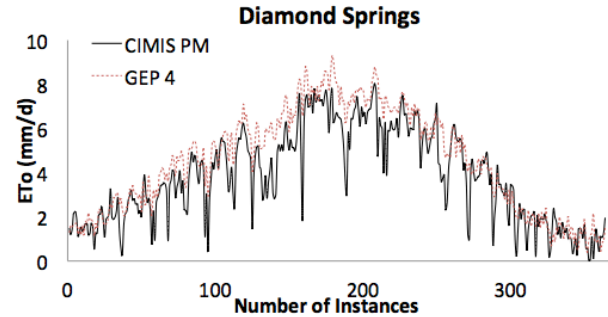
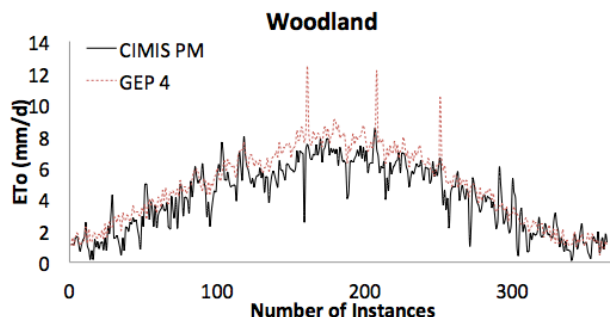
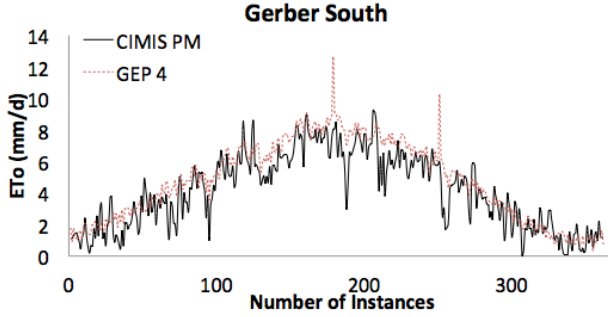
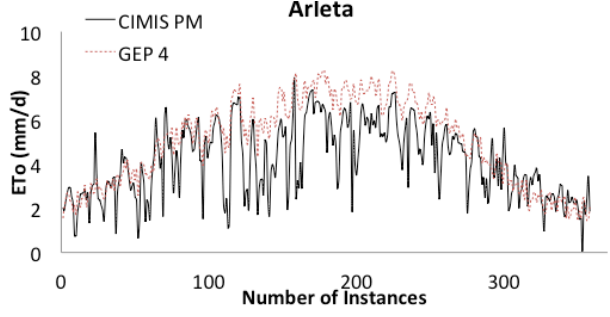
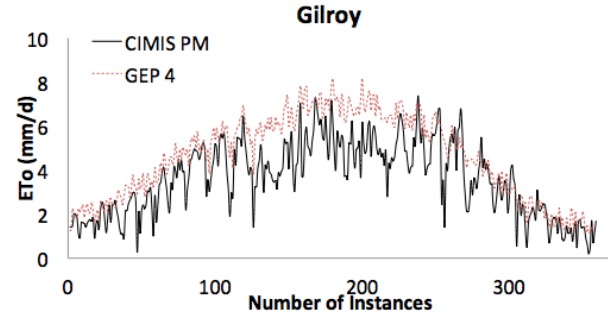
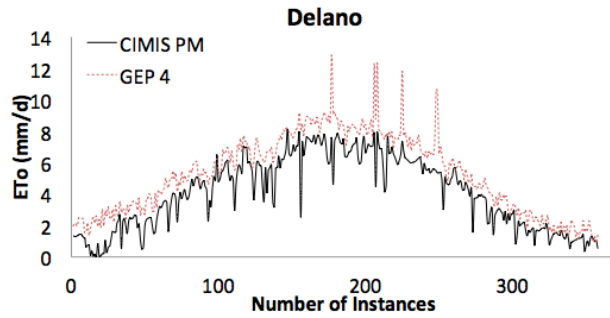
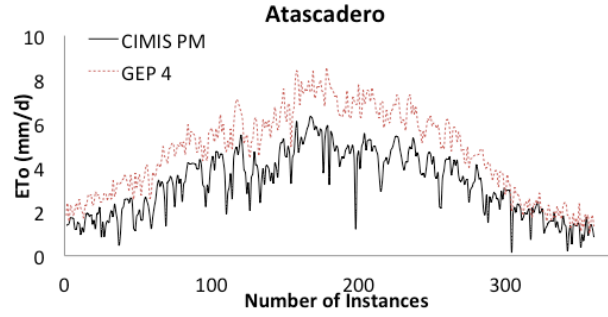
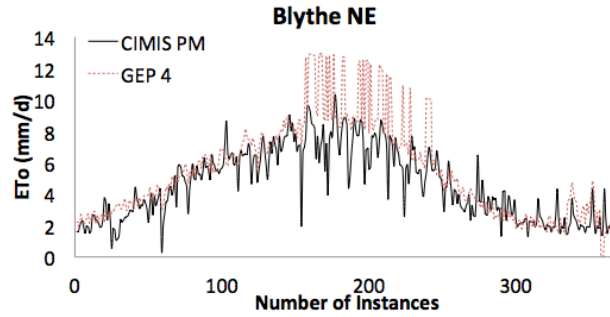
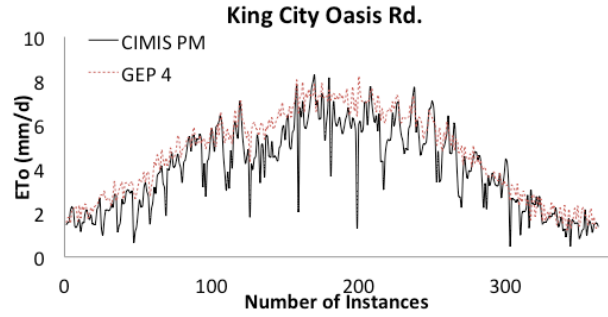
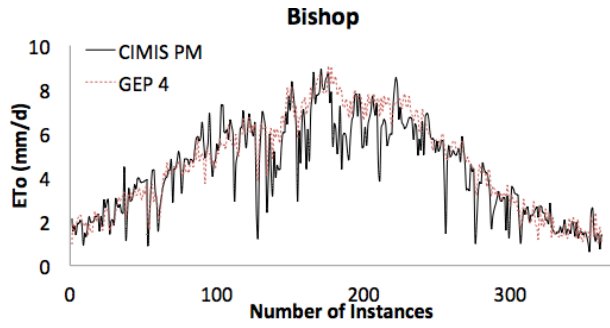


Figure 30. Time series of observed and estimated  $ET_0$  values from GEP3.



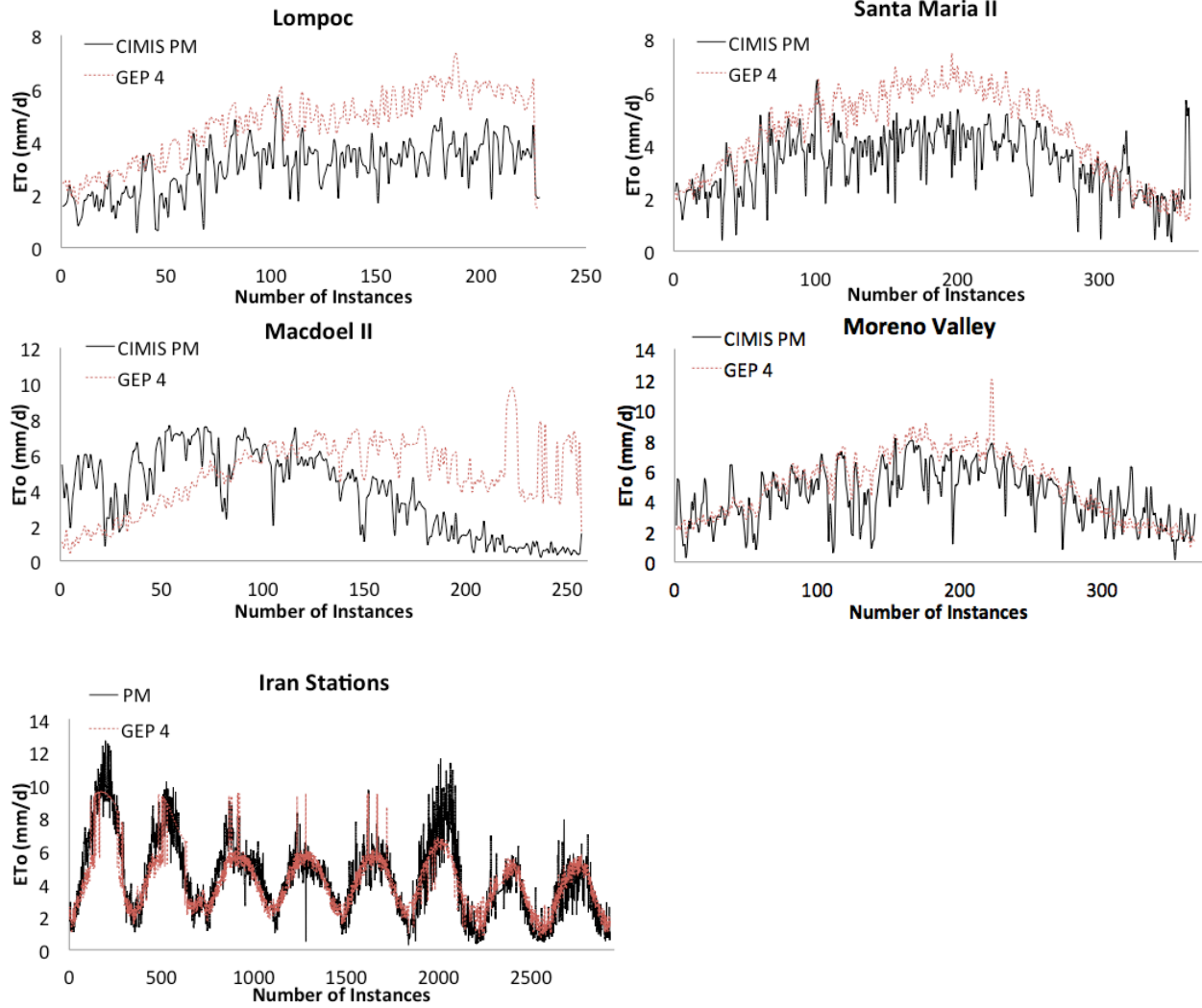


Figure 31. Time series of observed and estimated  $ET_0$  values from GEP4.

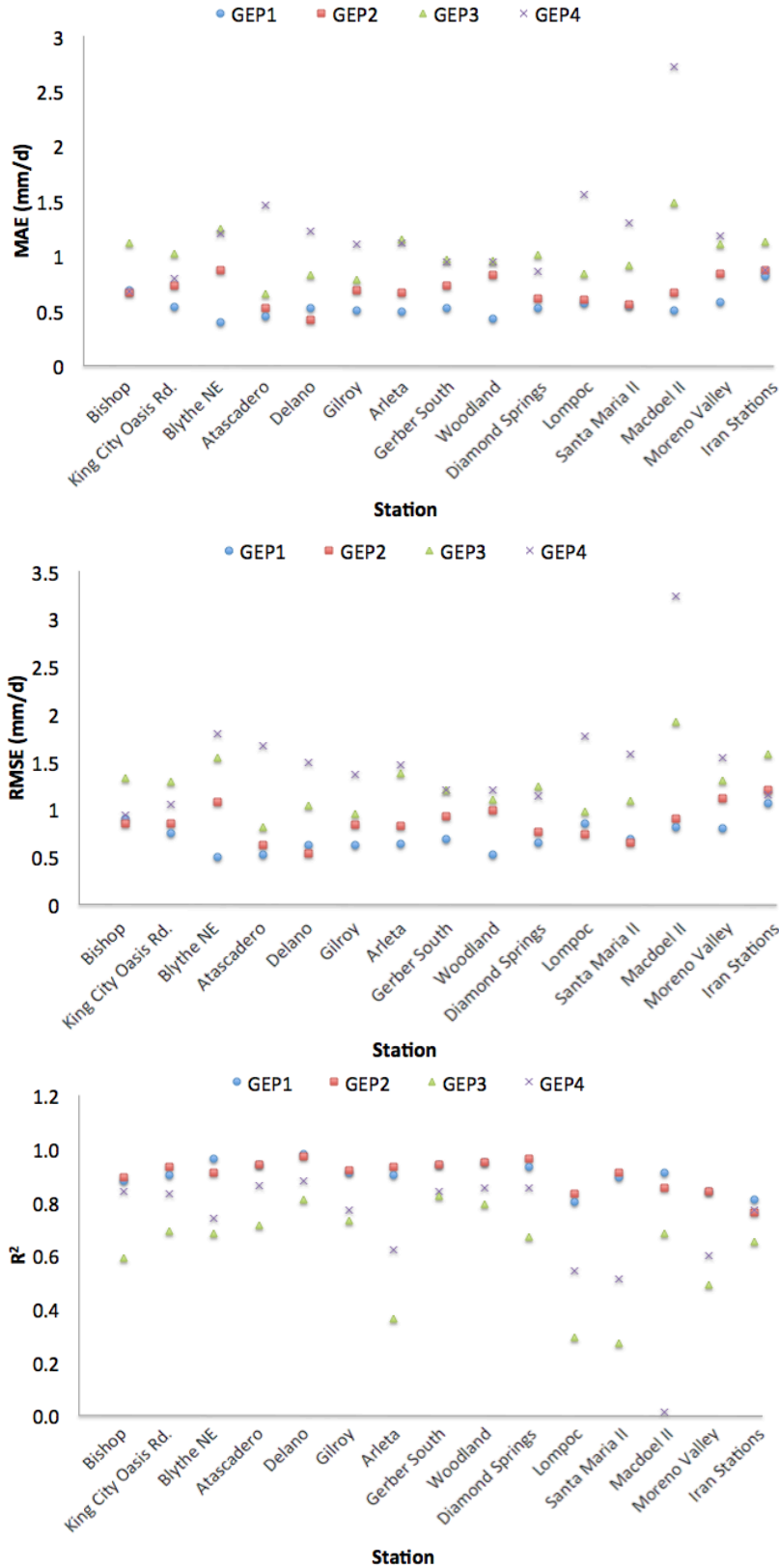


Figure 32. Comparing performance of GEP models in different stations.

Table 17. Statistical metrics of  $ET_0$  estimates from GEP1 and GEP2.

<b>Model</b>	<b>Station</b>	<b>MAE (mm/d)</b>	<b>RMSE (mm/d)</b>	<b>R<sup>2</sup></b>
GEP1	Bishop	0.68	0.90	0.88
	King City Oasis Rd.	0.53	0.75	0.90
	Blythe NE	0.39	0.50	0.96
	Atascadero	0.44	0.52	0.94
	Delano	0.52	0.62	0.98
	Gilroy	0.50	0.62	0.91
	Arleta	0.49	0.63	0.90
	Gerber South	0.52	0.68	0.94
	Woodland	0.42	0.52	0.95
	Diamond Springs	0.52	0.65	0.93
	Lompoc	0.56	0.85	0.80
	Santa Maria II	0.54	0.68	0.89
	Macdoel II	0.50	0.81	0.91
	Moreno Valley	0.57	0.79	0.84
	All Iran Stations	0.81	1.06	0.81
GEP2	Bishop	0.66	0.84	0.89
	King City Oasis Rd.	0.72	0.84	0.93
	Blythe NE	0.86	1.07	0.91
	Atascadero	0.52	0.62	0.94
	Delano	0.41	0.53	0.97
	Gilroy	0.68	0.83	0.92
	Arleta	0.66	0.82	0.93
	Gerber South	0.73	0.92	0.94
	Woodland	0.82	0.98	0.95
	Diamond Springs	0.61	0.76	0.96
	Lompoc	0.60	0.73	0.83
	Santa Maria II	0.55	0.65	0.91
	Macdoel II	0.66	0.90	0.85
	Moreno Valley	0.83	1.11	0.84
	All Iran Stations	0.87	1.20	0.76



Table 18. Statistical metrics of  $ET_0$  estimates from GEP3 and GEP4.

<b>Model</b>	<b>Station</b>	<b>MAE (mm/d)</b>	<b>RMSE (mm/d)</b>	<b>R<sup>2</sup></b>
GEP3	Bishop	1.11	1.33	0.59
	King City Oasis Rd.	1.02	1.28	0.69
	Blythe NE	1.24	1.54	0.68
	Atascadero	0.65	0.81	0.71
	Delano	0.82	1.03	0.81
	Gilroy	0.78	0.95	0.73
	Arleta	1.15	1.37	0.36
	Gerber South	0.96	1.20	0.82
	Woodland	0.95	1.10	0.79
	Diamond Springs	1.01	1.23	0.67
	Lompoc	0.83	0.97	0.29
	Santa Maria II	0.91	1.08	0.27
	Macdoel II	1.48	1.91	0.68
	Moreno Valley	1.10	1.30	0.49
All Iran Stations	1.12	1.57	0.65	
GEP4	Bishop	0.67	0.93	0.84
	King City Oasis Rd.	0.79	1.05	0.83
	Blythe NE	1.20	1.79	0.74
	Atascadero	1.46	1.66	0.86
	Delano	1.22	1.49	0.88
	Gilroy	1.10	1.36	0.77
	Arleta	1.11	1.46	0.62
	Gerber South	0.94	1.20	0.84
	Woodland	0.94	1.20	0.85
	Diamond Springs	0.85	1.13	0.85
	Lompoc	1.56	1.77	0.54
	Santa Maria II	1.30	1.58	0.51
	Macdoel II	2.72	3.23	0.01
	Moreno Valley	1.18	1.54	0.60
All Iran Stations	0.87	1.15	0.77	

#### 4.4 Comparing Performance of MARS, M5MT, and GEP

The average performance of the MARS, M5MT, and GEP approaches for all stations are compared in Table 19 and Figure 33. According to Table 19, the GEP approach performed better than MARS and M5MT. Also, the MARS approach provided better results than M5MT. Average *MAE* and *RMSE* of  $ET_0$  estimates from the MARS approach decreased respectively, by 9% and 18% compared to M5MT. Compared to GEP, MARS average *MAE* (*RMSE*) was 9% (5%) higher and  $R^2$  was 29% lower. Also, M5MT average *MAE* (*RMSE*) was 19% (25%) higher and  $R^2$  was 3% lower than GEP.

Comparing the average accuracies of the four different configurations, Table 19 shows configuration 1 to provide the best  $ET_0$  estimates, followed by configuration 2. This was true for all approaches. These results demonstrated that the use of only two input parameters,  $T_{mean}$  and  $R_s$  (configuration 2), can provide results comparable to the use of four input parameters,  $T_{mean}$ ,  $RH_{mean}$ ,  $W_s$ , and  $R_s$  (configuration 1). The results also suggested that  $RH_{mean}$ ,  $T_{min}$ ,  $T_{max}$ , or  $R_a$  used with  $T_{mean}$  (configurations 3 and 4) did not have a significant role in predicting  $ET_0$ .




Of the four GEP models, GEP1 achieved the best accuracy, followed by GEP2, GEP3, and GEP4. GEP1 had the lowest *MAE* (0.53 mm/d) and *RMSE* (0.71 mm/d). *MAE* and *RMSE* of GEP2 increased by 28% and 20%, respectively compared to those of GEP1. *MAE* and *RMSE* of GEP3 increased by 91% and 75%, respectively, and  $R^2$  decreased by 45% in comparison with GEP1. Furthermore, compared to GEP1, *MAE* and *RMSE* of GEP4 increased by 126% and 111%, respectively, and  $R^2$  decreased by 29%.

Based on the previously mentioned results, GEP demonstrated superior accuracy in estimating  $ET_0$  compared to MARS and M5MT. It was observed that for all approaches, the performance of configuration 1 surpassed the performances of configurations 2, 3, and 4. The

results also indicated that configuration 2 can provide similar results to configuration 1, and yielded better results than configurations 3 and 4.

Table 19. Mean  $R^2$ ,  $MAE$ , and  $RMSE$  of  $ET_0$  estimates from MARS, M5MT and GEP models (tested with Iran and California stations).

Approach	Model	Tested with Iran and California		
		MAE (mm/d)	RMSE (mm/d)	$R^2$
MARS	MARS1	0.71	0.84	0.75
	MARS2	0.85	1.01	0.70
	MARS3	1.08	1.33	0.49
	MARS4	1.10	1.35	0.49
M5MT	M5MT1	0.76	0.94	0.86
	M5MT2	0.90	1.10	0.89
	M5MT3	1.13	1.56	0.63
	M5MT4	1.29	1.78	0.65
GEP	GEP1	0.53	0.71	0.90
	GEP2	0.68	0.85	0.90
	GEP3	1.01	1.24	0.62
	GEP4	1.20	1.50	0.70

 Best Approach  
 Best Model Performance  
 Second Best Model Performance

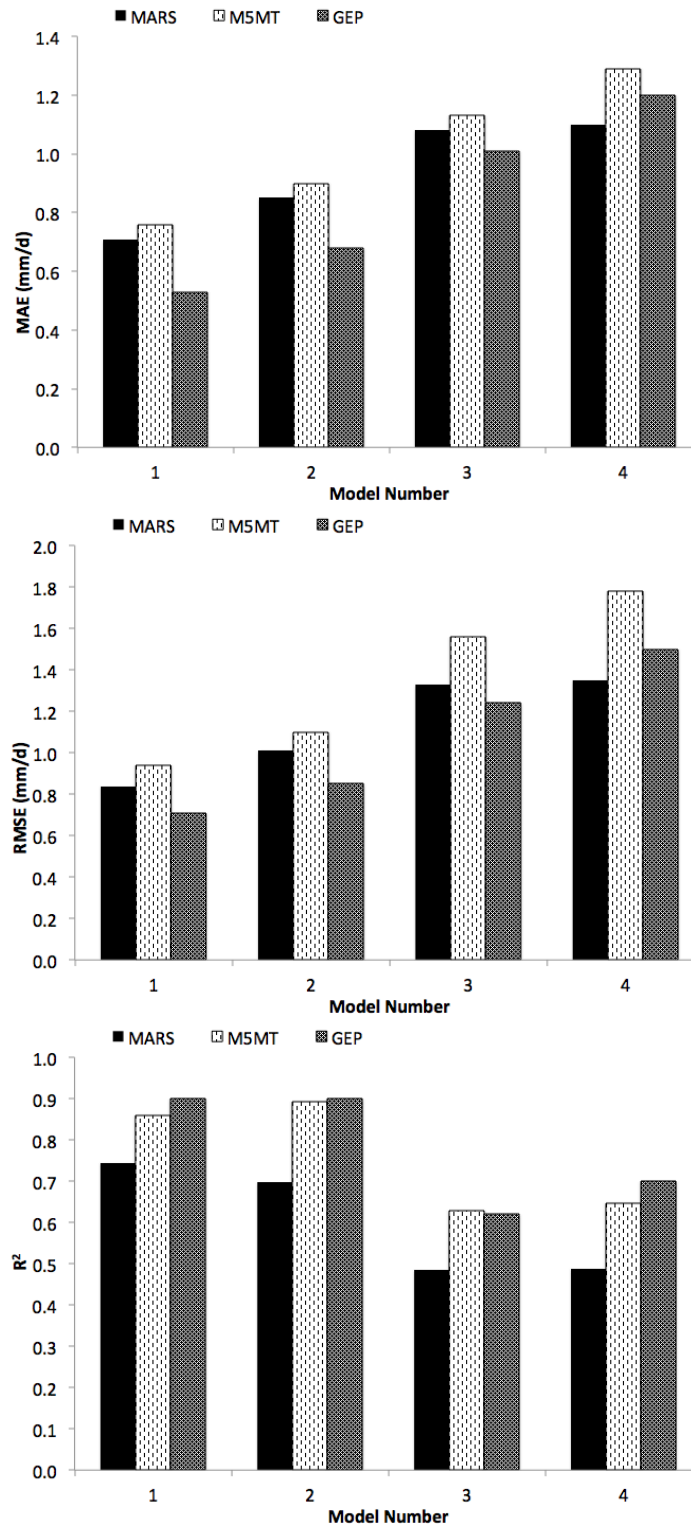


Figure 33. Performance of MARS, M5MT, and GEP models tested with Iran and California stations.

## 5. CONCLUSION

In this study, Multivariate Adaptive Regression Splines (MARS), M5 Model Tree (M5MT), and Gene Expression Programming (GEP) were used to estimate  $ET_0$  from climatic data. Four different input configurations were used: daily mean air temperature ( $T_{mean}$ ), daily mean wind speed ( $W_s$ ), daily mean relative humidity ( $RH_{mean}$ ), and solar radiation ( $R_s$ ) [configuration 1]; daily mean air temperature ( $T_{mean}$ ) and solar radiation ( $R_s$ ) [configuration 2]; daily mean air temperature ( $T_{mean}$ ) and daily mean relative humidity ( $RH_{mean}$ ) [configuration 3]; daily maximum, minimum, and mean air temperature ( $T_{max}$ ,  $T_{min}$ , and  $T_{mean}$ ) and extraterrestrial radiation ( $R_a$ ) [configuration 4]. MARS, M5MT and GEP were trained with climatic data from 8 weather stations in Iran for the years 2000-2007. These models were tested with the data from the same weather stations in Iran for the year 2008 and fourteen stations in California for the year 2015. Their performance was evaluated based on mean absolute error ( $MAE$ ), root mean square error ( $RMSE$ ), and coefficient of determination ( $R^2$ ).

It was shown that configuration 1 yielded the most accurate results with the lowest  $MAE$  and  $RMSE$  in all approaches. In GEP, configuration 1 reduced  $RMSE$  by 20%, 75%, and 111% compared to configurations 2, 3, and 4, respectively. Similarly, in MARS, the reduction in  $RMSE$  was 20% 59%, and 61%, respectively. Finally, the decrease in  $RMSE$  was respectively, 17%, 66%, and 89% in M5MT. Therefore, it was concluded that configuration 1 consisted of variables that have the most significant effect on  $ET_0$ . Moreover, the accuracy of configuration 1 was not region dependent and it generated the best results in both Iran and California.

M5MT and GEP showed configuration 4 to be region dependent, performing better when tested locally. M5MT4 tested with Iran stations decreased  $RMSE$  by 125% compared to testing

with California stations. Likewise, GEP4 tested with Iran stations reduced *RMSE* by 33%. Thus, configuration 4 is suggested when only air temperature is obtainable for a specific region.

This study demonstrated that modeling  $ET_0$  is possible through the use of MARS, M5MT, and GEP. However, results showed GEP to be the best approach, followed by MARS. Compared to MARS, the average *MAE* and *RMSE* of  $ET_0$  estimates from GEP were respectively 9% and 5% lower. Also, average *MAE* and *RMSE* of  $ET_0$  estimates from GEP were respectively, 19% and 25% lower than those of M5MT. As a result, GEP is the recommended approach to most accurately model  $ET_0$ .

Summarizing, configuration 1 was not region dependent and provided the most accurate  $ET_0$  estimates compared to configurations 2, 3, and 4. Configuration 4 was shown to be region dependent and would be useful in areas where only temperature data is available. GEP provided better results over MARS and M5MT, and is the suggested approach to model  $ET_0$ .

Future work should be directed to validate GEP, MARS and M5MT approaches in other regions as well. Also, their performance should be compared with commonly used equations such as Makkink, Romanenko and Hargreaves-Samani equations.

## APPENDIX: M5MT Output Reference Guide

1. Starting from the left column of Table 10, " $R_s \leq 16.271$ " is stated. This means  $R_s$  is the first node with a branching decision statement  $\leq 16.271$  (refer to Figure 1d for general configuration of model tree).
2. Following the symbol "|" down the same indentation, " $R_s > 16.271$ " is stated. This represents the second branch of the node previously established ( $R_s$ ) and its corresponding decision statement.
3. Following the symbol "|" down the same indentation, there are no other decision statements. This concludes the first tier of the model tree.
4. The second indentation from the top left of Table 10 starts the second tier. " $T_{mean} \leq 19.175$ " and " $T_{mean} > 19.175$ " are stated and  $T_{mean}$  is a node in the second tier with decision statements  $\leq 19.175$  and  $> 19.175$ . A data value from the testing dataset would reach this node if the statement " $R_s \leq 16.271$ " is true.
5. Similarly, following the same indentation down the table, " $T_{mean} \leq 28.837$ " and " $T_{mean} > 28.837$ " are also in the second tier, which is another  $T_{mean}$  node with decision statements  $\leq 28.837$  and  $> 28.837$ . A data value from the testing dataset would reach this node if the statement " $R_s > 16.271$ " is true.
6. Following the symbol "|" down the same indentation, there are no other decision statements. This concludes the second tier of the model tree.
7. The third indentation from the top left of Table 10 represents the nodes in the third tier and so on.

**Note:** Statements, such as " $T_{mean} \leq 8.55$ : LM1", signify the node does not have any more branches below, and linear model 1 (LM1) can be used.

## REFERENCES

- Adamowski, J., H.F. Chan, S.O. Prasher, and V.N. Sharda (2012). Comparison of multivariate adaptive regression splines with coupled wavelet transform artificial neural networks for runoff forecasting in Himalayan micro-watersheds with limited data, *Journal of Hydroinformatics*, 14 (3), 731–744.
- Allen, R., L.S. Pereira, D. Raes, and M. Smith (1998). Crop evapotranspiration. Guidelines for computing crop evapotranspiration. FAO Irrigation and Drainage Paper 56, Rome, Italy.
- Atiaa, A. M., and H. B. Ghalib (2008). Rainfall-Runoff modeling by using M5 model trees technique: an example of Tigris catchment area in Baghdad, Middle of Iraq, *MARSH BULLETIN*, 3 (2), 125–135.
- Azamathulla, H., and Z. Ahmad (2012). Gene-expression programming for transverse mixing coefficient, *Journal of Hydrology*, 434-435, 142-148.
- Azamathulla, H., and R.D. Jarrett (2013). Use of Gene expression programming to estimate Manning’s roughness coefficient for high gradient streams. *Water Resource Management*, 27, 715-729.
- Bansal, P. and J. Salling. “Multivariate Adaptive Regression Splines (MARS).” Data Mining, UT ECE. 16 Feb. 2013.
- Bhattacharya, B., and D.P. Solomatine (2005). Neural networks and M5 model trees in modelling water level–discharge relationship, *Neurocomputing*, 63, 381-396.
- Emamgolizadeh, S., S.M. Bateni, D. Shahsavani, T. Ashrafi, and H. Ghorbani. Estimation of soil cation exchange capacity using Genetic Expression Programming (GEP) and Multivariate Adaptive Regression Splines (MARS). *J. Hydrol.* (2015), <http://dx.doi.org/10.1016/j.jhydrol.2015.08.025>
- Etemad-Shahidi, A., and J. Mahjoobi (2009). Comparison between M5 model tree and neural networks for prediction of significant wave height in Lake Superior, *Ocean Engineering*, 36.15, 1175-1181.
- “Evapotranspiration – The Water Cycle.” Evapotranspiration – The Water Cycle, from USGS Water-Science School. 2 Dec. 2016. USGS. <http://water.usgs.gov/eduwatercycleevapotranspiration.html>.



- Ferreira, C. (2001). Gene Expression Programming: A New Adaptive Algorithm for Solving Problems, *Complex Systems*, 13 (2), 87–129.
- Frank, E., M.A. Hall, and I.H. Witten, 2016. The WEKA Workbench. Online Appendix for “Data Mining: Practical Machine Learning Tools and Techniques”, Morgan Kaufmann, Fourth Edition, 2016.
- “Fresh Water Crisis.” National Geographic: Environment. 2 May 2016. National Geographic. <<https://environment.nationalgeographic.com>>.
- Friedman, J.H. “Multivariate Adaptive Regression Splines (with discussion)”. *Annals of Statistics*, 1991. <<http://www.salfordsystems.com/doc/MARS.pdf>>
- Garcia-Navarro, M.C., R.Y. Evans, and R.S. Montserrat (2004). Estimation of relative water use among ornamental landscape species, *Scientia Horticulturae*, 99 (2), 163–174.
- Güven, A. and M. Günel (2008). Genetic programming for prediction of local scour downstream of grade-control structures, *Journal of Irrigation and Drainage Engineering*, 134 (2), 241–249.
- Güven, A., A. Aytekin, M.I. Yüce, and H. Aksoy (2008). Genetic programming-based empirical model for daily reference evapotranspiration estimation, *Clean Soil, Air, Water*, 36, 905–912.
- Hargreaves, G.H. and Z.A. Samani (1985). Reference crop evapotranspiration from temperature, *American Society of Agricultural Engineers*, 1 (2), 96-99.
- Hashmi, M.Z., A.Y. Shamseldin, B.W. Melville (2011). Statistical downscaling of watershed precipitation using gene expression programming (GEP), *Environmental Modeling Software*, 26, 1639-1646.
- Jekabsons, G., ARESLab: Adaptive Regression Splines toolbox for Matlab/Octave, 2016, available at <http://www.cs.rtu.lv/jekabsons/>.
- Kisi, O. (2015). Pan evaporation modeling using least square support vector machine, multivariate adaptive regression splines and M5 model tree, *Journal of Hydrology*, 528, 312-320.
- Kisi, O. and K.S. Parmar (2016). Application of least square support vector machine and multivariate adaptive regression spline models in long term prediction of river water pollution, *Journal of Hydrology*, 534, 104–112.

- Lui, J., A.J. B Zehnder, and H. Yang (2009). Global consumptive water use for crop production: the importance of green water and virtual water, *Water Resources Research*, 45, W05428, doi: 10.1029/2007WR006051.
- Makkink, G.F. (1957). Testing the Penman formula by means of lysimeters, *Journal of the Institution of Water Engineering*, 11 (3), 277-288.
- Oltean, M., and C. Grosan (2003). A Comparison of Several Linear Genetic Programming Techniques, *Complex Systems*, 14, 285–313.
- Pal, M. and S. Deswal (2009). M5 model tree based modeling of reference evapotranspiration, *Hydrological Processes*, 23, 1437–1443.
- Postel, S. “Climate Change Poses Existential Water Risks.” National Geographic: Voices. 2 May 2016. National Geographic. <voices.nationalgeographic.com>.
- Pour Ali Baba, A., J. Shiri, O. Kisi, A. Fakheri Fard, S. Kim, and R. Amini (2013). Estimating daily reference evapotranspiration using available and estimated climatic data by adaptive neuro-fuzzy inference system and artificial neural networks, *Hydrology Research*, 44 (1), 131–146.
- Rahimikhoob, A. (2008). Comparative study of Hargreaves’s and artificial neural network’s methodologies in estimating reference evapotranspiration in a semiarid environment, *Irrigation Science*, 26 (3), 253–259.
- Rahimikhoob, A., M. Asadi, and M. Mashal (2013). A Comparison Between Conventional and M5 Model Tree Methods for Converting Pan Evaporation to Reference Evapotranspiration for Semi-Arid Region, *Water Resour Manage*, 27, 4815–4826.
- Romanenko, V.A. (1961). Computation of the autumn soil moisture using a universal relationship for a large area, In: Proceedings of Ukrainian Hydrometeorological Research Institute, no. 3 Kiev.
- Sattari, M.T., M. Pal, K. Yurkekl, and A. Unlukara (2013). M5 model trees and neural network based modeling of ET<sub>0</sub> in Ankara, Turkey, *Turkish Journal of Engineering and Environmental Sciences*, 37.2, 211–219.
- Shahidian, S., R.P. Serralheiro, J. Serrano, J. Teixeira, N. Haie, and F. Santos. *Hargreaves and other reduced-set methods for calculating evapotranspiration*. InTech, 2012.

- Sharda, V.N., R.M. Patel, S.O. Prasher, P.R. Ojasvi, and C. Prakash (2006). Modeling runoff from middle Himalayan watersheds employing artificial intelligence techniques, *Agricultural Water Management*, 83, 233 – 242.
- Shiri, J. and O. Kisi (2011). Application of Artificial Intelligence to Estimate Daily Pan Evaporation Using Available and Estimated Climatic Data in the Khozestan Province (South Western Iran), *Journal of Irrigation and Drainage Engineering*, 137, 412–425.
- Shiri, J., O. Kisi, G. Landaras, J.J. Lopez, A.H. Nazemi, and L. Stuyt (2011). Daily reference evapotranspiration modeling by using genetic programming approach in the Basque Country (Northern Spain), *Journal of Hydrology*, doi: 10.1016/j.jhydrol.2011.11.004, in press.
- Shiri, J., A. A. Sadraddini, A.H. Nazemi, O. Kisi, P. Marti, A.F. Fard, and G. Landaras (2013). Evaluation of different data management scenarios for estimating daily reference evapotranspiration, *Hydrology Research*, 44 (6), 1058–1070.
- Shiri, J., A.A. Sadraddini, A.H. Nazemi, O. Kisi, G. Landaras, A.F. Fard, and P. Marti (2014). Generalizability of Gene Expression Programming-based approaches for estimating daily reference evapotranspiration in coastal stations of Iran, *Journal of Hydrology*, 508, 1–11.
- Traore, S., Y. Wang, and T. Kerh (2010). Artificial neural network for modeling reference evapotranspiration complex process in Sudano-Sahelian zone, *Agricultural Water Management*, 97, 707–714.
- Verstraeten, W., F. Veroustraete, and J. Feyen (2008). Assessment of Evapotranspiration and Soil Moisture Content Across Different Scales of Observation, *Sensors*, 8, 70–117.
- Wang, Y., and I.H. Witten (1997). Induction of model trees for predicting continuous classes. In: *Proceedings of the Poster Papers of the European Conference on Machine Learning*. University of Economics, Faculty of Informatics and Statistics, Prague.
- Witten, I.H., and E. Frank (2005). *Data Mining: Practical Machine Learning Tools and Techniques with Java Implementations*. Morgan Kaufmann: San Francisco.
- Xu, T., S. Bateni, S. Margulis, L. Song, S. Liu, and Z. Xu (2016). Partitioning Evapotranspiration into Soil Evaporation and Canopy Transpiration via a Two-Source Variational Data Assimilation System, *Journal of Hydrometeor*, doi: 10.1175/JHM-D-15-01781, in press.

Yang, C.C., S.O. Prasher, R. Lacroix, and S.H. Kim (2004). Application of multivariate adaptive regression splines (MARS) to simulate soil temperature, *Transactions of the ASAE*, 47 (3), 881-887.

Zakaria, N.A., H. Azamathulla, C.K. Chang, A.A. Ghani (2010). Gene expression programming for total bed material load estimation – a case study, *Sci. Total. Environ.*, 408, 5078-5085.